


DEVELOPING ALTERNATIVE POLYMERIC MEMBRANES FOR FUEL CELLS



by
Esra Yılmaz

Submitted to Graduate School of Natural and Applied Sciences
in Partial Fulfillment of the Requirements
for the Degree of Doctor of Philosophy in
Chemical Engineering

Yeditepe University

2017

DEVELOPING ALTERNATIVE POLYMERIC MEMBRANES FOR FUEL CELLS

APPROVED BY:

Assist. Prof. Dr. Erde Can
(Thesis Supervisor)



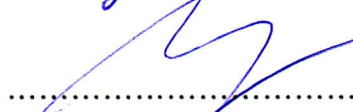
Prof. Dr. Nurcan Baç
(Thesis Co-Supervisor)



Prof. Dr. Birgöl TanteKin Ersolmaz



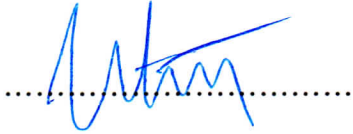
Prof. Dr. Mustafa ÖZilgen



Prof. Dr. Süheyla Uzman



Assist. Prof. Dr. Oktay Demircan



DATE OF APPROVAL : .../.../2017



*this thesis is dedicated to
my family and husband...*

ACKNOWLEDGEMENTS

I would like to express my gratitude to my supervisor Assist. Prof. Erde Can for her continuous support and encouragement with patience and also sharing her immense knowledge with me throughout the research. I would like to also express my gratitude to my thesis co-supervisor Prof. Nurcan Baç for his support and guidance during my whole education and research period in the department.

Furthermore, I would like to thank to the Chemical Engineering Department and Laboratory personnel for their technical support and friendship. I am also thankful to the Yeditepe University for granting me PhD student scholarship. Last but not the least; I would like to thank my all friends for their support and existence.

I am indebted to my family for their love, patience, understanding, motivation and psychological support they provide throughout this study. Special thanks to my father Zafer Yılmaz, mother Gülay Yılmaz and sister Yasemin Çolak for their encouragement to achieve the doctoral degree. They have been always with me by supporting with their love and concern.

Finally, I would like to express deepest gratitude to my precious husband Zeki Sincar for his endless support, concern and love which I always felt being with me all time.

ABSTRACT

DEVELOPING ALTERNATIVE POLYMERIC MEMBRANES FOR FUEL CELLS

Fuel cells are electrochemical devices that convert chemical energy to electrical energy. They are attractive alternative power sources because they have a higher efficiency than diesel or gas engines, they can operate silently and they can eliminate pollution caused by burning fossil fuels. One of the most important components of polymer electrolyte fuel cells and of direct methanol fuel cells (DMFCs) that use hydrogen and methanol as a fuel respectively are the polymer electrolyte membranes (PEMs). The PEM provides proton conduction and functions as a barrier to avoid direct contact between fuel and oxygen. High proton conductivity, low water or fuel permeability, thermal and mechanical stability as well as a low cost are desirable properties for fuel cell membranes. For DMFCs, the proton-conducting membranes must also exhibit low methanol permeability to minimize fuel crossover. In this study, polymer electrolyte membranes based on sulfonated poly(aryl ether sulfone)s and their cross-linked derivatives were prepared and characterized for DMFC applications. The partially sulfonated poly(aryl ether sulfone)s (PESS) were prepared via polycondensation of hydroquinone 2- potassium sulfonate, bisphenol A and 4-fluorophenyl sulfone. The resulting polymers were then methacrylated with glycidyl methacrylate (PESSGMA) and then cross-linked and copolymerized with comonomers, vinyl phosphonic acid (VPA) and styrene (STY) via radical polymerization to improve mechanical properties and decrease methanol permeability. Cross-linked membranes of PESSGMA and its copolymers were prepared via solution casting method through optimization steps both in the synthesis of the PESSGMA pre-polymer and curing cycles. The crosslinking of the PESS polymer significantly reduced ion exchange capacity, proton conductivity, swelling in water and methanol permeability of the membranes while increasing the modulus and the glass transition temperature. However the introduction of the VPA co-monomer to the PESSGMA network increased the proton conductivity while maintaining excellent resistance to methanol cross-over which was significantly higher as compared to both PESS and the commercial Nafion membranes.

ÖZET

YAKIT PİLLERİ İÇİN ALTERNATİF POLİMERİK MEMBRANLAR

Yakıt pilleri, kimyasal enerjiyi elektrik enerjisine dönüştüren elektrokimyasal cihazlardır. Dizel veya benzinli motorlara göre daha yüksek verime sahip olduklarından dolayı ilgi çeken alternatif güç kaynaklarıdır, sessiz çalışabilirler ve fosil yakıtların yanması sonucu oluşan kirliliği azaltabilirler. Yakıt olarak hidrojen kullanan polimer elektrolit yakıt pillerinin ve yakıt olarak metanol kullanan doğrudan metanol yakıt pillerinin (DMFC'lerin) en önemli birleşenlerinden biri, polimer elektrolit membranlar (PEM'ler) dir. Polimer elektrolit membran, proton iletkenliği sağlar ve yakıt ile oksijen arasında oluşabilecek doğrudan teması engellemek amacıyla bariyer görevi görür. Yüksek proton iletkenliği, düşük su veya yakıt geçirgenliği, termal ve mekanik dayanıklılık ve de düşük maliyet, yakıt pilli membranları için arzu edilen özelliklerdir. Doğrudan metanol yakıtlı yakıt pillerinde, proton iletkenliği sağlayan membranların yakıt geçişini en aza indirmek üzere düşük metanol geçirgenliği göstermeleri gerekir. Bu çalışmada, sulfone edilmiş poli(aril eter sulfon) ve çapraz bağlanmış türevleri polimer elektrolit membran olarak hazırlanmış ve doğrudan metanol yakıtlı yakıt pillerinde kullanılmak üzere karakterize edilmiştir. Kısmen sulfone edilmiş poli(aril eter sulfon) (PESS); hidrokinon 2- potasyum sulfonat, bisfenol A ve 4-Florofenil sulfon, monomerlerinin çözelti polikondenzasyonu ile hazırlanmıştır. Sentezlenen polimerler gisidil metakrilatla reaksiyona sokularak metakrile edilmiş (PESSGMA) ve sonrasında mekanik özelliklerini geliştirmek ve metanol geçirgenliğini azaltmak üzere homopolimerizasyon ile veya stiren (STY) ve vinil fosfonik asit (VPA) gibi komonomerlerle radikal ko-polimerizasyona sokularak çapraz bağlı türevleri hazırlanmıştır. Çapraz bağlanmış olan PESSGMA ve kopolimerleri, hem PESSGMA pre-polimer sentezi hem de kür döngülerindeki optimizasyon çalışmaları sonucunda çözelti dökme yöntemi ile hazırlanmıştır. PESS polimerinin çapraz bağlanması, membranların modül ve camsı geçiş sıcaklığını artırırken; iyon değiştirme kapasitesini, proton iletkenliğini, suda şişme ve metanol geçirgenliğini belirgin bir şekilde düşürmüştür. Ancak, VPA ko-monomerinin PESSGMA ağına dahil edilmesi, proton iletkenliğini artırırken, hem PESS hem de ticari Nafyon membranlarına kıyasla mühim oranda yüksek olan mükemmel metanol geçişi direncinin korunmasına neden olmuştur.

TABLE OF CONTENTS

ACKNOWLEDGEMENTS.....	iv
ABSTRACT.....	v
ÖZET	vi
TABLE OF CONTENTS.....	vii
LIST OF FIGURES	xi
LIST OF TABLES.....	xix
LIST OF ABBREVIATIONS.....	xxi
1. INTRODUCTION	1
2. THEORETICAL BACKGROUND.....	4
2.1. FUEL CELLS	4
2.1.1. H ₂ /O ₂ Fuel Cell	6
2.1.2. Direct Methanol Fuel Cell (DMFC).....	7
2.1.2.1. Requirements for DMFC Membranes.....	9
2.1.2.2. Disadvantages of Nafion ® Membranes.....	10
2.2. POLYMERS	10
2.2.1. Polymer Classification Based on Polymerization Mechanism	11
2.2.1.1. Step Reaction Polymerization.....	11
2.2.1.2. Chain Reaction Polymerization	11
2.2.2. Polymer Classification Based on Monomer Composition.....	14
2.2.2.1. Homopolymers.....	14
2.2.2.2. Copolymers	14
2.2.3. Polymer Classification Based on Polymer Architecture.....	16
2.2.3.1. Linear Polymers	17
2.2.3.2. Branched Polymers	17
2.2.3.3. Crosslinked Polymers	17
2.2.4. Polymer Classification Based on Reaction to Temperature.....	18
2.2.4.1. Thermoplastics	19
2.2.4.2. Thermosets	20
2.2.5. Thermal Transition in Polymers	21
2.2.5.1. Crystallization	22
2.2.5.2. Melting.....	23

2.2.5.3. Glass Transition	24
2.2.6. Mechanical Properties of Polymers	25
2.3. POLYMER ELECTROLYTE MEMBRANES FOR DIRECT METHANOL FUEL CELLS (DMFC's)	28
2.3.1. Perflourinated Ionomeric Membranes	29
2.3.2. Non-Fluorinated Hydrocarbon Membranes	30
2.3.3. Acid – Base Complexes	31
2.4. AIM OF THE THESIS	32
3. MATERIALS AND METHODS.....	34
3.1. CHEMICALS	34
3.1.1. Chemicals Used in PESS Synthesis	34
3.1.2. Chemicals Used in PESSGMA Synthesis.....	35
3.1.3. Chemicals Used in the Cure of PESSGMA and Membrane Preparation.....	35
3.2. METHODS	36
3.2.1. FT-IR Spectroscopy	37
3.2.2. ¹ H-NMR Spectroscopy	39
3.2.3. Gel Permeation Chromatography (GPC)	40
3.2.4. Differential Scanning Calorimetry (DSC)	42
3.2.5. Dynamic Mechanical Analysis (DMA)	44
3.2.6. Thermal Gravimetric Analysis (TGA).....	46
3.2.7. Scanning Electron Microscopy (SEM)	48
3.2.8. Proton Conductivity Measurements.....	49
3.2.9. Methanol Permeability Measurements.....	52
4. EXPERIMENTAL STUDY.....	54
4.1. SYNTHESIS OF PESS AND PESS(K)	54
4.1.1. Procedure of the Reaction	54
4.1.2. The Purification of the PESS and PESS(K) Polymer	56
4.2. SYNTHESIS OF PESSGMA AND PESSGMA(K).....	58
4.2.1. The Procedure of the Reaction.....	58
4.3. CURE OF PESSGMA AND PESSGMA(K) POLYMERS AND PREPARATION OF MEMBRANES	62
4.4. CHARACTERIZATION OF PESS AND PESSGMA POLYMERS	68

4.4.1. FT-IR Analysis	68
4.4.2. ¹ H-NMR Analysis	68
4.4.3. Gel Permeation Chromatography (GPC) Analysis	69
4.4.4. Ion Exchange Capacity (IEC) Analysis	69
4.4.5. Swelling Tests	70
4.4.6. Differential Scanning Calorimetry (DSC) Analysis	70
4.4.7. Dynamic Mechanical Analysis (DMA)	70
4.4.8. Thermal Gravimetric Analysis (TGA)	71
4.4.9. Scanning Electron Microscopy (SEM) Analysis	71
4.4.10. Proton Conductivity Measurements	71
4.4.11. Methanol Permeability Measurements	73
5. POLY ARYL ETHER SULFONE (PESS) AND METHACRYLATED POLY ARYL ETHER SULFONE (PESSGMA) SYNTHESIS AND CHARACTERIZATION	75
5.1. CHARACTERIZATION OF THE PESS AND PESSGMA POLYMERS VIA FT-IR SPECTROSCOPY	76
5.2. CHARACTERIZATION OF THE PESS AND PESSGMA POLYMERS VIA ¹ H-NMR SPECTROSCOPY	78
5.3. CHARACTERIZATION OF THE PESS(K ⁺) AND PESSGMA(K ⁺) POLYMERS VIA FT-IR AND ¹ H-NMR SPECTROSCOPY	82
5.4. GPC ANALYSIS OF THE PESS AND PESSGMA POLYMERS	85
6. STRUCTURAL CHARACTERIZATION OF CROSS-LINKED PESSGMA POLYMERS	87
6.1. FT-IR ANALYSIS	87
6.1.1. Self Polymerization of PESSGMA and PESSGMA(K)	88
6.1.2. Polymerization of PESSGMA(K) with Styrene	95
6.1.3. Polymerization of PESSGMA(K) with Sulfonated Styrene (Sodium 4-vinyl benzene sulfonate)	96
6.1.4. Polymerization of PESSGMA(K) with Vinyl Phosphonic Acid	97
6.1.5. Polymerization of PESSGMA with Styrene	98
6.1.6. Polymerization of PESSGMA with Sulfonated Styrene (Sodium 4-vinyl benzene sulfonate)	99
6.1.7. Polymerization of PESSGMA with Vinyl Phosphonic Acid	100

6.1.8. Polymerization of PESSGMA with Styrene and Vinyl Phosphonic Acid.....	102
6.1.9. Self Polymerization of PESSGMA After Cure Optimization	104
6.1.10. Polymerization of PESSGMA with Styrene After Cure Optimization	105
6.1.11. Polymerization of PESSGMA with Vinyl Phosphonic Acid After Cure Optimization.....	106
6.1.12. Polymerization of PESSGMA with Styrene and Vinyl Phosphonic After Cure Optimization.....	107
6.2. ION EXCHANGE CAPACITY (IEC) ANALYSIS	108
6.3. WATER SWELLING PROPERTIES	111
6.3.1. Swelling Experiments at Room Temperature.....	111
6.3.2. Swelling Experiments at 80°C	113
7. ANALYSIS OF PROPERTIES OF PESS AND PESSGMA POLYMERS FOR FUEL CELL APPLICATIONS.....	115
7.1. DSC ANALYSIS	115
7.2. THERMOMECHANICAL PROPERTIES (DMA)	118
7.3. THERMAL GRAVIMETRIC ANALYSIS (TGA).....	122
7.4. PROTON CONDUCTIVITY RESULTS	127
7.4.1. Effect of Temperature	130
7.4.2. Effect of Initiator Content.....	131
7.5. METHANOL PERMEABILITY	131
7.6. SCANNING ELECTRON MICROSCOPY (SEM) ANALYSIS	134
7.7. COST ANALYSIS	139
8. CONCLUSIONS AND FUTURE WORK	141
8.1. CONCLUSIONS	141
8.2. FUTURE WORK.....	148
REFERENCES	150

LIST OF FIGURES

Figure 2.1. Schematic of a fuel cell	5
Figure 2.2. Schematic of a proton exchange membrane fuel cell.....	7
Figure 2.3. DMFC principle scheme.....	8
Figure 2.4. Free-radical chain polymerization.....	13
Figure 2.5. Linear, branched, and cross-linked polymer structures.....	16
Figure 2.6. The branched chain structure of thermoplastics	20
Figure 2.7. Molecular structure of thermosets	21
Figure 2.8. Typical heat flow vs. temperature plot of a crystallization transition in a polymer.....	22
Figure 2.9. Typical heat flow vs. temperature plot of a melting transition in a polymer.....	24
Figure 2.10. Typical heat flow vs. temperature plot of a glass transition in a polymer.....	25
Figure 2.11. A typical tensile stress-strain curve for a polymeric material that exhibits plastic deformation.....	28

Figure 2.12. Representative tensile stress-strain curves of different types of polymeric material.....	28
Figure 2.13. The scheme for the synthesis of the Nafion membrane	30
Figure 2.14. Structure of basic polymers (a-d) and acidic polymers (e,f)	31
Figure 2.15. The schematic representations of (a) PESS and (b) PESSGMA polymers.....	33
Figure 3.1. Basic components of a FT-IR spectrometer.....	37
Figure 3.2. Typical infrared absorption frequencies for some common functional groups.....	38
Figure 3.3. Schematic representation of a NMR spectrometer	40
Figure 3.4. Schematic of the basic components of a gel permeation chromatograph.....	41
Figure 3.5. Molecular weight distribution curve of a gel permeation chromatograph.....	42
Figure 3.6. Schematic view of the interior components of a DSC	42
Figure 3.7. Schematic of a DSC thermogram	43
Figure 3.8. Clamp of film tension for DMA.....	46

Figure 3.9. A typical TGA instrument.....	47
Figure 3.10. A typical SEM instrument.....	48
Figure 3.11. Schematic of a four-probe conductivity cell designed to measure proton conductivity.....	51
Figure 3.12. Nafion 115 membrane's AC impedance spectra generated via four probe method.(0.4, 1.6, and 2.7 stand for the distance (cm) between the two voltage probes).....	52
Figure 3.13. The schematic of the two compartment diffusion cell and a typical methanol permeability measurement set-up.....	53
Figure 4.1. The schematic representation of the PESS synthesis reaction	54
Figure 4.2. The experimental set up for PESS synthesis	55
Figure 4.3. The precipitation and vacuum filtration processes of PESS product	56
Figure 4.4. The final form of the PESS product	57
Figure 4.5. The schematic representation of PESSGMA synthesis reaction.....	59
Figure 4.6. Experimental set up for the PESSGMA synthesis	60
Figure 4.7. The solution of the synthesized PESSGMA product at the end of reaction.....	60

Figure 4.8. The filtered product and residual particals	61
Figure 4.9. The filtrated PESSGMA polymer	61
Figure 4.10. Films of PESSGMA(K) polymer cured with styrene(1), sodium4- vinyl benzene sulfonate (2) and vinyl phosphonic acid(3).....	67
Figure 4.11. Films of a) PESSGMA(4wt% TBPB) polymer and b) PESSGMA (3wt%TBPB) polymer c)PESSGMA/STY polymer d)PESSGMA/VPA polymer cured under the conditions listed in Table 4.3.....	67
Figure 4.12. The proton conductivity measurement set-up (left) and the conductivity cell (right).....	72
Figure 4.13. Representation of membrane dimensions for the proton conductivity measurement set up.....	72
Figure 4.14. Two-compartment diffusion cell used in methanol permability measurements.....	74
Figure 5.1. FT-IR spectrum of the PESS polymer.....	77
Figure 5.2. FT-IR spectrum of the PESSGMA polymer	78
Figure 5.3. The ¹ H-NMR spectrum of the PESS polymer	80
Figure 5.4. The ¹ H-NMR spectrum of (a) the PESSGMA polymer and (b) its magnified version.....	81

Figure 5.5. The FT-IR spectrum of the PESS (K) polymer	82
Figure 5.6. The ¹ H-NMR spectrum of the PESS(K) polymer version.....	83
Figure 5.7. FT-IR spectrum of the PESSGMA (K) polymer.....	84
Figure 5.8. The ¹ H-NMR spectrum of PESSGMA(K) polymer.....	85
Figure 6.1. The FT-IR spectrum of PESSGMA polymerized with 4% of tert-butyl peroxy benzoate (100°C for 3 hours, 130°C for 3 hours).....	89
Figure 6.2. The FT-IR spectrum of PESSGMA(K) polymerized with 4% of tert-butyl peroxy benzoate (100°C for 3 hours, 130°C for 3 hours).....	90
Figure 6.3. The FT-IR spectrum of PESSGMA (K) polymerized with 4% of tert-butyl peroxy benzoate (100°C for 3 hours, 130°C for 6 hours).....	91
Figure 6.4. The FT-IR spectrum of PESSGMA polymerized with 6% of tert-butyl peroxy benzoate (100°C for 3 hours, 130°C for 6 hours).....	92
Figure 6.5. The FT-IR spectrum of PESSGMA (K) polymerized with 6% of tert-butyl peroxy benzoate (100°C for 3 hours, 130°C for 6 hours).....	93
Figure 6.6. The FT-IR spectrum of PESSGMA polymerized with 10% of tert-butyl peroxy benzoate (100°C for 3 hours, 130°C for 6 hours).....	94
Figure 6.7. The FT-IR spectrum of PESSGMA(K) polymerized with 10% of tert-butyl peroxy benzoate (100°C for 3 hours, 130°C for 6 hours).....	95

Figure 6.8. FT-IR spectrum of PESSGMA (K) - styrene polymerized with 4% benzoyl peroxide (90°C for 5 hours, 130°C for 3 hours).....	96
Figure 6.9. The PESSGMA(K) - sulfonated styrene film prepared with benzoyl peroxide (90°C for 5 hours, 130°C for 3 hours).....	97
Figure 6.10. FT-IR spectrum of PESSGMA (K) and vinyl phosphonic acid polymerized with 4% benzoyl peroxide (90°C for 5 hours, 130°C for 3 hours).....	98
Figure 6.11. FT-IR spectrum of PESSGMA and styrene polymerized with 4% benzoyl peroxide (100°C for 5 hours, 130°C for 3 hours, 150°C for 12 hours).....	99
Figure 6.12. FT-IR spectrum of PESSGMA and vinyl phosphonic acid polymerized with 4% benzoyl peroxide (100°C for 5 hours, 130°C for 9 hours).....	100
Figure 6.13. FT-IR spectrum of PESSGMA and vinyl phosphonic acid polymerized with 4wt% benzoyl peroxide (100°C for 5 hours, 180°C for 9 hours).....	101
Figure 6.14. FT-IR spectrum of PESSGMA polymerized with styrene and vinyl phosphonic acid in the presence of 4wt% benzoyl peroxide (100°C for 5 hours, 130°C for 9 hours).....	102
Figure 6.15. FT-IR spectrum of PESSGMA polymerized with styrene and vinyl phosphonic acid in the presence of 4wt% benzoyl peroxide (100°C for 5 hours, 180°C for 9 hours).....	103
Figure 6.16. The FT-IR spectrum of PESSGMA self-polymerized in the presence of 4wt% of tert-butyl peroxy benzoate by drying sample at 100°C for 5 hours and then at 110°C for 15 hours under vacuum.....	105

Figure 6.17. FT-IR spectrum of PESSGMA/STY(70/30) sample polymerized in the presence of 4wt% of benzoyl peroxide by drying the sample at 100°C for 5 hours and then 110°C for 15 hours, under vacuum.....	106
Figure 6.18. FT-IR spectrum of PESSGMA/VPA(70/30) sample polymerized in the presence of 4wt% of benzoyl peroxide by drying the sample at 100°C for 5 hours and then at 110°C for 5 hours and at 120°C for 10 hours, under vacuum.....	107
Figure 6.19. FT-IR spectrum of PESSGMA/STY/VPA(70/15/15) sample polymerized in the presence of 4wt% of benzoyl peroxide by drying the sample at 100°C for 5 hours and then at 110°C for 5 hours and at 120°C for 10 hours, under vacuum.....	108
Figure 6.20. a) Weight % change data of the PESS and PESSGMA membranes in water for 400 hrs at room temperature b) weight % change values of the PESS and PESSGMA membranes after 24 hrs in water, at room temperature.....	113
Figure 6.21. Weight % change values of the PESS and PESSGMA membrane after swelling in water for 24 hrs at 80°C.....	114
Figure 7.1. The DSC spectra of the PESS and PESSGMA polymer membranes	116
Figure 7.2. The DSC spectra of the PESSGMA/VPA polymer membranes	117
Figure 7.3. (a) Loss modulus versus temperature (b) Storage modulus versus temperature for PESS, PESSGMA and PESSGMA co-polymer membranes.....	120

Figure 7.4. The weight% vs temperature plots of (a) PESS, PESSGMA and PESSGMA co-polymers (b) PESS and PESSGMA polymers.....	124
Figure 7.5. The weight% vs temperature plots of PESSGMA/VPA co-polymers	126
Figure 7.6. SEM images of (a) PESS at 5500x magnification (b) PESSGMA at 6000x magnification, (c) PESSGMA/STY at 6000x magnification and (d) PESSGMA/VPA at 6000x magnification.....	137
Figure 7.7. SEM images of PESSGMA/STY/VPA at (a) 1000X (b) 4000X (c) 10000X magnifications.....	139
Figure 8.1. Bar graphs for the T_g 's, and the values of storage modulus, proton conductivity, methanol permeability and selectivity ratio at 60°C as well as the cost for all the PESS, PESSGMA and PESSGMA copolymer membranes.....	148

LIST OF TABLES

Table 3.1. Chemicals used in preparation of PESS and PESS(K) polymers.....	34
Table 3.2. Chemicals used in preparation of PESSGMA and PESSGMA(K) polymers.....	35
Table 3.3. Chemicals used in the cure of PESSGMA and PESSGMA(K) polymers and membrane preparation.....	36
Table 4.1. The compositions of all the prepared PESSGMA samples and the curing conditions applied in initial trials.....	63
Table 4.2. The compositions of all the prepared PESSGMA(K) samples and the curing conditions.....	65
Table 4.3. The compositions of all the prepared PESSGMA samples and the curing conditions after curing optimization.....	65
Table 5.1. The molecular weight data of the PESS and PESSGMA polymers as determined from GPC analysis. (\bar{M}_n is number average molecular weight, \bar{M}_w is weight average molecular weight and \bar{D} is the polydispersity index).....	86
Table 6.1. IEC values of the PESS, PESSGMA and PESSGMA copolymers at room temperature.....	110

Table 7.1. Storage modulus (E') values at 25°C and 60°C and glass transition temperatures (T_g) for the PESS and PESSGMA polymers as determined by DMA.....	122
Table 7.2. The temperatures for 5,10 and 20wt% loss for the PESS and PESSGMA polymer membranes.....	127
Table 7.3. Proton conductivity data of the different polymer membranes at the end of 48hrs at 60°C and 80°C.....	130
Table 7.4. Methanol permeability and selectivity ratios of the PESS,PESGMA and PESSGMA copolymer membranes at 60°C.....	134
Table 7.5. Cost values of the PESS, PESSGMA, PESSGMA copolymer membranes and the commercial Nafion® 117 membranes.....	140

LIST OF SYMBOLS/ABBREVIATIONS

AC	Alternating Current
CL	Catalyst Layer
C_p	Heat Capacity
DC	Direct Current
DL	Diffusion Layer
GPa	Giga Pascal
KBr	Potassium Bromide
kW	Kilo Watt
mA	Mili Ampere
meq g ⁻¹	Milliequivalent Per Gram
mHz	Mili Hertz
MHz	Mega Hertz
MPa	Mega Pascal
mS	Mili Siemens
mW	Mili Watt
nm	Nano Meter
Pt	Platinum
RH	Relative Humidity
Ru	Ruthenium
S	Siemens
UV	Ultra Violet
μL	Micro Liter
μm	Micro Meter



1. INTRODUCTION

Power generation is one of the world's most important and growing problems. Proton exchange membrane fuel cells and direct methanol fuel cells (DMFC)s which are electrochemical devices that convert chemical energy to electrical energy are the most promising power sources in the future due to their high energy efficiency and environmental friendliness.

Polymer electrolyte membranes (PEMs) are main components of polymer electrolyte fuel cells that use hydrogen as a fuel and of direct methanol fuel cells (DMFCs). The basic roles of a PEM are acting as an electrolyte medium for proton conduction and as a barrier to avoid direct contact between the fuel and oxygen[1]. Fuel cell membranes must exhibit high proton conductivity, low water or fuel permeability, good mechanical and thermal stability and low cost. DMFC technology needs proton-conducting membranes that have low methanol permeability to minimize methanol cross-over [2,3]. Most commercially available proton exchange membranes use a fluorinated ionomer, such as Nafion® produced by DuPont because of its high proton conductivity and high chemical stability. However, Nafion® membranes have several drawbacks like low proton conductivity at high temperature (>80°C) under low humidity, high cost and an undesirably high methanol permeability. A high methanol crossover through the proton exchange membrane causes to a decreased fuel cell performance owing to depolarization of the oxygen reducing cathode. As a result, considerable effort has been expended to minimize methanol permeability and keep a high proton conductivity for membranes used in DMFC applications. To get over the disadvantages of perfluorinated membranes, many sulfonated polymers, such as sulfonated polysulfone, sulfonated poly(aryl ether sulfone), sulfonated polyetherether ketone, sulfonated poly(styrene) and sulfonated poly(phenylene sulfide) have been developed as alternatives to Nafion for fuel cell applications [4–5].

Recently, the synthesis of sulfonated poly(aryl ether sulfone) copolymers by direct copolymerization of bisphenol A, precursor-activated aromatic halide monomers and disulfonated-activated aromatic halide monomers for fuel cell membrane applications has been performed[6–8]. Poly(aryl ether sulfone)s attract a considerable interest, since these materials are well known for their excellent mechanical and thermal properties as well as their stability under acidic conditions and their resistance to oxidation[6,7].

The aim of this study was to prepare new polymer electrolyte membranes (PEM) for direct methanol fuel cells (DMFC). Common requirements for a polyelectrolyte membrane in DMFC applications include high ionic conductivity, high chemical and mechanical durability, low methanol permeability at operation conditions and low cost. In order to satisfy these requirements poly(aryl ether sulfones) and their sulfonated derivatives were prepared. The sulfonate groups were introduced to the polymer structure to increase the proton conductivity of the resulting polymers. However, complete sulfonation of polymers also increases the methanol permeability, therefore to decrease the methanol permeability, partially sulfonated poly(aryl ether sulfone)s were prepared via polycondensation of sulfonated and non-sulfonated monomers that are hydroquinone 2- potassium sulfonate, bisphenol A and 4- fluorophenyl sulfone. The resulting polymers were then functionalized with glycidyl methacrylate (GMA) to polymerize them via radical polymerization in order to produce cross-linked network structures to improve mechanical properties and decrease methanol permeability. The synthesized PESSGMA polymer was then cross-linked and copolymerized with comonomers, vinyl phosphonic acid (VPA) and styrene (STY) via radical polymerization. The effects of cross-linking and the different monomer types on membrane properties such as thermal stability, thermomechanical properties, water uptake, proton conductivity and methanol permeability were evaluated. Five types of polymer membranes were prepared namely the partially sulfonated polyarylether sulfone (PESS), sulfonated polyarylether sulfone glycidyl methacrylate (PESSGMA), and the copolymers of PESSGMA with styrene and vinyl phosphonic acid; PESSGMA/STY, PESSGMA/VPA and PESSGMA/STY/VPA via solution casting method using dimethyl sulfoxide as the solvent. For the PESSGMA polymer and copolymers the cross-linking was carried out in the presence of a radical initiator using a high temperature cure cycle. The comonomer content was fixed at 30wt% for the PESSGMA/STY and PESSGMA/STY/VPA polymers. The PESSGMA/VPA polymers were prepared at (70/30,60/40,50/50) weight compositions to see the effect of VPA content on the proton conductivity of the membranes.

In addition to these studies, the potassium salt form of the PESSGMA polymer; PESSGMA(K) was also prepared and self-polymerized and copolymerized with styrene and vinyl phosphonic acid in an effort to examine and prevent the possible inhibiting effect of sulfonic acid groups on radical polymerization. However as the PESSGMA(K)

synthesis led to an undesirable product, this route was not explored further for preparation of membranes.

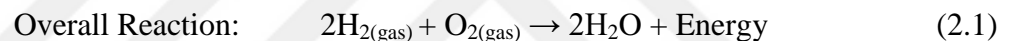
The structural characterization of the PESS and PESSGMA polymers was carried out using FT-IR and $^1\text{H-NMR}$ spectroscopic techniques. The molecular weights of the PESS and PESSGMA polymers were determined via Gel Permeation Chromatography (GPC). The thermal transitions, thermal stability and thermomechanical properties of the prepared membranes were analyzed via Differential Scanning Calorimetry (DSC), Thermal Gravimetric Analysis (TGA) and Dynamic Mechanical Analysis (DMA), methods respectively. The ion exchange capacity (IEC) of the polymers were determined using a titration method and the proton conductivity of the polymer membranes under fully hydrated conditions were evaluated by an AC impedance spectrometer over the frequency range of 100mHz - 1MHz. Swelling of the polymer membranes in different solvents and the water uptake of the membranes both at room temperature and at 80°C were also evaluated. Finally, measurement of methanol permeability of the membranes was carried out by using a diffusion cell which consists of two compartments separated by a membrane.

This thesis starts with a theoretical background section that includes general information about fuel cells, polymers as well as literature on different types of polymer membranes used for DMFC applications. After this section, the following section includes the chemicals used for the preparation of the polymer membranes and methods used in the characterization of the synthesized polymers and prepared membranes. Then, in the experimental section, the experimental procedures for the synthesis of the polymers and preparation of the membranes as well as the procedures for the characterization methods are explained in detail. The results obtained from the experimental data and related discussions are presented in the following three chapters. Finally, the last chapter consists of the conclusions based on the results and discussion presented in the previous chapters as well as some suggestions for the future work of this study.

2. THEORETICAL BACKGROUND

2.1. FUEL CELLS

A fuel cell is an equipment that produces electricity by a chemical reaction. All fuel cells have two electrodes, one positive and one negative which are called respectively, the cathode and anode. The reactions that generate electricity take place at the electrodes. Every fuel cell has also an electrolyte that carries electrically charged particles from one electrode to another and a catalyst that speeds the reactions at the electrodes. The basic fuel in the fuel cell is hydrogen however fuel cells also require oxygen. One great attraction of fuel cells is; they produce electricity with a low pollution that much of the oxygen and hydrogen used in producing electricity finally combine to form a harmless byproduct which is water.



The aim of a fuel cell is to generate an electrical current that can be directed through outside of the cell to do work, such as enlightening a light bulb or powering an electric motor. Because of the way electricity acts, this current returns to the fuel cell to complete an electrical circuit. The chemical reactions that generate this current are the key to how the fuel cell performs.

The fuel cells have several kinds that each works a bit differently. But in general, hydrogen atoms enter at the anode part of fuel cell where a chemical reaction takes them of their electrons. This way, the hydrogen atoms are ionized and carry a positive electrical charge. The negatively charged electrons supply the current through the wires to do work. If alternating current (AC) is required, the DC output of the fuel cell should be removed through a conversion equipment called an inverter [9].

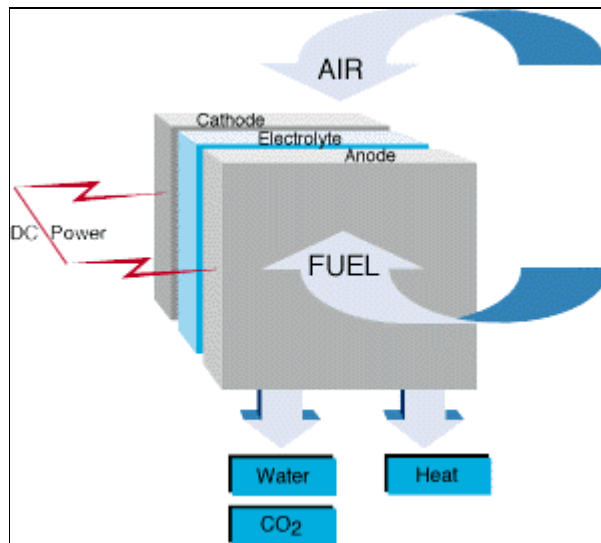


Figure 2.1. Schematic of a fuel cell [10].

Oxygen enters at the cathode part of the fuel cell and in many cell types, as the one shown in Figure 2.1, it there combines with hydrogen ions that have traveled through the electrolyte from the anode and electrons returning from the electrical circuit. For other cell types, the oxygen collects electrons and then goes through the electrolyte to the anode where it combines with hydrogen ions.

The electrolyte acts a key role. It must allow only the suitable ions to cross between the anode and cathode. If any free electrons or substances could pass through the electrolyte, they would disturb the chemical reaction.

If the oxygen and hydrogen combine at cathode or anode, together they form water, which discharges from the cell. As far as a fuel cell is supplied with oxygen and hydrogen, it will produce electricity [9].

All the better, as fuel cells produce electricity chemically instead of combustion, they do not obey the thermodynamic laws which limit a traditional power plant. So, fuel cells are more effective to take out energy from a fuel. Waste heat exists from some cells can also be utilized and improve system efficiency still further.

There are generally five fuel cell systems which contain their different electrochemical reactions as well as operation requirements. The different fuel cells are actually classified

according to electrolyte used. These are; molten carbonate fuel cells (MCFC), phosphoric acid fuel cells (PAFC), alkaline fuel cells (AFC), solid oxide fuel cells (SOFC) and proton exchange membrane fuel cells (PEMFC).

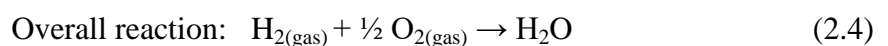
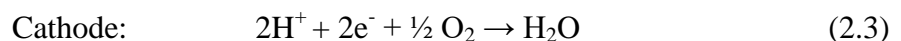
Proton Exchange Membrane (PEM) fuel cells perform with a thin and permeable polymer electrolyte which has an operating temperature about 80°C (about 175°F) and efficiency about 40 to 50 percent. Cell outputs usually range from 50 to 250 kW. The flexible, solid electrolyte must not crack or leak and these cells work at a low temperature to make them appropriate for cars and homes. But their fuels should be purified and a platinum catalyst which is applied on both sides of the membrane increase costs [9].

2.1.1.H₂/O₂ Fuel Cell

The basic concept included in Proton Exchange Membrane Fuel Cell (PEMFC) for electric power production is the electrochemical reaction between oxygen and hydrogen in the presence of catalyst that generates electrical energy in the form of a DC current. The byproducts are water and heat. Hydrogen is mostly used as either pure hydrogen or hydrogen rich fuel in PEMFC because, it has one of the highest catalytic chemical reactivities. The fuel is provided on the anode side. In the fuel cells, the anode reaction is direct oxidation of hydrogen as;



The electrons produced at the anode are run through external load to the cathode. Protons (H⁺) are transferred through the proton exchange membrane to the cathode part. The electrons and protons that arrive at the cathode react with oxygen from air. The cathode reaction is oxygen reduction from air as;



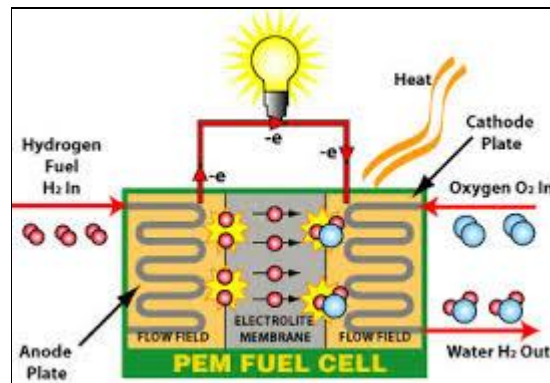


Figure 2.2. Schematic of a proton exchange membrane fuel cell [12].

The schematic diagram of a simplified proton exchange membrane fuel cell is illustrated in Figure 2.2. The proton exchange membrane fuel cell (PEMFC) is a low temperature fuel cell working at around 80°C that has a polymer membrane (eg. Nafion membrane) which when hydrated with water becomes the electrolyte for the proton transfer from anode to cathode. The gas diffusion layer of cathode and anode are thin, porous carbon papers (graphite sheets) or cloth. Pt or Pt/Ru catalyst layer with about $10\text{-}100\ \mu\text{m}$ is placed on each side of the membrane. PEMFCs exhibit fast start up - load response and high power density. Extensive gas cleaning for hydrogen generated from hydrocarbon reforming is essential since carbon monoxide is a strong poison for PEM. These fuel cells are mainly utilized for mobile applications [11].

2.1.2. Direct Methanol Fuel Cell (DMFC)

Principally, the direct methanol fuel cell is a proton exchange membrane fuel cell that is fed with an aqueous solution of methanol. Polymer membrane which conducts protons from anode to cathode and blocks the diffusion of other compounds, is placed between the two catalytic electrodes where the methanol oxidation (anode) and the oxygen reduction (cathode) occur. A membrane electrode assembly (MEA) is known as the combination of electrodes and membranes. Each electrode is made of a catalytic layer and a gas diffusion layer as shown in Figure 2.3. Nafion which is produced by addition of sulfonic acid groups into the bulk polymer matrix of Teflon, is the state of the art in membranes. The sulfonic acid groups act as proton exchange sites and have strong ionic properties. Aqueous methanol is fed at the anode side and diffuses through the diffusion layer to the catalytic

layer where it is electrochemically oxidized into carbon dioxide, protons and electrons. Protons which are formed during this reaction pass through the Nafion membrane to the cathode catalytic layer. They join to oxygen reduction to produce water at cathode side. Oxygen can be pure but also may come from air. Graphite bipolar plates which are the two poles of the cell, collect the electrons[13].

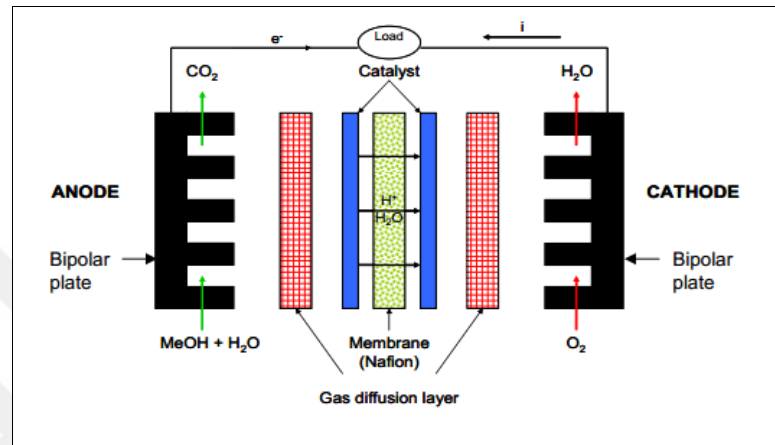
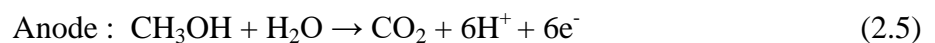
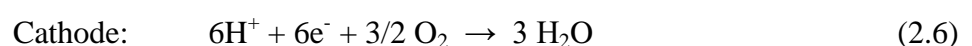


Figure 2.3. DMFC principle scheme [13].

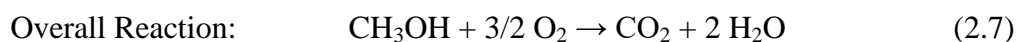
On the anode part, methanol solution is provided through the anode flow field to the anode CL where part of methanol is oxidized to create protons, electrons, and CO₂ while the remainder is transported directly to the cathode through membrane; the diffusion of methanol from anode to the cathode through the membrane is called as methanol crossover which generates a mixed potential and decreases the cathode potential. The electrochemical reaction on the anode part is;



On the cathode part, oxygen/air is provided through the cathode flow field and transferred through cathode DL to the cathode CL where main part of oxygen reacts with the protons which are conducted through the membrane from the anode and the electrons which come from the external circuit to produce water while the remaining part of oxygen reacts electrochemically with the permeated methanol. The electrochemical reaction on the cathode part is;



Finally, the overall reaction in the DMFC is:



The liquid water generated on the cathode and the gas generated on the anode are then vented out of the cell [14].

The ease of storage of the methanol fuel is an important advantage for DMFCs. They also have an advantage of higher energy density per unit volume among the different types of fuel cells. But, at temperatures below 100°C, the slow oxidation kinetics of methanol can not allow the development of DMFC units with efficiencies as high as proton exchange fuel cell (PEFC). Hence, an invention would be needed to increase the working temperature and develop the performance of the methanol fed devices.

Unfortunately, perfluorosulphonic membranes that are currently used do not keep extended operation at temperatures higher than 130°C due to the fact that dehydration phenomena happens at these temperatures with lower conductivity and performance. Then, in order to support the acceptability of DMFC technology worldwide, the development of high temperature resistant proton exchange electrolytes is an ambitious goal to be maintained [15].

2.1.2.1. Requirements for DMFC Membranes

Although requirements for DMFC membranes may change with the application area, common necessities for an ideal polymer electrolyte membrane in DMFC applications include operation at high temperature, low methanol crossover (MCO) ($<10^{-6} \text{ mol min}^{-1} \text{ cm}^{-1}$) or low methanol diffusion coefficient in the membrane ($<5.6 \times 10^{-6} \text{ cm}^2 \text{ s}^{-1}$ at $T = 25^\circ\text{C}$), high ionic conductivity (e.g. $>80 \text{ mS cm}^{-1}$) [16], high chemical and mechanical durability especially at $T > 80^\circ\text{C}$ (for increased CO tolerance), low ruthenium crossover (in the case that the anode catalyst contains Ru) and low cost (e.g. $<\$10 \text{ kW}^{-1}$ based on a PEMFC) [17].

2.1.2.2. Disadvantages of Nafion® Membranes

Nafion, which is the most important commercial membrane used in PEMFC applications, is derived from a polyethylene polymer. In Nafion, the hydrogen atoms of polyethylene are displaced by fluorine atoms. The monomer is termed as tetrafluoroethylene. The polymer synthesized from this monomer is called polytetrafluoroethylene (PTFE) or Teflon. PTFE is stable to chemical attack and has a strongly hydrophobic feature that is used in fuel cell electrodes to remove the water from the electrode and therefore, disallow flooding. The Nafion membrane which is formed via sulfonation of PTFE, is highly mechanically and chemically resistant, acidic and can absorb large amounts of water. Therefore, Nafion exhibits high proton conductivity, chemical and mechanical durability. However, it also shows some disadvantages like, a high level of fuel (methanol) crossover and the fuel cell operation must be limited to 80°C because of its inability to keep water at higher temperatures. The conductivity of Nafion increases as the relative humidity increases but does not rise up significantly with increasing temperature. In addition to these limitations, Nafion membranes have a very high cost. Hence, in order to commercialize PEMFCs there is a requirement to develop new proton conducting polymers [18].

2.2. POLYMERS

Polymers constitute a very important class of materials that are all around us in everyday use; in resins, in plastics, in rubbers and in adhesives. The word polymer comes from Greek words, *poly* defining many and *mers* defining parts. Polymers are also called macromolecules which are giant molecules of high molecular weight formed by connecting together of a large number of small molecules that are called *monomers*. The reaction in which the monomers link together to form a polymer is termed as *polymerization*. It is a chemical reaction in which two or more items join together with or without evolution of anything like heat, water, or any other solvents to create a molecule with a high molecular weight. The starting material is called monomer and the product is called polymer [19].

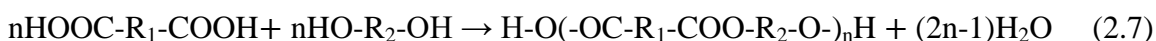
2.2.1. Polymer Classification Based on Polymerization Mechanism

As defined in the previous section, the connecting together of a large number of small molecules called as monomers with each other to create a polymer molecule or macromolecule through a chemical reaction is called as polymerization. It can also be described as the fundamental process that the low molecular weight compounds are changed into high molecular weight compounds. The polymerization can be classified into step growth and chain growth polymerization by current terminology [19].

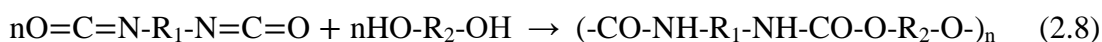
2.2.1.1. Step Reaction Polymerization

Step-growth polymerization usually involves a chemical reaction in which polymer is formed together with a lower molecular weight by-product. The by-product that is released is termed as condensate. These polymerization reactions can occur between two similar or different monomers [19].

Step-growth polymerization reactions in which small molecules are released as the byproduct are called as polycondensations. These polymerizations include the reaction between an organic acid (such as an acid chloride or a carboxylic acid) and an organic base (such as an amine or an alcohol) and in which small molecules (like water) are released. The formation of polyesters is an example of such a polycondensation reaction:



In some some, step growth polymerization reactions, the monomers react without the elimination of other small molecules, such polymerization reactions are called polyadditions. The formation of polyurethanes is an example of such a polyaddition reaction;



2.2.1.2. Chain Reaction Polymerization

In chain-growth polymerization, two or more molecules of monomers link together to form a polymer. There is no elimination of any molecule in this type of polymerization reaction.

It is a chain reaction without the formation of any by-products. The chain-growth polymerization reaction takes place by linking the monomer molecules together by a chain reaction to obtain a polymer whose molecular weight is exactly an integral multiple of that of the monomer just as in the case of polyethylene produced via polymerization of ethylene. This type of polymerization reaction is usually initiated by a catalyst, heat or light for breaking the double bond of the monomer and forming the reactive sites [19].

Chain-growth polymerizations progress in a completely different mechanism from step-growth polymerizations. The most important difference is that, high molecular weight polymer is created immediately in a chain-growth polymerization. A radical, cationic or anionic reactive center once formed, attaches many monomer units during a chain reaction and grows quickly to a large size. As the number of high-polymer molecules increases, the monomer concentration decreases during the reaction. At any time during the reaction, the reaction mixture consists of only monomer, high polymer and growing chains. The molecular weight of the polymer does not change significantly during polymerization reaction even though the overall percent conversion of monomer to polymer rises with reaction time [20].

In step-growth polymerization, the conditions are quite different. While only the propagating species and monomer can react with each other in chain-growth polymerization, any two molecular species in the system can react in step-growth polymerization. Thus in step-growth polymerization reactions, monomer disappears very fast as one progresses slowly to create dimer, trimer, tetramer and so on. Extended reaction times are required for both high molecular weights and high percent conversion in step reaction polymerizations [20].

- ***Free-Radical Chain Polymerization***

Many organic reactions occur through the formation of intermediates that possess unpaired electrons and an odd number of electrons. These intermediates are called free radicals. Free radicals can be created in a number of ways such as the application of heat or light. The stability of radicals changes significantly depending on their structure. Primary radicals for example, are more reactive and less stable than secondary radicals which also have less stability than tertiary ones. The free radical chain polymerization proceeds through the following steps:

- Initiation

When free radicals are produced through the application of heat or light to an initiator molecule, in the existence of a vinyl monomer, the radical formed joins to the double bond of the monomer with the formation of another radical [21].

- Propagation

The chain radical generated in the initiation step can add sequential monomers to propagate the chain [21].

- Termination

In addition to propagation reactions taking place, radicals have a strong tendency to react in pairs to form a paired-electron covalent bond with loss of activity leading to termination reactions. The termination step can occur in two ways: via combination (coupling) where two radical species combine to form a covalent bond and disproportionation where a growing radical abstracts a hydrogen radical from another growing radical terminating itself causing the formation of a new terminal double bond in the other molecule [21]. Figure 2.4 represents the initiation, propagation and termination steps of free radical chain polymerization.

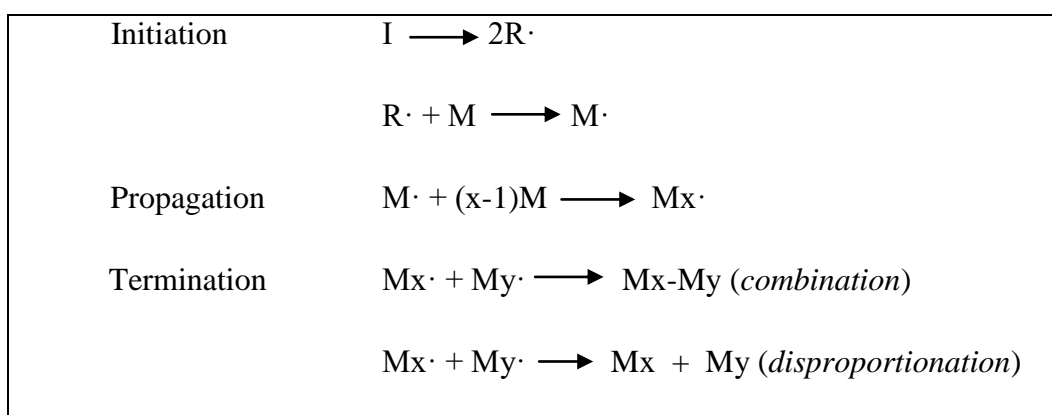


Figure 2.4. Free-radical chain polymerization [22].

• Ionic Chain Polymerization

Nearly all monomers possessing a carbon-carbon double bond can participate in radical polymerization whereas ionic polymerizations can occur with only specific types of monomers. Cationic polymerization is essentially restricted to those monomers which have

electron releasing substituents such as vinyl, phenyl and alkoxy. Anionic polymerization on the other hand can occur with monomers having electron-withdrawing groups like vinyl, phenyl, nitrile and carboxyl. Ionic polymerizations are highly selective because of the severe necessity for stabilization of cationic and anionic propagating species. The commercial usage of anionic and cationic polymerizations is quite limited due to this high selectivity of ionic polymerizations in comparison to radical polymerization [20].

Anionic and cationic polymerizations have some similar properties. Both of these polymerizations depend on the generation and propagation of ionic species, a negative one in one case and a positive one in the other. The generation of ions with enough long life times for propagation generally needs stabilization of propagating centers by dissolution in an appropriate solvent to yield high molecular weight products. Moderate or relatively low temperatures are also required to prevent termination, transfer and other chain breaking reactions that deactivate the propagating centers [20].

2.2.2. Polymer Classification Based on Monomer Composition

2.2.2.1. Homopolymers

Homopolymer is generally defined as a polymer derived from one type of a monomer. But, the word homopolymer is used more widely to define polymers whose structure can be shown by multiple iteration of a single type of repeat unit that can include one or more types of monomer unit. The latter is occasionally called as a structural unit.

The chemical structure of a polymer is often shown by the repeat unit symbol or structure in brackets. Therefore, the hypothetical homopolymer -----A-A-A-A-A-A-A----- is shown by $-[A]_n-$ where n is the number of repeating units attached together to create the macromolecule [23].

2.2.2.2. Copolymers

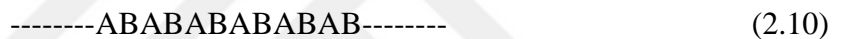
The polymer that consists of two or more different monomers is termed as a *copolymer*. Different arrangements of the repeating units throughout the polymer chains are feasible depending on the polymerization process and relative fractions of these repeating unit

types. On the copolymer chain, the repeating units may be arranged to different degrees of order along the backbone. In some cases, it is possible to have branches of one monomer type on another monomer type of backbone. There are basically four types of copolymer systems; [24]

- **Random copolymer** — The repeating units are randomly positioned on the polymer chain. If the repeating units are illustrated as A and B, the random copolymer structure may be represented as shown below:



- **Alternating copolymer** — The polymer chain consists of an ordered (alternating) arrangement of the two repeating units.



- **Block copolymer** — Long sequences (blocks) of each repeating unit are chemically bound together along the polymer chain:



- **Graft copolymer** — Sequences of one monomer (repeating unit) are “grafted” onto a backbone of another monomer type:[24]

2.2.3.1. Linear Polymers

The polymers in which the repeat units are linked end to end in single chains are linear polymers. These long chains are quite flexible and they may be visualized as a mass of spaghetti as depicted in Figure 2.5. Linear polymers may have extensive hydrogen and van der Waals bonding between the chains. Some examples of polymers that have linear structures are polyethylene, nylon, fluorocarbons, poly(methyl methacrylate), polystyrene and poly(vinyl chloride) [25].

2.2.3.2. Branched Polymers

Branched polymers typically have branches at irregular intervals through the polymer chain. These branches prevent the packing of the polymer molecules in a regular array resulting in less dense and less crystalline structures. The type and amount of branching may also alter physical properties such as elasticity and viscosity. Branches usually prevent chains from being close to each other and therefore decrease the effectiveness of intermolecular forces [26]. The type and amount of branching effects also physical properties such as elasticity and viscosity. Branches usually prevent chains to become close each other for intermolecular forces to work effectively [26].

The branches which are actually a part of the main chain molecule may result from side reactions that take place during the synthesis of the polymer. The chain packing efficiency is decreased with the generation of side branches that in turn results in a decrease of the polymer density. Polymers which form linear structures can also be branched depending on the synthesis reaction and conditions [25].

2.2.3.3. Crosslinked Polymers

Adjacent linear chains are linked to each other at different positions by covalent bonds in crosslinked polymers, as shown in Figure 2.5. The process of crosslinking takes place during the synthesis or by a nonreversible chemical reaction. Usually, the crosslinking reaction is achieved by additive molecules or atoms which are covalently bonded to the

chains. Most of the elastic rubber materials are cross-linked; this cross-linking process in rubbers is called "vulcanization" [26].

For example, the vulcanization of rubber occurs by the introduction of short chains of sulfur atoms which connect the polymer chains by covalent bonds. Cross-linking also rises the viscosity of polymers. The flow of polymers is achieved by the movement of chains through each other but cross-linking prevents this.

Elastomers are elastic polymers generated by limited cross-linking. When the number of cross-links rises, the polymer gets more rigid and cannot stretch so much; the polymer will be less elastic and less viscous and may also become brittle. The decision to categorize a polymer as cross-linked is based on the extent to which the side-chains or main chains on the polymer backbone connect covalently to adjacent polymer chains. This categorization is not always easy however, since stronger intermolecular forces might imitate cross-linking. Polymer chains might have a particular geometry or include chemical groups which enhance the intermolecular forces between chains. Although these intermolecular forces do not represent the covalent cross-linking, they effect the physical properties like viscosity and elasticity just as cross-linking does. The simple way to differentiate between these categories is to work on the effect of different solvents on the polymer. Cross-linked polymers are generally insoluble in solvents since the polymer chains are connected together by strong covalent bonds. Other polymers are generally soluble in one or more solvents since it is possible to move apart the polymer chains that are not covalently bonded [26].

2.2.4. Polymer Classification Based on Reaction to Temperature

The word plastic is derived from the Greek word Plastikos that has a meaning of "able to be shaped and molded". Plastics can be categorized into two main groups based on their response to temperature changes and chemical structure as thermosetting plastics and thermoplastics [28].

2.2.4.1. Thermoplastics

If a material softens when heated above its glass transition temperature or melting temperature, and it becomes hard after being cooled, then it is classified as a thermoplastic. A thermoplastic can be melted by heating and solidified by cooling reversibly in a restricted number of cycles without influencing its mechanical properties. As the number of recycling processes of thermoplastics increases, color degradation, changes in appearance and properties may occur. Thermoplastics are liquids in the molten state, and partially crystalline or glassy in the mushy state. The molecules are linked end to end in a series of long chains however these chains are not connected to each other via covalent bonds. All crystalline arrangement and order disappears and the long chains become randomly oriented above the melting temperature.

The polymer chains of a thermoplastic maybe linear or branched, the latter structure is illustrated in Figure 2.6. The molecular structure has an effect on both chemical resistance and resistance towards environmental effects such as UV radiation. The molecular structure also determines other properties such as crystallinity, the material's being opaque or optically transparent. The key properties of the thermoplastics are high toughness and strength, better hardness, durability, chemical resistance, transparency, self lubrication and water proofing [28].

There are several types of thermoplastics such as, acrylics, acetals, polyamides, fluorocarbons, cellulosics, polypropylenes (PP), polyethylene (PE), polycarbonates, polyetheretherketone, polyvinyl chloride (PVC), polystyrenes, polyphenylene sulphide (PPS), acrylonitrile-butadiene-styrene (ABS) and liquid crystal polymers (LCP) [28].

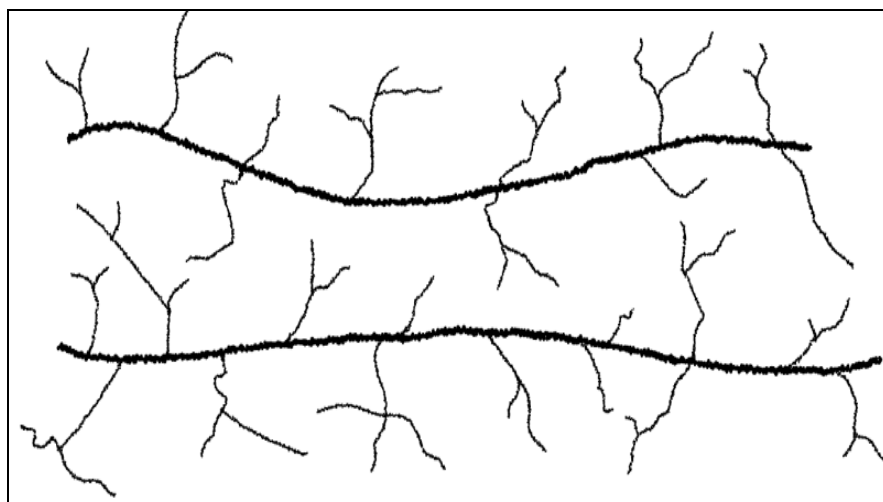


Figure 2.6. The branched chain structure of thermoplastics [28].

2.2.4.2. Thermosets

A material is classified as a thermoset if it transforms into a permanently hard and rigid solid when heated as a consequence of a chemical reaction. This solidification process is called curing. The transformation of a thermosetting material from the liquid state to the solid state is an irreversible process which means that thermosets can not be recycled. Further heating after solidification of thermosets will result only in chemical decomposition. In most curing processes, small molecules are chemically linked together, combining polymer chains via covalent bonds, forming complex inter-connected network structures as illustrated in Figure 2.7. The slippage of individual chains is inhibited by this cross-linking. Thus, in contrast to thermoplastics, the mechanical properties after solidification (e.g. hardness, compressive strength and tensile strength) do not vary significantly with temperature. Therefore, thermosets are usually stronger than thermoplastics [28].

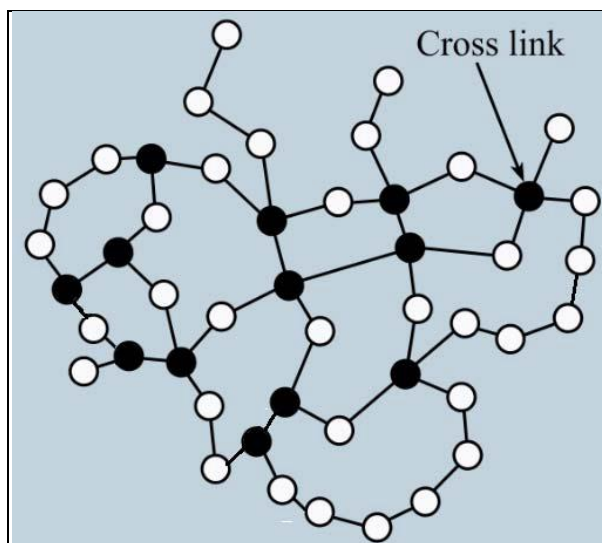


Figure 2.7. Molecular structure of thermosets [28].

The connection of thermosets by thermal processes such as gas welding, laser welding and ultrasonic welding is not possible, however adhesive bonding and mechanical fastening maybe used for applications that require low mechanical strength. Some of the common thermosets are epoxy, polyester, vinyl ester, alkyds, bakelite, allylics, phenolic (PF), polyurethane (PUR) and silicone.

2.2.5. Thermal transitions in Polymers

A thermal transition or a phase change for polymers results in remarkable changes in material behavior. The phase change happens as a result of either a chemical curing reaction or a reduction in material temperature. A thermoplastic polymer will harden if its temperature is decreased to below either glass transition temperature in liquid crystalline polymers or the melting temperature for semi-crystalline polymers. A thermoplastic can soften again when its temperature is increased above the solidification temperature, however in thermosets the solidification results in cross-linking of molecules. Crosslinking is an irreversible process that results in a network that limits the free movement of the polymer chains without dependence on the material temperature [29].

2.2.5.1. Crystallization

The crystallization of a molten polymer happens via nucleation and growth processes. For polymers, with cooling to temperatures below the melting temperature, nuclei develop where the small regions of the random and tangled molecules get ordered and aligned as chain-folded layers. At temperatures above the melting temperature, these nuclei are not stable because of the thermal atomic vibrations which tend to break down the ordered molecular arrangements. Following the nucleation during the crystallization growth process nuclei expand by the continued ordering and sequencing of additional molecular chain moieties; this means, the chain-folded layers get an increase in lateral dimensions or there is an increase in spherulite radius for spherulitic structures[30].

The polymer chains exhibit a significant mobility above the glass transition. They squirm and wiggle, and never stay in one position for a long time. When they come to the right temperature, they will have won sufficient energy to drive into very ordered arrangements that we call as crystals. When polymers are locked in these crystalline arrangements, they emit heat to the system, therefore the process is exothermic. Actually, the heat flow falls from the big dip in the plot of (q/t) vs. temperature at the crystallization temperature, as represented in Figure 2.8 [33].

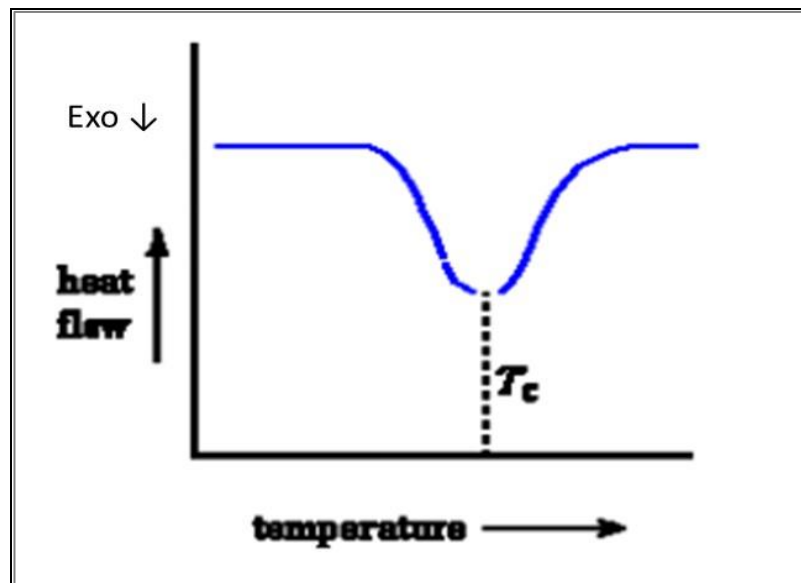


Figure 2.8. Typical heat flow vs. temperature plot of a crystallization transition in a polymer [33].

From the plot in Figure 2.8 one can:

- have confirmation of the existence of the crystallization;
- detect the crystallization temperature (T_c) of the polymer as the lowest point of the dip;
- get information of the latent energy of crystallization for the polymer by using the area of the dip.

2.2.5.2. Melting

Melting is a significant step for any polymer processes. The material must be first molten or softened before to be shape into its final form.

Melting is a significant step in processing of polymers. The material must be first molten or softened before being shaped into its final form. The melting of a polymer crystal represents the transformation of a solid material that have an ordered structure of arranged molecular chains to a viscous liquid form in which the structure becomes highly random. This situation happens heating upon melting temperature, T_m . For the crystalline polymer, there is a discontinuity in the specific volume vs temperature plot at the melting temperature T_m [31].

The polymer chains are free to move around at the melting temperature (T_m), therefore they do not exhibit an ordered arrangement. Polymers absorb heat during the melting phenomena, hence melting is an endothermic phase transition. Typical heat flow (q/t) vs. temperature plot of a melting transition in a polymer is depicted in Figure 2.9. Melting is known as a first order transition because when the polymer comes to the melting temperature, its temperature does not increase till all the crystals completely melt[33].

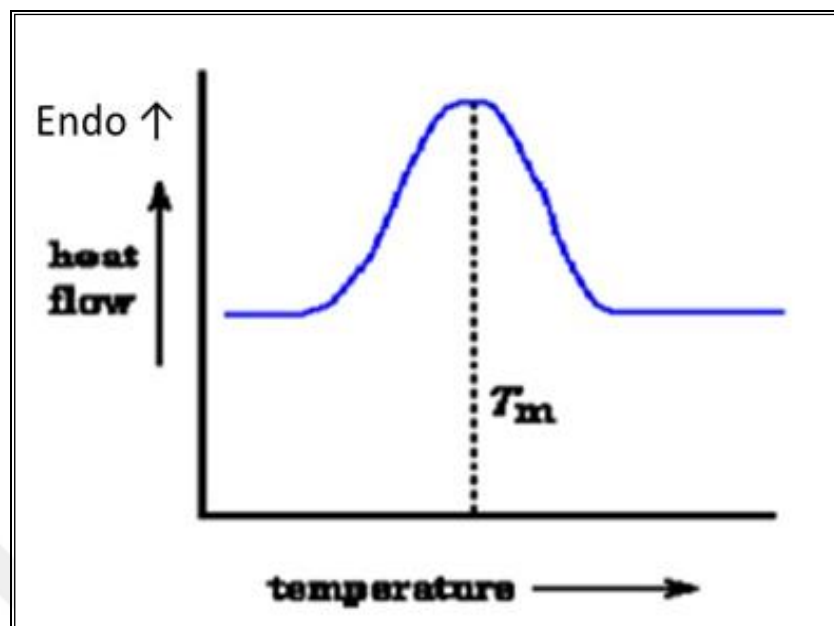


Figure 2.9. Typical heat flow vs. temperature plot of a melting transition in a polymer [33].

2.2.5.3. Glass Transition

Glass transition happens in semi-crystalline and amorphous polymers due to a decrement in movement of large segments of molecular chains with reducing temperature. During cooling, the glass transition occurs as the gradual transformation from liquid to a rubbery state and then to a rigid solid. The glass transition temperature, T_g is defined as the temperature at which the polymer makes the transition from rubbery to rigid state. Surely, this series of events happen inversely when a rigid glass that is below its T_g is heated to a temperature above its T_g [32].

The solid amorphous polymer transforms from rigid to a rubbery state by heating through the glass transition temperature. Appropriately, the molecules which are nearly frozen in position below T_g start to experience translational and rotational motions above T_g . Therefore, the value of the glass transition temperature will rely on molecular characteristics which effect chain stiffness. The majority of these factors and their effects are same as for melting temperature. As chain flexibility is diminished (eg. with bulky side groups, polar side atoms or groups of atoms, double-chain bonds and aromatic chain groups) T_g is increased[32].

Increasing the molecular weight also leads to an increase in glass transition temperature. A low density of branching will act to lower the T_g whereas a large amount of branching decreases chain mobility and rises the glass transition temperature. For cross-linked polymers increasing cross-link density elevates the T_g [32].

A typical heat flow vs. temperature plot of a glass transition for a polymer is shown in Figure 2.10. For both of two regimes before and after the T_g , polymers have distinct heat capacities (C_p): generally polymers have a lower C_p below T_g and a greater C_p above T_g . Owing to this distinction in C_p , the DSC is a precious method to detect the T_g . As can also be seen from Figure 2.10, the transition does not happen suddenly but generally occurs over a temperature range. The T_g therefore is determined as the temperature in the middle of the step change in the heat flow curve as depicted in the figure [33].

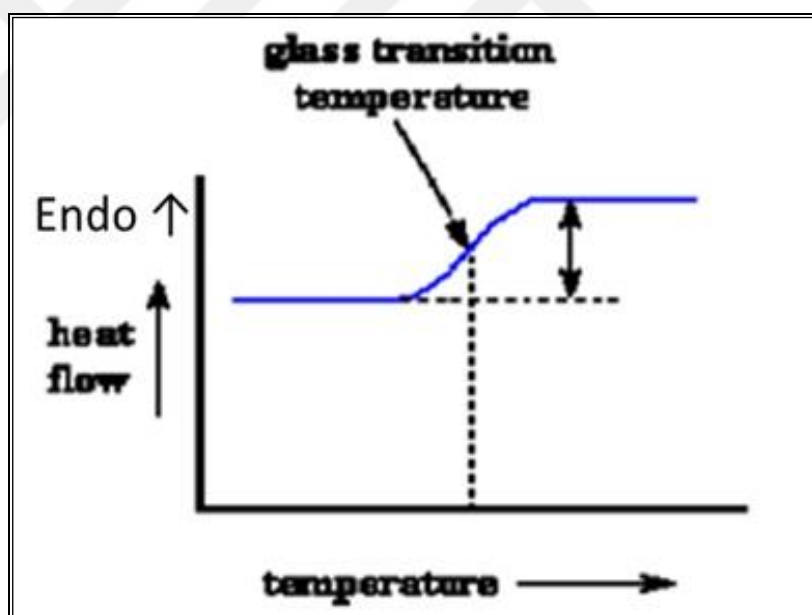


Figure 2.10. Typical heat flow vs. temperature plot of a glass transition in a polymer [33].

2.2.6. Mechanical Properties of Polymers

A polymer can behave as a glassy, brittle solid or an elastic rubber, or a viscous liquid, contingent on both the time scale and the temperature of measurement. Therefore, to determine the mechanical properties of polymers, tests can be performed by subjecting

them to some type of mechanical stress either continuously or periodically at different rates. Tensile strength, elastic modulus, flexural and compressive strength, creep, fatigue and impact resistance and hardness are some of the important features of polymers in considering their applications as engineering materials.

Toughness of a polymer can be described as the capability to absorb mechanical energy without breaking. Tensile strength represents the maximum amount of tensile load per unit area that the material can resist, while the tensile elongation shows a measure of extension in length as a result of an applied tensile load, given as a percent value of the original length. Elongation at break therefore represents the maximum elongation the polymer can endure[34].

Like for most materials, the simple tensile stress-strain curve can give significant information about the mechanical properties of a particular polymer. This curve is generally formed by continuously determining the force exerted as the sample is extended at a constant rate of extension to the point it breaks. A representative tensile stress-strain curve is shown in Figure 2.11, any polymer's stress strain behavior can be described by certain portions of this curve. This tensile stress-strain curve can be used to define several important properties of the material. The modulus of elasticity (*Young's modulus*) which is a direct measure of the stiffness of the material is given by the initial slope of the curve. As represented in Figure 2.11, the curve also points out the elongation at break and yield stress and strength. The work necessary to fracture the polymeric material, given by the area under the curve is an approximate indication of the toughness of the polymer. The stress that corresponds to the knee in the curve (*the yield point*) represents the resistance to permanent deformation and is therefore a measure of the strength of the material. The ultimate strength which is a direct measure of the force necessary for complete cracking of the material corresponds to the stress at the breaking point.

An amorphous polymer far below its glass transition temperature which is hard and brittle will exhibit an initial slope corresponding to a quite high modulus, a low elongation at break, modest strength and a small area under the stress-strain curve as depicted in Figure 2.12. Poly (methyl methacrylate), polystyrene and many phenol-formaldehyde resins are some examples of polymeric materials showing hard, brittle behaviour at room temperature or below room temperature [34].

Strong and hard polymers exhibit high strength, high modulus of elasticity and elongation at break of nearly 5 percent. The form of the curve usually proposes that the material has broken where a yield point can occur. Some polystyrene polyblends and rigid poly(vinyl chloride) formulations exhibit this type of curve. Tough and hard behaviour is exhibited by polymers like nylons, cellulose nitrate and cellulose acetate; they have high modulus and high yield points, large elongation at break values and high strength. Most polymers in this group exhibit 'necking' or 'cold-drawing' during an applied stretching process. Cold-drawing which is used to develop strength has great importance in synthetic fiber technology. Soft and tough polymeric materials show moderate strength at break, low modulus and yield values and quite high elongations that can change from 20 to 100 percent. Rubbers (elastomers) and plasticized PVCs show this type of stress-strain behavior. Figure 2.12 shows the typical stress-strain curves of the various types of polymeric materials described.

The creep and stress relaxation which are the two mechanical performances of polymeric materials are related to one another. In creep, the polymer exhibits elongation in response to a constant applied stress, whereas in stress relaxation, the polymer responds with a decrease in stress when an instantaneously induced strain is applied and held at constant. The change in stress or strain is followed as a function of time. Repeated deformation of a sample at a given strain often causes the failure of the sample at a lower stress than would be observed for a single straining. This property is termed as fatigue. Fatigue testing can be performed by applying the polymeric material alternating tensile and compressive stress. Increase in rigidity generally causes a decrease in fatigue resistance. Impact strength which is another important mechanical property for certain engineering applications, is a measure of resistance to breaking or failure when an impact with high velocity is applied [34].

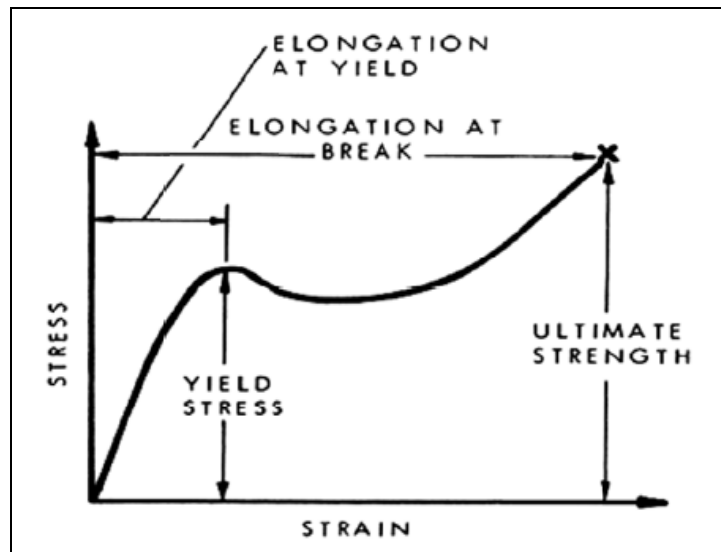


Figure 2.11. A typical tensile stress-strain curve for a polymeric material that exhibits plastic deformation [34].

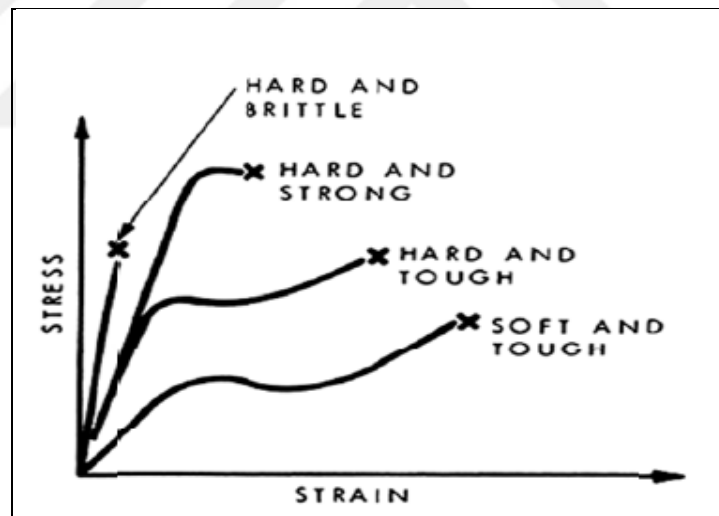


Figure 2.12. Representative tensile stress-strain curves of different types of polymeric material [34].

2.3. POLYMER ELECTROLYTE MEMBRANES FOR DIRECT METHANOL FUEL CELLS (DMFC's)

Membrane is the key component of both H_2/O_2 fuel cells and direct methanol fuel cells (DMFCs). There are basically three roles of a polymeric membrane used in a DMFC, these

are; separation of the reactant gases, charge carrier for protons and electronic insulator to hinder the movement of electrons towards the membrane.

Usually the materials utilized in the synthesis of polymer electrolyte membranes can be categorized into three major groups: partially or completely perfluorinated ionomers, non-fluorinated aliphatic or aromatic hydrocarbons and acid–base complexes.

2.3.1. Perfluorinated Ionomeric Membranes

Because of the small size and the high electronegativity of the fluorine atom, the perfluorinated polymers have a low polarizability and a strong C–F bond. Owing to the chemical inertness, thermal stability and improved acidity of sulfonic acid group in the $-\text{CF}_2\text{SO}_3\text{H}$ structure, these polymers have been widely used in chlor-alkali processes and as polymer electrolyte membranes for DMFC applications. These polymeric membranes are produced by the polymerization of monomers that include a group that can be modified as either anionic or cationic by further treatment. These membranes which are prepared from fluorocarbon-based ion-exchange polymers, possess good chemical and thermal stability. They have been first prepared by DuPont in 1966, under the commercial name of Nafion. The four-step procedure followed for the synthesis of Nafion polymeric membrane, can be outlined as follows: (a) the reaction of SO_3 with tetrafluoroethylene producing the sulfone cycle; (b) the condensation of the products produced in a) in the presence sodium carbonate and then copolymerization with tetrafluoroethylene forming an insoluble resin; (c) the hydrolysis of the polymer synthesized in b) forming a perfluorosulfonic polymer, finally (d) the exchange of the counter ion, Na^+ with the H^+ ion. This four step synthesis-procedure is depicted in Figure 2.13. Although there are similar polymers such as Flemion[®] and Aciplex-S[®] produced by Asahi Glass and Asahi Chemical companies respectively, the Dupont product, Nafion membrane is more successful owing to its mechanical strength, good chemical stability and high proton conductivity[35].

2.3.3. Acid – Base Complexes

Acid–base complexes have been developed as a feasible alternative for membranes that can keep the high conductivity at high temperatures without being affected from dehydration. Usually, the acid–base complexes designed for fuel cell membranes include an acid moiety introduced into an alkaline based polymer to provide proton conduction. Figure 2.14 shows the chemical structures of some important acidic and basic polymers and their complexes.

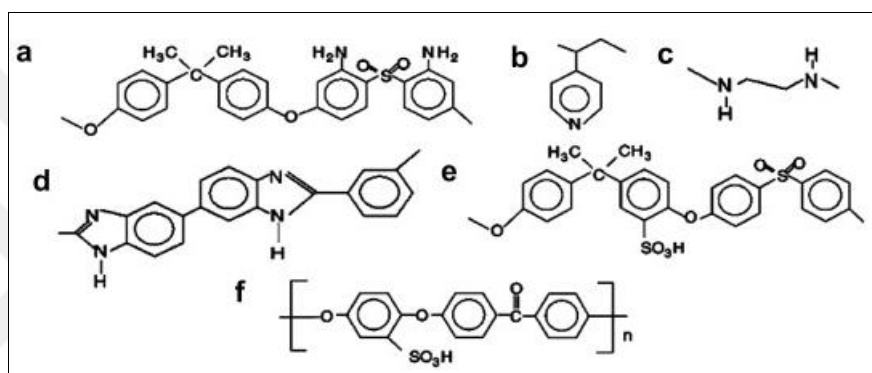


Figure 2.14. Structure of some important basic polymers (a-d) and acidic polymers (e,f) [37].

In this category, membranes based on polybenzimidazole doped with phosphoric acid (PBI/H₃PO₄) exhibit the most promising properties for high temperature PEMFC applications generally under ambient pressures. The development of these membranes has encouraged a wide range of research activities including polymer synthesis, physicochemical characterizations, membrane casting and fuel cell technologies in recent years. Thus these acid-doped PBI membranes have been characterized in detail. With the development of related fuel cell technologies, the application of PEMFCs at temperatures as high as 200 °C at ambient pressures has been demonstrated. Different from the Nafion cells, no gas humidification and therefore complicated humidification system are necessary. Some advantageous operating characteristics of the PBI cell are easy control of cell temperature and air flow rate.

2.4. AIM OF THE THESIS

The main objective of this study is to develop novel poly(aryl ether sulfone) based polymer electrolyte membranes for direct methanol fuel cells (DMFCs). Poly(aryl ether sulfones) have been selected due to their relatively high mechanical and thermal resistance, high T_g , good hydrolytic stability and low cost. A polymer electrolyte membrane designed to be used in DMFC applications must exhibit a high proton conductivity, high chemical and mechanical durability, low methanol permeability at operation conditions and low cost. Thus in this study, first partially sulfonated poly(aryl ether sulfones) (PESS) will be synthesized by the reaction of 4-Fluorophenyl sulfone (FPS), bisphenol A (BPA) and hydroquinone 2-potassium sulfonate (HPS) using an approximate ratio of BPA to HPS of 4:6, the product will be acidified and characterized. This synthesis will also be carried out first in a slight excess of FPS monomer and then BPA monomer will be added and reacted to ensure that all the chains terminate with BPA monomer. Sulfonation is necessary for proton conductivity however complete sulfonation will be avoided as it also increases the methanol permeability of the resulting membranes. The partially sulfonated poly(aryl ether sulfones) will then be methacrylated via reaction with glycidyl methacrylate through an addition reaction to the phenol end groups. The schematic presentation of the BPA terminated PESS and PESSGMA polymer structures are depicted in Figures 2.15 (a) and (b) respectively. The resulting glycidyl methacrylated and partially sulfonated poly(aryl ether sulfones) (PESSGMA) will then be self polymerized and copolymerized with comonomers such as styrene and vinyl phosphonic acid in the presence of radical initiators applying thermal cure cycles, in an effort to improve mechanical properties, reduce swelling in water and to reduce the methanol permeability. Membranes of these polymers will be prepared via the solution casting method. The effects of cross-linking and the different monomer types on membrane properties such as swelling in water, thermomechanical and thermal properties, proton conductivity and methanol permeability will be evaluated to examine the future applications of these membranes as PEM candidates for DMFCs.

In the first part of the study, the synthesis and characterization of the partially sulfonated poly(arylether sulfone) (PESS) and its glycidyl methacrylated derivative (PESSGMA) via spectroscopic methods will be carried out. In the second part of the study the resulting

PESSGMA pre-polymer will be self polymerized and copolymerized with styrene and vinyl phosphonic acid by radical polymerization via the solution casting method using a high temperature cure cycle. Studies will be carried out to optimize the cure cycle to obtain membranes with mechanical integrity and for successful cure and network formation. Then various properties such as ion exchange capacity, swelling in water, thermochemical and thermal properties, proton conductivity and methanol permeability of the membranes will be determined and analyzed with respect to their composition. Also as mentioned in the introduction section, the potassium salt form of the PESSGMA polymer; PESSGMA(K) will also prepared and self-polymerized and copolymerized with styrene and vinyl phosphonic acid in an effort to examine the possible inhibiting effect of sulfonic acid groups on radical polymerization.

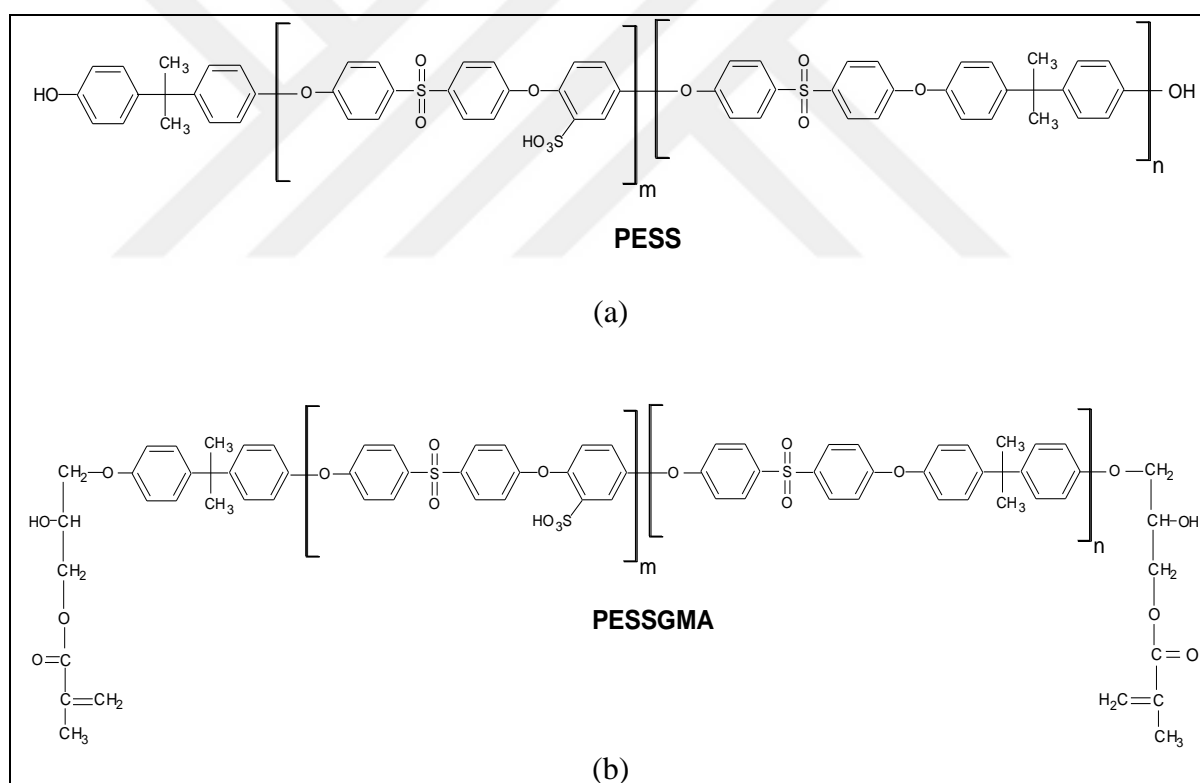


Figure 2.15. The schematic representations of (a)PESS and (b) PESSGMA polymers.

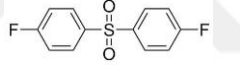
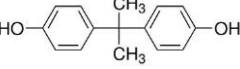
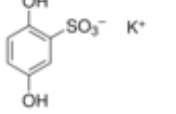
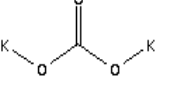
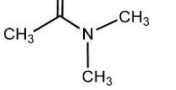
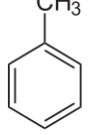
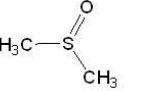
3. MATERIALS AND METHODS

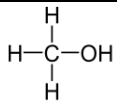
3.1. CHEMICALS

3.1.1. Chemicals Used in PESS Synthesis

The chemicals used in the synthesis of partially sulfonated poly(arylethersulfone) (PESS) and the potassium (K) salt form of PESS (PESS(K)) (potassium (K) salt form) are listed in Table 3.1.

Table 3.1. Chemicals used in preparation of PESS and PESS(K) polymers.

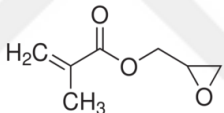
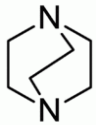
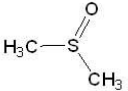
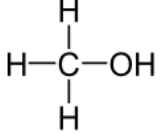
Chemical Name	Formula	Structure	Provider	Purity (%)
Bis(4-fluorophenyl sulfone)	$C_{12}H_8F_2O_2S$		Acros Organics	99
Bisphenol A	$(CH_3)_2C(C_6H_4OH)_2$		Sigma Aldrich	99
Hydroquinone 2-potassium sulfonate	$C_6KSO_5H_2$		Sigma Aldrich	
Potassium carbonate	K_2CO_3		Sigma Aldrich	99
Dimethyl acetamide	$CH_3C(O)N(CH_3)_2$		Merck	99
Toluene	C_7H_8		Sigma Aldrich	99.5
Dimethyl sulfoxide	$(CH_3)_2SO$		Merck	99.9

Methanol	CH ₃ OH		Sigma Aldrich	99.7
Hydrogen chloride	HCl	H—Cl	Sigma Aldrich	37

3.1.2. Chemicals Used in PESSGMA Synthesis

The chemicals used in the synthesis of partially sulfonated polyarylethersulfone-glycidyl methacrylate derivative (PESSGMA) and its potassium salt form (PESSGMA(K)) are listed in Table 3.2.

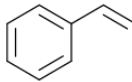
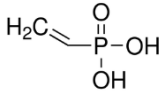
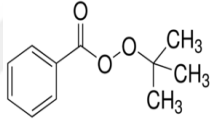
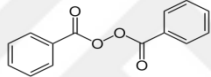
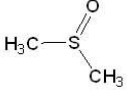
Table 3.2. Chemicals used in preparation of PESSGMA and PESSGMA(K) polymers.

Chemical Name	Formula	Structure	Provider	Purity (%)
Glycidyl Methacrylate	C ₇ H ₁₀ O ₃		Fluka	99
1,4-Diazobicyclo [2.2.2] octane	C ₆ H ₁₂ N ₂		Merck	98
Dimethyl sulfoxide	(CH ₃) ₂ SO		Merck	99.9
Methanol	CH ₃ OH		Sigma Aldrich	99.7

3.1.3. Chemicals Used in the Cure of PESSGMA and Membrane Preparation

The co-monomers and the radical initiators used in the cure of PESSGMA and PESSGMA(K) polymers and the solvent used in membrane preparation are listed in Table 3.3.

Table 3.3. Chemicals used in the cure of PESSGMA and PESSGMA(K) polymers and membrane preparation.

Chemical Name	Formula	Structure	Provider	Purity (%)
Styrene	C_8H_8		Sigma Aldrich	99
Vinyl phosphonic acid	$CH_2CHP(O)(OH)_2$		Merck	90
Tert-butyl Peroxy Benzoate	$C_{11}H_{14}O_3$		Fluka	91
Benzoyl Peroxide	$C_{14}H_{10}O_4$		Fluka	97
Dimethyl sulfoxide	$(CH_3)_2SO$		Merck	99.9

3.2. METHODS

In this study, the chemical structures of synthesized partially sulfonated poly arylether sulfone (PESS) and its glycidyl methacrylate derivative (PESSGMA) were characterized by fourier transform infrared (FT-IR) and proton nuclear magnetic resonance (1H -NMR) spectroscopic techniques. The molecular weights of the PESS and PESSGMA polymers were determined via gel permeation chromatography (GPC). The thermal transitions of the synthesized polymers were analyzed via differential scanning calorimetry (DSC) and the thermal degradation profiles were determined via thermal gravimetric analysis(TGA). Dynamic Mechanical Analysis (DMA) was used to determine the thermomechanical properties of the PESS and (PESSGMA) polymer membranes. Scanning electron microscopy (SEM) was also used to characterize morphology of the polymeric membranes. The ion exchange capacities (IEC) of the polymeric membranes were determined by titration methods and the proton conductivities of the polymer membranes under fully hydrated conditions were evaluated by an AC impedance spectrometer.

Swelling in water both at room temperature and at 80°C were determined for the prepared membranes and the methanol permeability of the membranes was measured using a diffusion cell which consists of two compartments separated by a membrane. Theoretical information about these methods will be presented in this section and the procedures for each method used in the analysis of the prepared polymers will be described in the following experimental section.

3.2.1. FT-IR Spectroscopy

Infrared (IR) spectroscopy is a common method for characterization of polymers. This technique depends on the vibrations of atoms of a molecule. An infrared spectrum is acquired by transition of infrared radiation through a sample and detecting which fraction of the incident radiation is directly absorbed at a particular energy. The energy at which a peak in an absorption spectrum occurs represents the frequency of vibration of a certain group of the sample molecule.

Most infrared spectroscopy is applied by using Fourier transform infrared (FTIR) spectrometers. This method relies on the interference of radiation among two beams to yield an interferogram, like a signal generated as a function of the variance of pathlength among the two beams. The two domains of frequency and distance are interconvertible by the mathematical method of Fourier transformation. The basic components of the FTIR spectrometer are illustrated schematically in Figure 3.1. The radiation generated from the source is directly passed through the interferometer to the sample present before reaching the detector. Upon amplification of the signal, at which high frequency contributions are sifted by a filter, obtained data are converted to the digital form by using a simple analog to digital converter and after then transferred to the computer so that the Fourier transformation can take place [45].

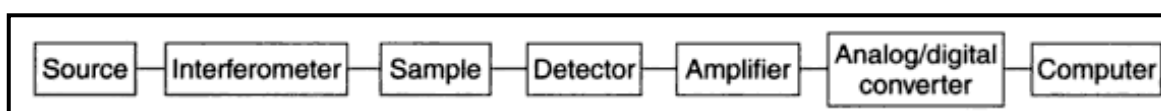


Figure 3.1. Basic components of an FT-IR spectrometer [45].

The output from the infrared instrument is called as spectrum. Inverse wavelength units i.e. (cm^{-1}) are used on the x-axis that is known as wavenumber scale. The y-axis is usually represented by transmittance percentage (%) with 100% at the top of the scale. One can also get the choice of transmittance or absorbance as a measure of band intensity. Absorbance is used for quantitative work while the transmittance is used traditionally for spectral interpretation.

The infrared spectrum can be classified into three regions, namely the near- infrared ($4000\text{--}13000\text{cm}^{-1}$), the mid infrared ($400\text{--}4000\text{cm}^{-1}$) and the far- infrared ($<400\text{cm}^{-1}$). Although the far and near- infrared regions can also supply specific information about materials, most infrared applications operate in the mid-infrared region. The near- infrared region largely consists of combination bands or overtones of fundamental modes that appear in the mid- infrared region. Moreover, the far- infrared region can supply information about the lattice vibrations.

The bands which appear in the FT-IR spectrum are assigned to particular part of the molecule, therefore giving useful information about the chemical structure of the molecule. Figure 3.2. shows the correlation table that belongs to infrared modes of polymers that can be useful in evaluating FT-IR spectra.

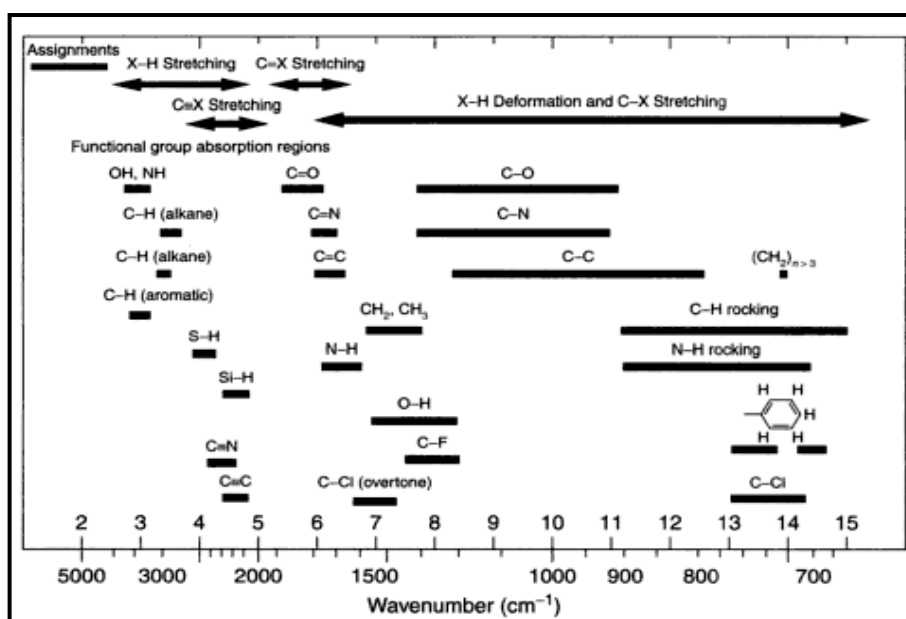


Figure 3.2. Typical infrared absorption frequencies for some common functional groups [45].

3.2.2. ^1H -NMR Spectroscopy

Nuclear Magnetic Resonance (NMR) Spectroscopy is a technique which provides a means to study both the structure and shape of molecules. It shows the different chemical environments of different types of hydrogen atoms present in a molecule, from which we can get information about the structure of the molecules. Also, if we already know what types of compounds exist in a mixture, NMR can also give a means of determining the amount of each component in the mixture. Therefore, it is a method of both quantitative and qualitative analysis, especially of organic compounds.

The most significant application of NMR is investigation of hydrogen atoms of organic molecules. Perhaps, the hydrogen atom is the simplest to analyze because of its physical properties. The nuclei of the other elements can not behave exactly in the same way as that of hydrogen.

NMR is especially useful in the structural analysis of organic compounds. The chemical shift shows what types of hydrogen exists e.g. hydrogen atoms of methyl groups, methylene groups, esters, aromatic compounds, and olefins. The multiplicity or spin-spin splitting shows which groups are next to each other in the molecule. The other important piece of information is acquired from the area or relative size of the absorption peaks in the spectrum that directly expresses how many hydrogen atoms (or nuclei) are in each group. For instance, the ratio of the areas of methyl (CH_3) and methylene (CH_2) peaks in propane ($\text{CH}_3\text{—CH}_2\text{—CH}_3$), would be 6:2; in butane ($\text{CH}_3\text{—CH}_2\text{—CH}_2\text{—CH}_3$) it would be 6:4. Appropriate interpretation of the spectra should give us significant information about the structure of an organic molecule. However, it does not directly tell us how much of this compound is present [46].

The area of the absorption peak (or peaks if spin-spin splitting is included) is directly controlled by the number of protons (hydrogen nuclei) included in absorption. For example, the total area of a methyl (CH_3) group should be 3/2 times as big as the total area of the CH_2 group. By using this fact, mixtures of organic liquids can be analyzed quantitatively [46].

The RF (radiofrequency) generator, permanent magnet, RF detector, magnetic coils and the sample holder are the most significant parts of an NMR instrument. Figure 3.3 shows how these components are arranged in a typical NMR instrument.

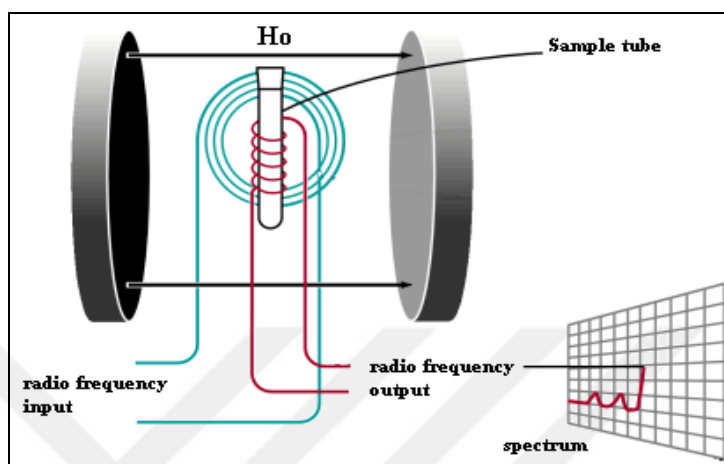


Figure 3.3. Schematic representation of an NMR spectrometer [46].

3.2.3. Gel Permeation Chromatography (GPC)

Gel permeation chromatography (GPC) allows the molecular weight distribution of a polymer sample to be obtained in two or three hours. Within the few years after its development it has reformed polymer characterization. It is now possible to get the molecular weight distribution of a very tiny sample of a polymer in two or three hours by this technique. For GPC analysis, a polymer solution is run down a chromatograph column which is packed with porous particles. It is experimentally observed that the volume of solvent needed to elute a molecule is a reducing function of molecular size.

GPC separates molecules present in a solution according to their "effective size in the solution". For sample preparation, the resin must be first dissolved in a suitable solvent. The dissolved resin is then directly injected into a continuously flowing stream of solvent (mobile phase) inside the gel permeation chromatograph. The mobile phase with the dissolved resin flows through densely packed highly porous and rigid particles (known as stationary phase) in a column. The pore sizes of these particles are important in separating molecules of different molecular weights and are available in a range of sizes.

Various components must be present in a typical GPC instrument. Injectors are required to present the polymer solution through the flowing system. Pumps pass the solvent and sample through the columns and system. Then, detectors monitor and also record the separation. Data acquiring accessories automatically control the test, make a record of the results and then finally calculate the average molecular weights. Figure 3.4 shows the basic components of a gel permeation chromatograph and the injection of the sample into the mobile phase.

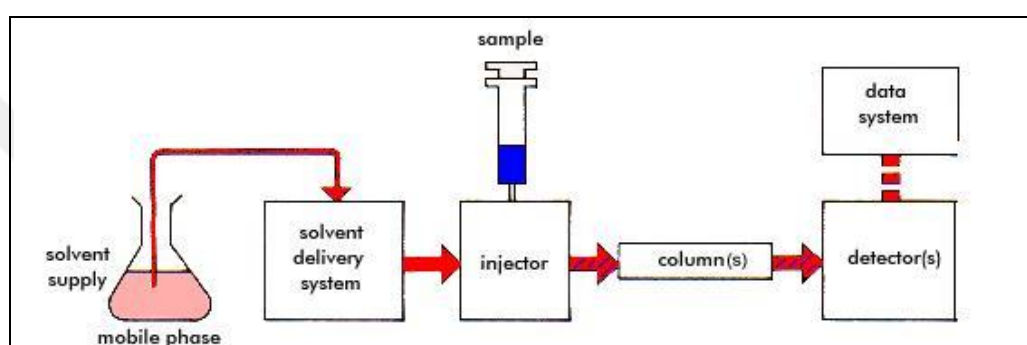


Figure 3.4. Schematic of the basic components of a gel permeation chromatograph [47].

GPC can deduce the weight average molecular weight, the number average molecular weight and the molecular weight distribution of a polymer which is its most significant characteristic. The distribution of the size of molecules for a given sample and its components is shown by the width of the individual peaks present in the chromatogram. This distribution curve is also commonly known as the molecular weight distribution (MWD) curve. The peaks all together represent the MWD of a sample. The broader the peaks, the broader the MWD of the polymer and vice versa. As the average molecular weight increases, the curve shifts further along the molecular weight axis [47].

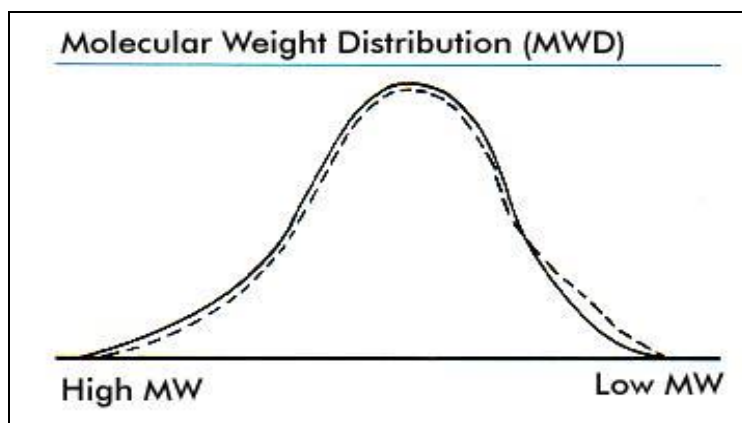


Figure 3.5. Molecular weight distribution curve of a gel permeation chromatograph [48].

3.2.4. Differential Scanning Calorimetry (DSC)

Differential scanning calorimetry (DSC) is a method that measures the energy produced (exotherm) or absorbed (endotherm) as a function of temperature or time. This method is commonly used to characterize processes like crystallization, melting, loss of solvents, resin curing and other processes resulting an energy change. Differential scanning calorimetry can also be used to characterize processes that involve a change in heat capacity like the glass transition. Generally, one test can be used to measure most of these properties, just as thermomechanical analysis. In a typical analysis, the sample is lodged in an aluminum pan and then an empty reference pan and the sample are located on small platforms present in the DSC chamber. Thermocouple sensors are present below the pans. Figure 3.6 shows the schematic view of the interior of a DSC instrument.

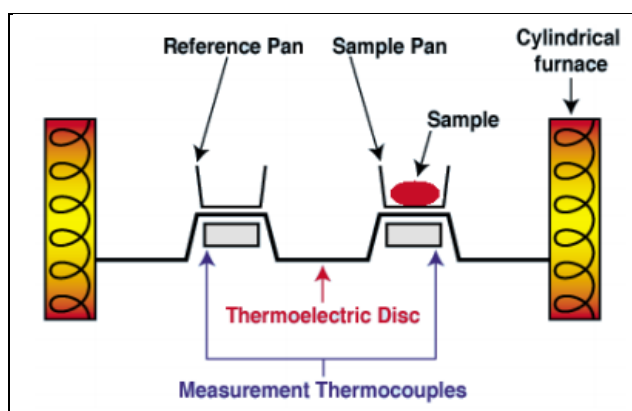


Figure 3.6. Schematic of the interior of a DSC [49].

DSC measurements can be performed in two ways: by measuring the heat flow as a function of sample temperature (heat flux) or by measuring the electrical energy supplied to heaters below the pans that is required to keep the two pans at the same temperature (power compensation).

The DSC finally outputs the differential heat flow (heat/time) between the empty reference pan and sample material. Heat capacity can be found out by calculating the ratio of heat flow to heating rate. Hence,

$$C_p = \frac{q}{\Delta T} \quad (3.1)$$

where C_p is the heat capacity of material, q is the heat flow along the material over a given time and ΔT is the variance in temperature over the same time period.

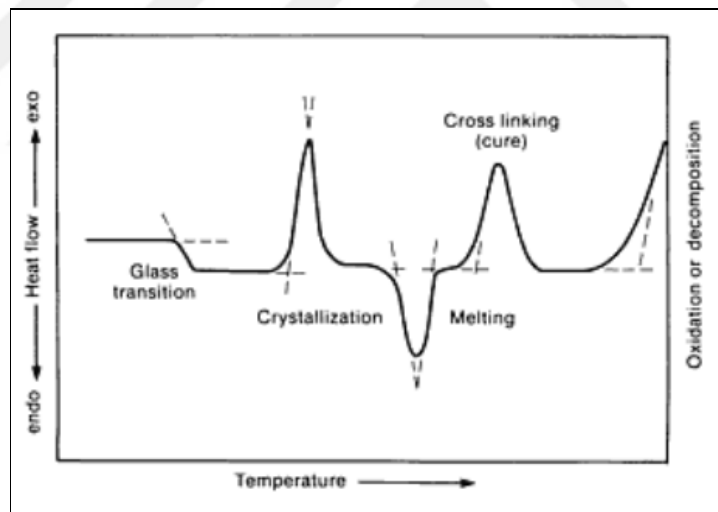


Figure 3.7. Schematic of a DSC thermogram [49].

Figure 3.7 shows the schematic of a DSC thermogram which is labeled for four critical points: the melting temperature (T_m), the crystallization temperature (T_c) and the glass transition temperature (T_g) and the curing temperature.

At a temperature below the glass transition temperature T_g , semicrystalline and amorphous polymers are generally brittle and hard since the polymer chains are locked in coiled and tangled positions. Above the glass transition temperature (T_g) on the other hand, the

polymeric chains can easily slip past each other and rotate with more ease and as a result the polymer becomes more ductile and also softer. The glass transition temperature of a polymer generally depends on its processing as well as the natural characteristics of the polymer such as its molecular weight, structure and bonding. On a DSC curve, the glass transition appears as an endothermic process because it gets energy to break the bonds between chains. In DSC analysis, the T_g can be detected by a permanent reduction in baseline heat flow and determined by taking the inflection point in the curve.

The crystallization temperature (T_c) which occurs in crystalline and semi-crystalline polymers is another significant transition. At the crystallization temperature, intermolecular bonds form and the chains become more ordered losing their random chain arrangement. During crystallization process, formation of bonds is an exothermic process, therefore an increase in heat flow (a peak on the DSC curve) shows up with the crystallization process. The T_c is generally found by discovering the onset point of the crystallization curve. It must be kept in mind that, many amorphous polymers never undergo crystallization.

When a material changes its phase from solid state to liquid, melting takes place. When the material begins to melt, its intermolecular bonds start absorbing energy and then loosen and break. Melting is an endothermic process since it includes absorption of energy and appears as a temporary, large decrease in heat flow on the DSC curve. When the material completely melts, the heat flow comes back to its original baseline value. Generally, the melting temperature is measured at the melting curve's onset point.

Curing of a polymer takes place when individual chains make strong bonds to other chains, this process is sometimes called as “crosslinking”. Like crystallization, this process of ordering of chains and bond formation are exothermic. Generally, the curing temperature is determined as the curing peak's onset on the DSC curve [49].

3.2.5. Dynamic Mechanical Analysis (DMA)

Dynamic Mechanical Analysis (DMA) is a method that measures the mechanical properties of materials as a function of frequency, time and temperature. It is also a thermal analytical method by which the mechanical response of a material exposed to a specific temperature program is analyzed under periodic stress. DMA is a high precision technique

for determining the viscoelastic features of materials. Most materials display mechanical responses to an applied stress, which are a combination of elastic and viscous behavior. Dynamic Mechanical Analyzer first deforms the material mechanically and afterwards, it measures the response of the material. As a force is exerted on a material, it is exposed to a change in shape, which means; it deforms. The deformation can be performed sinusoidal, under a fixed rate or in a constant (or step) fashion. The response of the material to the deformation may be monitored as a function of time or temperature. A force to resist the deformation is built up at the same time within the material and it rises as the deformation goes on. If the material is not able to resist to the external action, the deformation process continues till the failure of the material. Thus, the deformation of a material in response to an external action and resistance to deform are called as *strain* and *stress* respectively.

Polymers which are viscoelastic fluids exhibit viscous or elastic behaviour, depending on how fast they flow or are deformed in response to an applied stress in the process. Whether the polymer shows more liquid-like or solid-like properties is dependent on temperature as well as frequency or time. With the DMA method, a sinusoidal stress or force is exerted on a sample and the resulting sinusoidal strain or deformation is monitored. The sample strain response lags behind the input stress wave with respect to time, thus this lag is commonly known as the phase angle (δ). The proportion of the dynamic stress to dynamic strain gives the complex modulus (E^*) which involves the components of the loss modulus (E'') and storage modulus (E'). The storage modulus can be defined as the capability of a material to store energy and it is a measure of the stiffness of a material. The loss modulus stands for the heat given out by the sample in consequence of the material's given molecular motions and this represents the damping properties of the polymer. Due to the viscoelastic nature of most materials that involve all polymers, the mechanical properties described here are functions of time and frequency as well as temperature. The proportion of the loss modulus to the storage modulus is referred to as tan delta and is generally termed damping. Thus, tan delta is a measure of the energy dissipation or spread of a material [50].

DMA gives significant and practical information about the material tested. For example, damping behavior and glass transition temperature can be used to identify the using conditions of the material such as corresponding stiffness and temperature. Additionally,

Dynamic Mechanical Analysis can also clarify how the material behaves in present time and in future.

The dynamic mechanical analyzer is generally useful for the following tests: morphology of polymers, mechanical properties, loss angle (δ), loss factor ($\tan \delta$), dynamic viscosity, impact resistance, curing kinetics, ageing, correlation with materials formulation, glass transition temperature (T_g), damping, industrial products' stiffness, secondary transitions, rheological properties, specimen stiffness, creep behavior, thermal stability, stress-strain, tension test etc.

In DMA, there are seven types of clamps that are used with suitable materials. 3-point bending clamp, single and dual cantilever bending clamps, compression and shear clamps, tension fiber clamp, tension film clamp are the various types of clamps utilized for DMA measurements [50]. In this study, the polymer films were analyzed using the tension film clamp. A schematic presentation of the tension film clamp is shown in Figure 3.8.

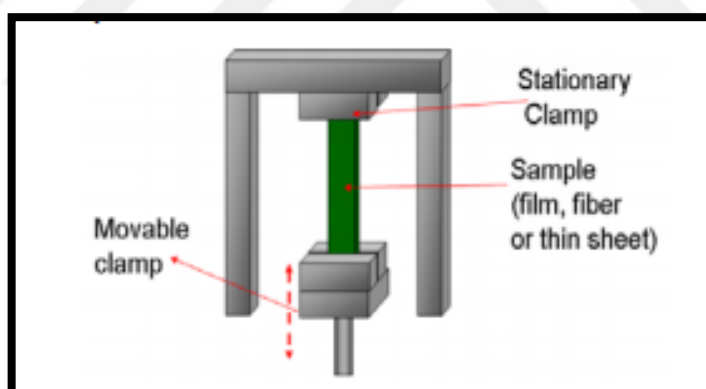


Figure 3.8. Clamp of film tension for DMA [76].

3.2.6. Thermal Gravimetric Analysis (TGA)

Thermal Gravimetric Analysis (TGA) is a technique that measures the amount and rate of variance in the mass of a sample as a function of time or temperature in a controlled atmosphere. Usually, the measurement is performed in an inert atmosphere such as Argon or Helium or in air and the weight is registered as a function of increasing temperature. The measurements can sometimes be performed in a low oxygen atmosphere (*eg.*, 1 -

5wt%O₂ in He or N₂) to decelerate oxidation. The measurements are primarily utilized to establish the oxidative and/or thermal stabilities of materials as well as their compositional features. This technique can survey materials that show either mass gain or loss because of oxidation, decomposition or loss of volatiles (like moisture). Thus, this method is convenient for the analysis of all types of polymeric materials, including thermosets, thermoplastics, composites, elastomers, fibers, films, coatings and paints [51].

The thermal gravimetric analyzer contains a sample pan which is connected to a precision balance. This pan stays in a furnace and is heated or cooled in the course of the experiment. The mass of the sample is directly recorded during the experiment. The sample environment is controlled by a sample purge gas. This gas may be reactive or an inert gas which runs through the sample and leaves the furnace through an exhaust. Within the instrument, the sample pan is held with a “hangdown” below the balance. A typical TGA instrument is shown in Figure 3.9. The thermal gravimetric analyzer uses the advantage of gravity to get very reproducible and accurate measurements. This technique can measure the loss of solvent, loss of water, loss of plasticizer, weight % filler, weight % ash, metallic catalytic residue content left on carbon nanotubes and the degree of decomposition, oxidation, decarboxylation and pyrolysis.



Figure 3.9. A typical TGA instrument [51].

3.2.7. Scanning Electron Microscopy (SEM)

The scanning electron microscope (SEM) is a handy instrument which can be utilized for the analysis and examination of the chemical composition characterizations, microstructure and morphology.

The scanning electron microscope (SEM) utilizes a focused beam of high-energy electrons to create various signals at the surface of solid materials. The signals created from electron-sample interactions give information about the material involving chemical composition, external morphology (texture), crystalline structure and orientation of the different components of the material. In many applications, data are gathered over a selected surface area of the sample and a 2-dimensional image is formed which exhibits spatial differences in these properties. Areas that range from approximately 1 cm to 5 microns in width may be pictured in a scanning mode via conventional SEM techniques. This roughly corresponds to magnification ranges from 20X to 30,000X and a spatial resolution of about 50 to 100 nm. SEM is also able to perform analysis of selected point places on the sample; this approach is particularly useful in determining crystal orientations, crystalline structure and qualitatively or semi-quantitatively analyzing chemical compositions. Figure 3.10 shows a typical SEM instrument with the sample chamber, electron column, electronics console, EDS detector together with the visual display monitors.



Figure 3.10. A typical SEM instrument [52].

In SEM analysis, accelerated electrons bear important amounts of kinetic energy and this energy is given off as various signals generated by electron-sample interactions when the incident electrons are slowed down in the solid sample. These signals involve secondary electrons (which create SEM images), diffracted backscattered electrons (EBSD which are utilized to analyze orientations and crystal structures of minerals), backscattered electrons (BSE), visible light (cathodoluminescence–CL), photons (characteristic X-rays which are used for elemental analysis and also continuum X-rays) and heat. Backscattered electrons and secondary electrons are utilized commonly for imaging samples: secondary electrons are the most precious for presenting topography and morphology on samples and backscattered electrons are most precious for showing contrasts in composition of multiphase samples (i.e. for identifying the different phases). X-rays are produced by inelastic collisions of the incident electrons with electrons in specific shells or orbitals of atoms in the sample. While the excited electrons come back to lower energy states, they emit X-rays which are of a specific wavelength (which is determined by the difference in energy levels of electrons in different orbitals for a given element). Therefore, characteristic X-rays are generated for each element in a mineral which is "excited" by the electron beam. SEM analysis can be classified as a non-destructive method, that is, X-rays produced by electron interactions do not cause a loss of volume of the sample, therefore it is also possible to scan the same materials repeatedly [52].

3.2.8. Proton Conductivity Measurements

The proton exchange membrane (PEM) is a core component of all PEM fuel cells. It enables the transportation of protons formed at the anode to the cathode while acting as a barrier to separate the cathodic and anionic compartments. The main charge carriers in the system are the protons in the membrane. Thus, the conductivity generated by this proton transport is referred to as proton conductivity.

Principally, proton conductivity may be measured by following the voltage drop across a membrane which is caused by the proton current flow as two H_2/H^+ metal electrodes, are fastened separately on both sides of the membrane. The metal electrodes can be made up of Pt black. The reversible electrochemical reactions on these Pt black electrodes are H_2/H^+ redox reactions that either supply or accept these protons. The fact that these redox

reactions are reversible or the activities of the electrodes which can alter the polarization potentials of the related reactions can effect the precision of voltage detection and therefore the conductivity measurements. The membrane water content and the operating temperature significantly effect the proton conductivity by influencing hydrogen ionization as well as proton concentration and the mobility of the protons in the membrane. Thus, a precise measurement of a PEM proton conductivity still stands as an important experimental challenge. A number of techniques have been proposed and also used to measure proton conductivity; these methods involve the electrochemical impedance spectroscopy, two-probe and four-probe methods, current interruption method, electrochemical atomic force microscopy and the solid-state pulsed field gradient nuclear magnetic resonance technique.

Relying on the same basis as the conventional measurement of electronic resistivity, Ohm's law is utilized to determine the resistivity of a proton-conductive membrane against the flow of either direct current (DC) or alternating current (AC). The following equation can be used to determine the proton conductivity;

$$\sigma = \frac{l}{RA} \quad (3.2)$$

where σ is the membrane conductivity (S cm^{-1}), l is the length among the two voltage probes in the case of in-plane measurements or the thickness of the membrane in the case of through-plane measurements, R is the resistance recorded, and A is the cross-sectional area of the tested membrane. The through-plane and/or in-plane proton conductivities of a membrane may be measured by using diverse approaches, like the four-probe method, the two-probe method and the coaxial-probe method.

Four-probe method has been commonly used to exclude effectively the interfacial impedance from conductivity measurements. If it is compared with the two-probe configuration, two additional Pt probes (these could be Pt strips or Pt wires, and are assigned as inner probes) are placed between the two outer Pt probes which function as voltage sensors, as illustrated in Figure 3.11. The two outer Pt strips function as AC current injectors. With this set up, the current is passed among the two outer Pt strips and the membrane conductance is determined from the difference in AC potential among the two inner probes. Relatively, this method is not sensitive to contact impedance at the

current-carrying electrodes and is thus appropriate for membrane conductivity measurements [53].

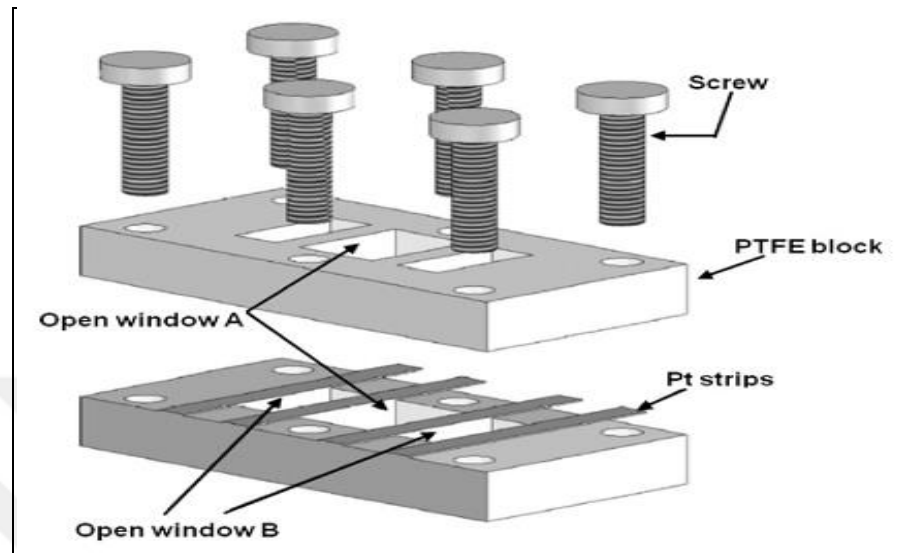


Figure 3.11. Schematic of a four-probe conductivity cell designed to measure proton conductivity [53].

Figure 3.12 illustrates the Nafion 115 membrane's AC impedance spectra generated via the four-probe method by employing Pt strips as both outer and inner probes under fully hydrated conditions, at room temperature. Each AC impedance spectrum includes an arc within the low-frequency domain and one semicircle within the high-frequency domain. Within this configuration, the low-frequency arc gets smaller with the rise in distance among the two voltage probes and the total AC impedance spectrum approaches to the shape of an ideal semicircle. This shows that the distance among the two inner probes can alter the obtained measurements and thus by increasing this distance, the low-frequency impedance can be decreased [53].

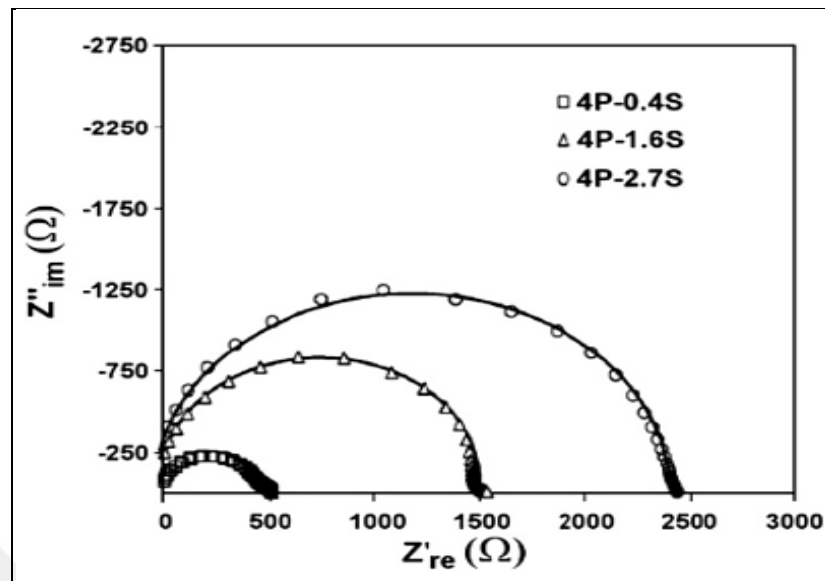


Figure 3.12. Nafion 115 membrane's AC impedance spectra generated via four probe method.(0.4, 1.6, and 2.7 stand for the distance (cm) between the two voltage probes) [53].

3.2.9. Methanol Permeability Measurements

It is quite critical to have reliable and accurate techniques for the measurement of methanol permeability of polymer electrolyte membranes designed for DMFCs. In principal, a very precise technique is necessary which is very responsive to methanol concentration because even a trace amount of methanol reaching the cathode will negatively influence the fuel cell performance. To determine the methanol cross-over of the polymer electrolyte membranes, several methods have been proposed and used. Previous studies on the methanol permeability problem in the DMFC's showed that the methanol reaching to the cathode is oxidized to carbon dioxide. Thus a commonly used method for measuring the methanol cross-over in a DMFC is to measure the carbon dioxide amount in the cathode exhaust gas via gas chromatography and mass spectrometry. But, a part of carbon dioxide generated on anode can permeate through the membrane to directly the cathode during the DMFC operation. Also, incomplete oxidation of the diffused methanol at the cathode always occurs.

So, the presence of anodic carbon dioxide and incomplete oxidation of methanol at cathode must be kept in mind so as to prevent reporting wrong methanol permeability values. It is

feasible to measure the exact amount of carbon dioxide crossing through the membrane by employing a methanol tolerant cathode layer which can not oxidize the permeated methanol. Additionally, via the gravimetric determination of Barium carbonate (BaCO_3) the amount of carbon dioxide being generated both at the cathode and the anode can be measured.

Gas chromatography (GC) is the other non-electrochemical method which is employed to measure the crossed methanol concentration with time. This technique is especially appropriate for preliminary screening of the membranes. It makes use of a two compartment diffusion cell equipment which is shown in Figure 3.13. During analysis, samples of the solution in the the receiving compartment are pulled at various time intervals and the concentration of methanol is determined. This technique works fine as long as an online GC device is available, but if not, the samples taken are vulnerable to contamination before their gas chromatographic analysis [54]. An image of a typical methanol permeability measurement set up is also illustrated in Figure 3.13.

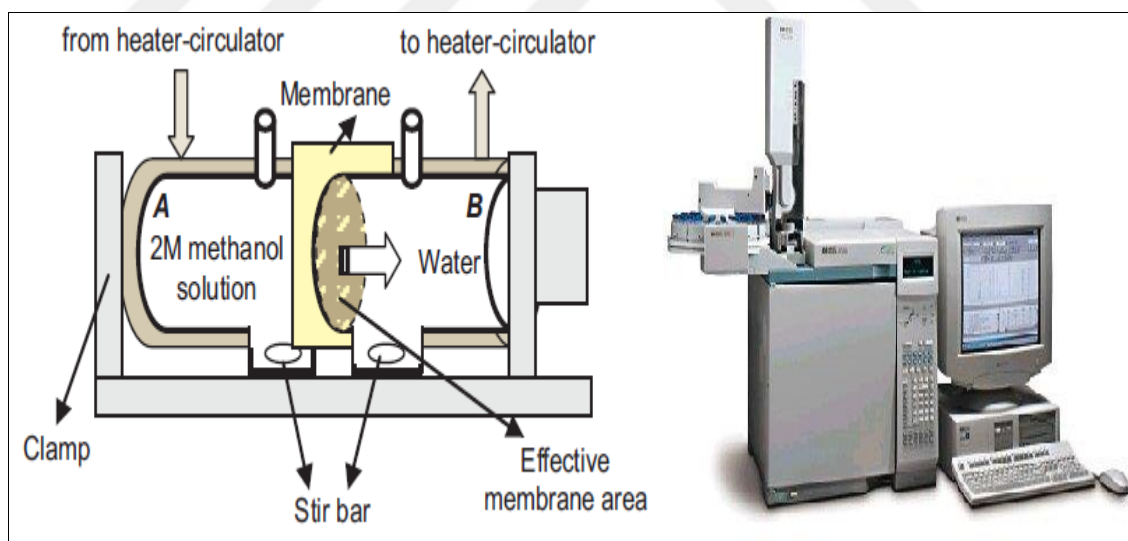


Figure 3.13. The schematic of the two compartment diffusion cell and a typical methanol permeability measurement set-up [55,56].

4. EXPERIMENTAL STUDY

In this section, first the detailed procedures for PESS, PESS(K), PESSGMA and PESSGMA(K) synthesis will be described. In the following sub-section, procedures used for the cure of the PESSGMA and PESSGMA(K) polymers and membrane preparation will be given. Finally the analytical methods used for the characterization of the PESS and PESSGMA polymers and their membranes will be presented.

4.1. SYNTHESIS OF PESS AND PESS(K)

4.1.1. Procedure of the Reaction

The partially sulfonated poly(aryl ether sulfone) (PESS) was synthesized by the reaction of 4-Fluorophenyl sulfone (FPS), bisphenol A (BPA) and hydroquinone 2-potassium sulfonate (HPS) using an excess of the diol monomers. The BPA : HPS mole ratio used was fixed as 4.4:6.0. The schematic representation of the PESS synthesis reaction is shown in Figure 4.1.

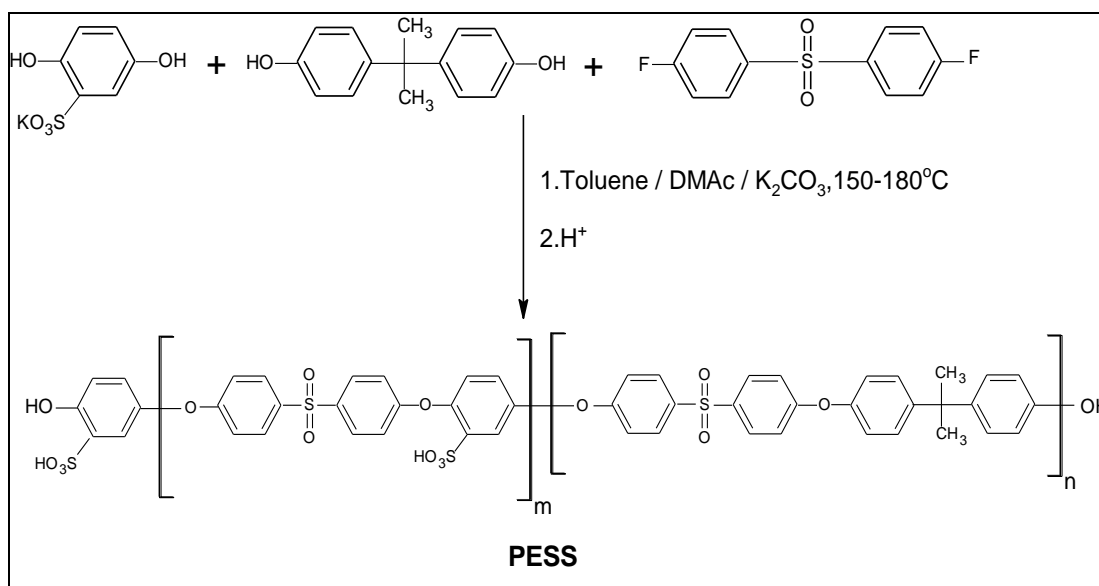


Figure 4.1. The schematic representation of the PESS synthesis reaction.

The procedure of the synthesis can be described in the following steps;

- 20 mmol (5.09 g) of 4-Fluorophenyl sulfone (FPS), 8.8 mmol (2.013 g) of Bisphenol A (BPA), 12 mmol (2.74 g) of hydroquinone 2- potassium sulfonate (HPS) and 40 mmol (5.70 g) potassium carbonate were added to a mixture of 25 ml of dimethyl acetamide(DMA), 40 ml of toluene and 40 ml of dimethyl sulfoxide (DMSO) in a 200 ml round bottom flask.
- The round bottom flask was placed in a heating mantle that was placed on a magnetic stirrer.
- The round bottom flask was equipped with a Dean- Stark apparatus, a nitrogen inlet and a temperature controller as shown in Figure 4.2.

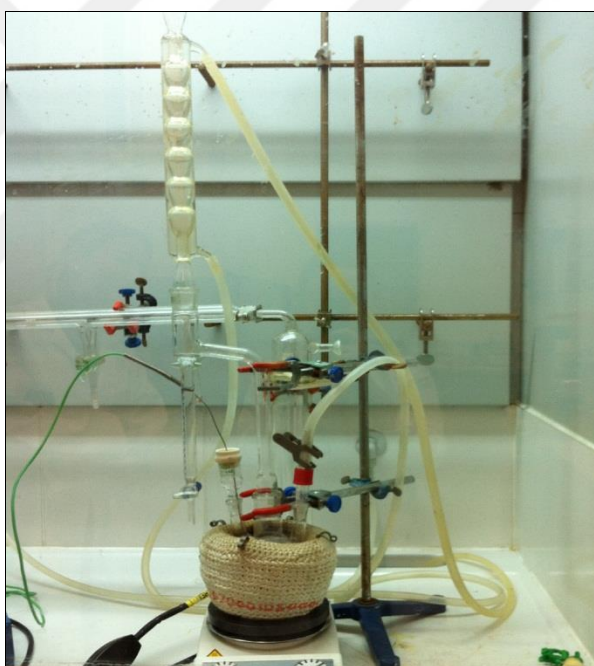


Figure 4.2. The experimental set up for PESS synthesis.

- The temperature of the reaction mixture was adjusted to 150°C and the reaction mixture was stirred at this temperature for 4 hours.
- At the end of 4 hours, the azeotropic mixture of toluene and water was distilled out and the temperature of the reaction mixture was raised to 180°C.
- The reaction mixture was stirred at this temperature for 10 hours.
- At the end of this time, the reaction solution was cooled to room temperature.

4.1.2. The Purification of the PESS and PESS(K) Polymer

After the outlined reaction steps were completed, the purification of the PESS polymer was performed as follows;

- The PESS product solution was poured into a 1000ml of methanol solution in order to precipitate the product. The precipitated product was then filtered using vacuum filtration as shown in Figure 4.3.

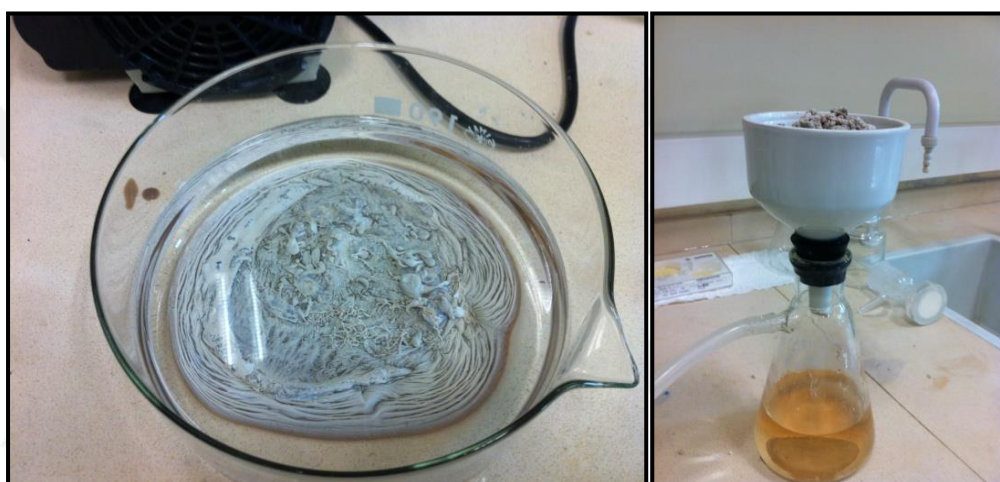


Figure 4.3. The precipitation and vacuum filtration processes of PESS product.

- The filtered product was dried at 45°C under vacuum for 1 hour.
- Then, the residual inorganic materials in the dried product was extracted by treatment with deionized water in the Soxhlet apparatus for 6 hours.
- The product was dried overnight in a vacuum oven at 40°C.
- The product was then dissolved in 50 ml of DMSO, and it was precipitated in a mixture of 500 ml hydrochloric acid (HCl) and 500 ml of methanol (MeOH) to convert the potassium sulfonate groups on the polymer to sulfonic acid groups.
- The precipitated product was filtered and after the soxhlet extraction of residual inorganic acid by using deionized water, it was dried overnight at 40°C. 7.8g of the PESS product was obtained with approximately 79% yield. The final form of the PESS product is shown in Figure 4.4.



Figure 4.4. The final form of the PESS product.

The synthesis procedure of the PESS(K) salt is the same with that of the PESS polymer, but for the purification steps of PESS(K) polymer, the precipitation of product in HCl acid solution and methanol mixture and the following steps were not performed to keep the resulting polymer in the potassium (K) salt form.

As will be discussed in the following chapters, the glycidyl methacrylated derivatives of the PESS polymer were found to be quite unreactive in radical polymerization due to possible inhibition effects of the sulfonic acid groups. As the diol monomers were used in excess for the PESS synthesis in the procedure described above, the obtained PESS polymer chains may terminate with both HPS and BPA monomers as depicted in Figure 4.1. Thus in addition to the procedure described above for the PESS synthesis, a modified procedure has also been carried out to ensure that all the PESS polymer chains terminate with BPA monomer. This can at least give a chance to keep the sulfonic acid groups a bit away from the glycidyl methacrylate functionality. In this modified procedure, the amount of reactants were all doubled and the poly condensation reaction was first carried out in a slight excess of 4- Fluorophenyl sulfone (FPS), then an additional amount of BPA was added and reacted with 4- Fluorophenyl sulfone (FPS) ends of the polymer chains for about 4 hours at 180°C. The BPA : HPS mole ratio used was again fixed as 4:6. The structure BPA terminated PESS product was shown in Figure 2.16(a).

The procedure of this modified synthesis method is described in the following steps;

- 40.2 mmol (10.24 g) of 4-Fluorophenyl sulfone (FPS), 16 mmol (3.66 g) of Bisphenol A (BPA), 24 mmol (5.48 g) of hydroquinone 2- potassium sulfonate (HPS) and 80 mmol (11.4 g) potassium carbonate were added to a mixture of 50 ml of dimethyl acetamide (DMA), 80 ml of toluene and 80 ml of dimethyl sulfoxide (DMSO) in a 250 ml round bottom flask.
- The round bottom flask was placed in a heating mantle that was placed on a magnetic stirrer.
- The round bottom flask was equipped with a Dean- Stark apparatus, a nitrogen inlet and a temperature controller.
- The temperature of the reaction mixture was adjusted to 150°C and the reaction mixture was stirred at this temperature for 4 hours.
- At the end of 4 hours, the azeotropic mixture of toluene and water was distilled out and the temperature of the reaction mixture was raised to 180 °C
- The reaction mixture was stirred at this temperature for 10 hours.
- Then, 0.1g (0.44mmol) excess BPA was added to the reaction mixture and the solution was kept at 180 °C for 4 hours with magnetic stirring.
- At the end of this time, the reaction solution was cooled to room temperature.

Similar purification steps were performed on this PESS product and at the end of the purification steps, 19.0g of the PESS polymer was obtained with approximately 97,5% yield.

4.2. SYNTHESIS OF PESSGMA AND PESSGMA(K)

4.2.1. The Procedure of the Reaction

The partially sulfonated poly(arylether sulfone) (PESS) was further reacted with glycidyl methacrylate (GMA) to convert the phenol hydroxyl end groups to glycidyl methacrylate groups, via an addition reaction as shown in Figure 4.5. 1,4-Diazobicyclo [2.2.2] octane (DABCO) was used as the catalyst. The amount of glycidyl methacrylate used was based on the amount of diol used in the synthesis of the PESS polymer and fixed at the molar ratio of $n\text{diol}:n\text{GMA} = 1.0 : 0.75$, thus an excess of GMA was used considering a major

portion of the diol hydroxyls were already consumed via polycondensation during the synthesis of the PESS polymer.

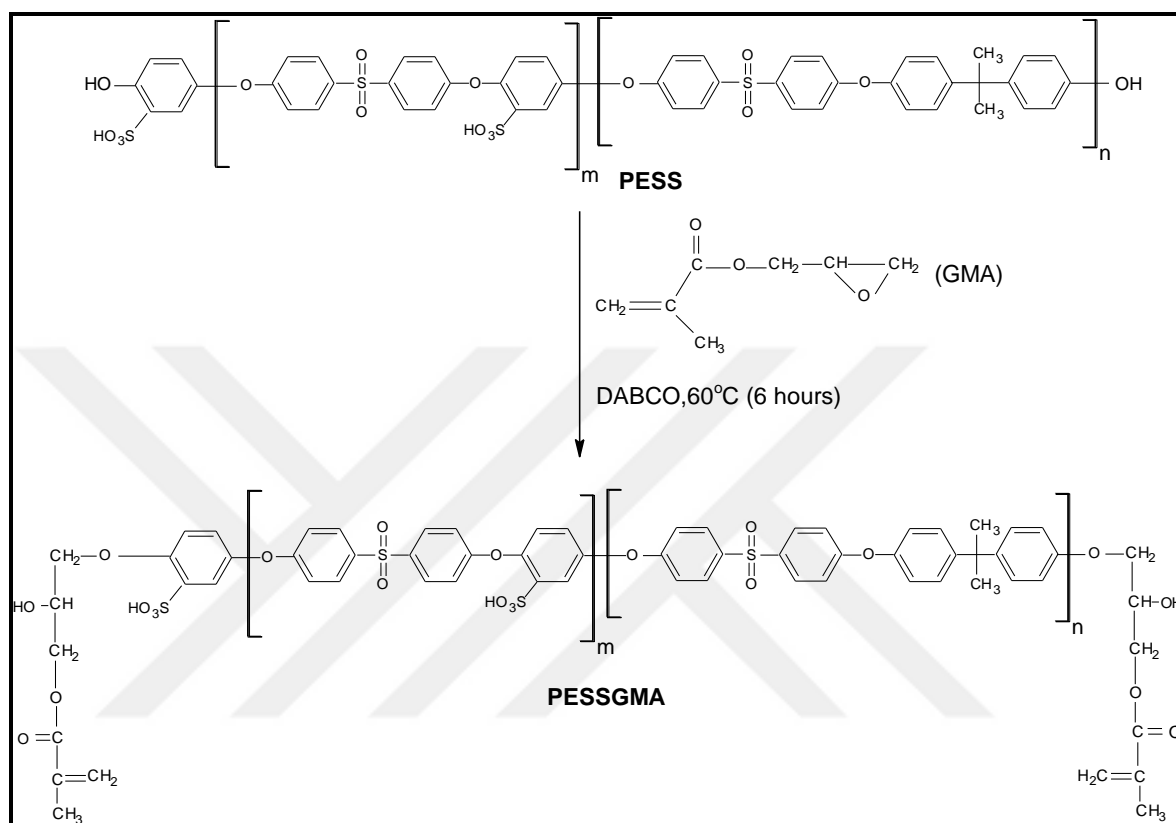


Figure 4.5. The schematic representation of PESSGMA synthesis reaction.

The procedure of the PESSGMA synthesis can be described in the following steps;

- 8 g of the PESS polymer, 1.719 ml of GMA and 0.29 g of DABCO were added to 50 ml DMSO in a 200 ml round bottom flask that was placed on a heating mantle.
- The round bottom flask was equipped with a nitrogen inlet, a thermometer, a condenser and a temperature controller. The experimental set up is shown in Figure 4.6.



Figure 4.6. Experimental set up for the PESSGMA synthesis.

- The temperature of the reaction mixture was adjusted to 60 °C, and the reaction mixture was allowed to stir for 6 hours at this temperature.
- At the end of 6 hours, the product was cooled to the room temperature. The solution of the product at the end of reaction is shown in Figure 4.7.

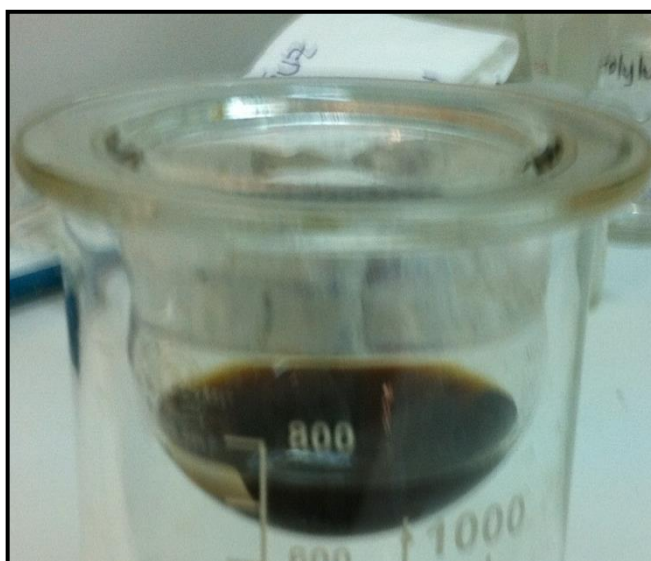


Figure 4.7. The solution of the synthesized PESSGMA product at the end of reaction.

The crude PESSGMA product was purified by filtration and extraction of residual inorganic materials according to the following procedure;

- Initially, the cooled PESSGMA solution was filtrated by using vacuum filtration to remove the catalyst. The residual particles stayed on the filter paper as shown in Figure 4.8.



Figure 4.8. The filtered product and residual particals.

- The filtrated product was then precipitated in 200 ml of methanol, and it was filtered again via vacuum filtration. The filtrated PESSGMA polymer which is in white powder form is shown in Figure 4.9.



Figure 4.9. The filtrated PESSGMA polymer

- The filtrated product was washed two times with deionized water and then with methanol.
- The product was finally dried in a vacuum oven at 30 °C for 12 hours. At the end, 3.72g of the PESSGMA polymer was obtained with about 45.6% yield.

The synthesis and purification procedure of the PESSGMA(K) polymer was the same with the synthesis and purification procedure of the PESSGMA polymer. At the end of the synthesis, 8.46 g of PESSGMA(K) polymer was obtained.

For the reaction of the BPA terminated PESS product (obtained from the second method of synthesis) with GMA, a similar procedure was carried out. The amount of glycidyl methacrylate used was again determined by using the amount of diol used in the synthesis of the PESS polymer and fixed at the molar ratio of ndiol:nGMA= 1.0 : 0.75, thus an excess of GMA was used. In this procedure, 19 g of the PESS polymer was reacted with 4.478 g of GMA in the presence of 0.704 g of DABCO catalyst for 6 hours at 60 °C. After similar purification and drying steps, 12.93g of the PESSGMA polymer was obtained with 67.5% yield.

4.3. CURE OF PESSGMA AND PESSGMA(K) POLYMERS AND PREPARATION OF MEMBRANES

The prepared PESSGMA polymer was self polymerized or copolymerized in the presence of co-monomers such as styrene and vinyl phosphonic acid via radical polymerization applying thermal cure cycles. Five types of polymer membranes were prepared namely the PESS, PESSGMA, and the copolymers of PESSGMA with styrene and vinyl phosphonic acid; PESSGMA/STY, PESSGMA/VPA, PESSGMA/STY/VPA via solution casting method using tert-butyl peroxy benzoate or benzoyl peroxide as the radical initiator and dimethyl sulfoxide as the solvent. Table 4.1 shows the compositions of all the prepared PESSGMA samples and the curing conditions applied in the initial trials for the cross-linking of the PESSGMA polymer. In the initial trials, the total co-monomer content was fixed at 30wt% for the copolymers, the initiator concentration used was 4wt% and (the total monomer + polymer weight)/(volume of solvent) ratio was fixed at 0.5g /5mL. For the self-polymerization of the PESSGMA polymer, samples were also prepared using

exceptionally higher contents of initiator (6 and 10wt%) as the cross-linking of PESSGMA was not successful at 4wt% or lower concentrations of initiator, under the conditions tabulated in Table 4.1. For each composition, all the ingredients were dissolved in DMSO, purged with N₂ gas for 5 minutes and the solution was then poured into a petridish (diameter : 3cm). The solution in the petridish was placed in a vacuum oven and the corresponding cure cycles were applied for the cure of the PESSGMA polymer and evaporation of the solvent.

Table 4.1. The compositions of all the prepared PESSGMA samples and the curing conditions applied in initial trials.

Composition	Initiator	Curing Conditions
0.5g PESSGMA	4wt% Tert-butyl Peroxy Benzoate	100°C 3 hours 130°C 3 hours
0.5g PESSGMA	6wt% Tert-butyl Peroxy Benzoate	100°C 3 hours 130°C 3 hours
0.5g PESSGMA	6wt% Tert-butyl Peroxy Benzoate	100°C 3 hours 130°C 6 hours
0.5g PESSGMA	10wt% Tert-butyl Peroxy Benzoate	100°C 3 hours 130°C 6 hours
PESSGMA/STY(70/30) 0.35 g PESSGMA +0.15g Styrene	4wt% Benzoyl peroxide	100°C 5 hours 130°C 3 hours 150°C 12 hours
PESSGMA/STY(70/30) 0.35 g PESSGMA +0.15g Styrene	6wt% Benzoyl peroxide	100°C 5 hours 130°C 3 hours 150°C 12 hours
PESSGMA/VPA(70/30) 0.35 g PESSGMA +0.15g Vinyl Phosphonic Acid	4wt% Benzoyl peroxide	100°C 5 hours 130°C 9 hours
PESSGMA/VPA(70/30) 0.35 g PESSGMA +0.15g Vinyl Phosphonic Acid	4wt% Benzoyl peroxide	100°C 5 hours 180°C 9 hours
PESSGMA/STY/VPA(70/15/15) 0.35 g PESSGMA +0.075 g Styrene + 0.075 g VPA	4wt% Benzoyl peroxide	100°C 5 hours 130°C 9 hours

PESSGMA/STY/VPA(70/15/15) 0.35 g PESSGMA +0.075 g Styrene + 0.075 g VPA	4wt% Benzoyl peroxide	100°C 5 hours 180°C 9 hours
---	--------------------------	--------------------------------

For the cure of the PESSGMA(K) polymers similar cure cycles were employed as listed in Table 4.2. However as will be discussed in the results and discussion section as well, the self polymerized PESSGMA and PESSGMA(K) samples cured under these conditions were found to be soluble in DMSO and therefore were not completely cured. In addition PESSGMA copolymers which were cured at the higher temperatures (*eg.* at 150-180°C) and which were insoluble in DMSO exhibited dark brown color and were quite brittle. Therefore longer times and lower temperatures were applied for the complete cure of the PESSGMA polymers in the following set of experiments. In addition the PESSGMA product obtained from the second method of synthesis (where the first step polycondensation reaction was run first in an FPS excess, then trace amount of BPA was added to produce the PESS polymer) was used in these experiments. The compositions of all the PESSGMA samples prepared and the curing conditions applied after curing optimization are listed in Table 4.3. The co-monomer content was again fixed at 30wt% for the PESSGMA/STY and PESSGMA/STY/VPA samples, however for the PESSGMA/VPA samples the VPA content was varied as 30, 40 and 50wt% of the total composition in order to increase the proton conductivity of the membranes. The (total monomer + polymer weight)/(volume of solvent) ratio was fixed at 1.5g /15mL. For each composition, a similar procedure was applied, all the ingredients were dissolved in DMSO, purged with N₂ gas for 5 minutes and the solution was poured into a petri-dish with a diameter of 5cm. The petri-dish with the solution was placed in a vacuum oven and the corresponding cure cycles were applied. For the self cure of the PESSGMA polymer, samples were also prepared using 2 and 3 wt% initiator to examine the effect of initiator content on proton conductivity of the PESSGMA membranes. All the PESSGMA polymers cured under these conditions were found to be insoluble in various solvents and in DMSO therefore cross-linked successfully. Thus, the PESSGMA obtained from the second method of synthesis and these optimized curing conditions were used for the preparation of all the PESSGMA polymer membranes for further characterization for use in DMFC applications. For the preparation of the PESS polymer films, the PESS polymer was also solvent cast using DMSO as the solvent (1.5g polymer/15mL solvent) and dried

in a vacuum oven at 100°C for 15 hours. All the films obtained, were cut into desired dimensions for the DMA and proton conductivity measurements and used for IEC analysis, swelling in water measurements, TGA and DSC analysis. For the preparation of the membranes for methanol permeability measurements, polymer solutions were poured into larger petri-dishes with a diameter of 9cm, cured under the same conditions and cut into desired dimensions for analysis.

Table 4.2. The compositions of all the prepared PESSGMA(K) samples and the curing conditions.

Composition	Initiator	Curing Conditions
0.5g PESSGMA(K)	4 wt% Tert-butyl Peroxy Benzoate	100 °C 3 hours 130 °C 3 hours
0.5g PESSGMA(K)	4 wt% Tert-butyl Peroxy Benzoate	100 °C 3 hours 130 °C 6 hours
0.5g PESSGMA(K)	6 wt% Tert-butyl Peroxy Benzoate	100 °C 3 hours 130 °C 6 hours
0.5g PESSGMA(K)	10 wt% Benzoyl peroxide	100 °C 3 hours 130 °C 6 hours
0.35g PESSGMA(K) +0.15 g Styrene	4 wt% Benzoyl peroxide	90 °C 5 hours 130 °C 3 hours
0.35g PESSGMA(K) +0.15 g Sodium 4- vinyl benzene sulfonate	4 wt% Benzoyl peroxide	90 °C 5 hours 130 °C 3 hours
0.35g PESSGMA(K) +0.15 g vinyl phosphoric acid	4 wt% Benzoyl peroxide	90 °C 5 hours 130 °C 3 hours

Table 4.3. The compositions of all the prepared PESSGMA samples and the curing conditions after curing optimization.

Composition	Initiator	Curing Conditions
1.5 g PESSGMA	2wt% Tert-butyl Peroxy Benzoate	100°C 5 hours 110°C 15 hours
1.5 g PESSGMA	3wt% Tert-butyl Peroxy Benzoate	100°C 5 hours 110°C 15 hours

1.5g PESSGMA	4wt% Tert-butyl Peroxy Benzoate	100°C 5 hours 110°C 15 hours
PESSGMA/STY(70/30) 1.05 g PESSGMA +0.45g Styrene	4wt% Benzoyl peroxide	100°C 5 hours 110°C 15 hours
PESSGMA/VPA(70/30) 1.05 g PESSGMA +0.45 g VPA	4wt% Benzoyl peroxide	100°C 5 hours 110°C 5 hours 120°C 10 hours
PESSGMA/VPA(60/40) 0.9 g PESSGMA +0.6 g VPA	4wt% Benzoyl peroxide	100°C 5 hours 110°C 5 hours 120°C 10 hours
PESSGMA/VPA(50/50) 0.75 g PESSGMA +0.75 g VPA	4wt% Benzoyl peroxide	100°C 5 hours 110°C 5 hours 120°C 10 hours
PESSGMA/STY/VPA(70/15/15) 1.05 g PESSGMA +0.225 g Styrene + 0.225 g VPA	4wt% Benzoyl peroxide	100°C 5 hours 110°C 5 hours 120°C 10 hours

In addition to the comonomers listed in Tables 4.1 - 4.3, sodium 4-vinyl benzene sulfonate (sulfonated styrene) was also used as the co-monomer for the crosslinking of PESSGMA and PESSGMA(K) polymers in the presence of 4wt% benzoyl peroxide via solution casting method using DMSO as the solvent. Samples were dried and polymerized at 90°C for 5 hours then at 130°C for 3 hours in a vacuum oven applying the same cure cycle used for the PESSGMA(K)/STY(70/30) sample. The intention of using this co-monomer was to acidify the resulting membranes to convert the styrene sodium sulfonate groups to sulfonic acid groups and improve the proton conductivity of the resulting membranes. However the sodium4- vinyl benzene sulfonate did not co-polymerize successfully with the PESSGMA or PESSGMA(K) polymer and phase separated at the end of the cure cycle. The films obtained had no mechanical integrity. Thus this co-monomer was no longer used for the cure of PESSGMA polymer. Films of PESSGMA(K) polymer cured with styrene, sodium4- vinyl benzene sulfonate (sulfonated styrene) and vinyl phosphonic acid are shown in Figure 4.10. Films of PESSGMA, PESSGMA/STY and PESSGMA/VPA polymers cured under the conditions listed in Table 4.3 are shown in Figure 4.11.

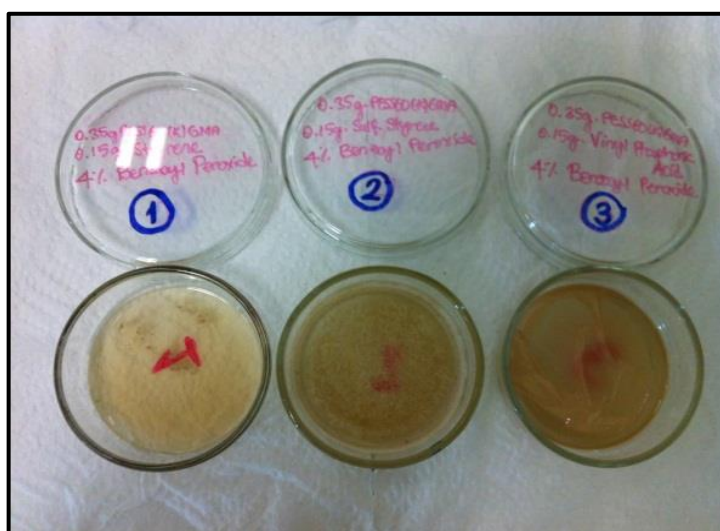


Figure 4.10. Films of PESSGMA(K) polymer cured with styrene(1), sodium4- vinyl benzene sulfonate (2) and vinyl phosphonic acid(3).

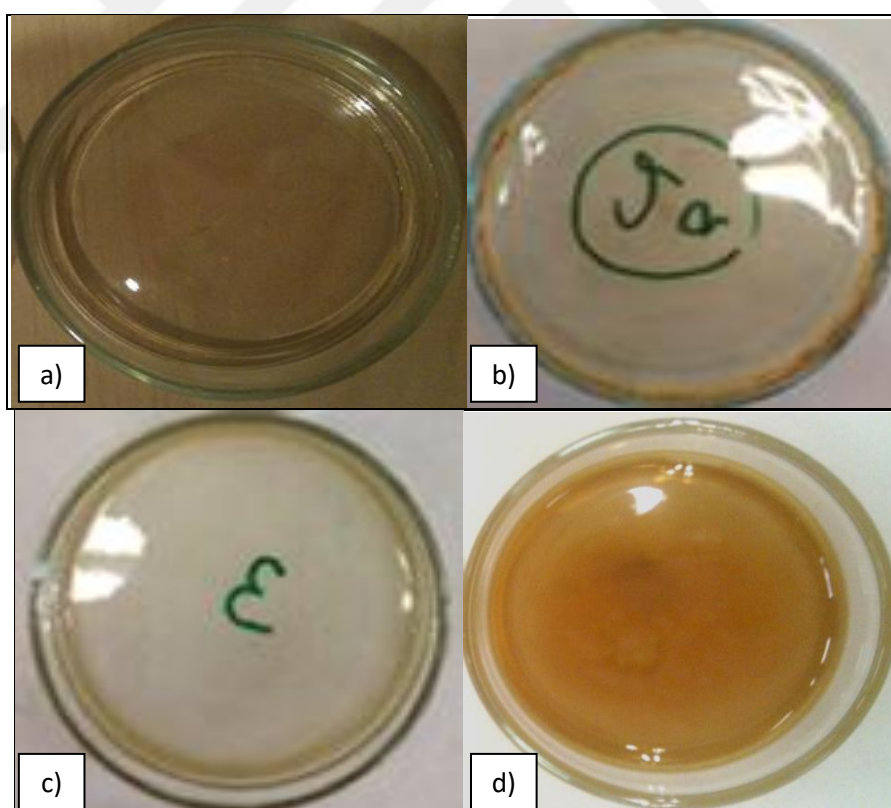


Figure 4.11. Films of a) PESSGMA(4wt% TBPB) polymer b) PESSGMA(3wt% TBPB) polymer c) PESSGMA/STY polymer d) PESSGMA/VPA polymer cured under the conditions listed in Table 4.3.

For the self polymerization of the PESSGMA polymer, tert-butyl peroxy benzoate was found to be the more effective initiator however tert-butyl peroxy benzoate was not able to cure the PESSGMA copolymers. Benzoyl peroxide was found to be the more effective initiator for the cure of the PESSGMA copolymers. Thus PESSGMA polymer membranes were prepared using tert-butyl peroxy benzoate as the initiator and PESSGMA copolymer membranes were prepared using benzoyl peroxide as the initiator.

4.4. CHARACTERIZATION OF PESS AND PESSGMA POLYMERS

4.4.1. FT-IR Analysis

In this work, FT-IR spectroscopy was mainly used to characterize the chemical structures of the synthesized PESS, PESS(K), PESSGMA, and PESSGMA(K) polymers and to follow the cross-linking reaction of the PESSGMA and PESSGMA(K) pre-polymers. All samples were run on an ATI Mattson Genesis Series FT-IR instrument. Firstly KBr pellets were prepared by pounding KBr using a mortar and pestle and applying pressure to it. For the PESS, PESS(K), PESSGMA and PESSGMA(K) polymers, the polymer was mixed with KBr and pellets were prepared in the same way. After a background scan was performed with the KBr pellet, the polymer containing pellets were also scanned in the 4000-450 cm^{-1} wavelength region, 16 times with a resolution of 4 cm^{-1} . For the cross-linked PESSGMA and PESSGMA(K) films, the IR scans were performed by placing the films on the IR beam path.

4.4.2. ^1H -NMR Analysis

In this work, ^1H -NMR spectroscopy was used to characterize the synthesized PESS, PESS(K), PESSGMA and PESSGMA(K) polymers. Samples were prepared for NMR analysis by dissolving ~0.1 g sample in ~1 mL deuterated dimethyl sulfoxide (DMSO-d_6). A Bruker AM250 instrument with a magnetic field strength of 250MHz was used as NMR spectrometer. A spectral window of 2000Hz, and a pulse width of 90° were used and the digital resolution was 0.427 Hz/pt. All measurements were carried at room temperature (25°C) and 32 scans of each sample were taken. MestRe-C NMR analysis software was

used to process the spectra. A Fourier transform was performed on the scans and the spectrum was phased. The relevant peaks were integrated to yield quantitative results.

4.4.3. Gel Permeation Chromatography (GPC) Analysis

Gel Permeation Chromatography (GPC) analysis of the PESS and PESSGMA polymers were performed in dimethyl formamide (DMF) at a flow rate of 0.7 ml/min, using a Agilent 1100 Series GPC modular system equipped with a refractive index detector. Stationary phase was PL-gel 5 μm , Mixed D type column and the mobile phase was 0.01M LiBr/DMF solution with flow marker toluene. The column was kept at 50°C. In order to prepare samples for GPC, 2mg sample was dissolved in 1 ml DMF and introduced to the GPC column, after being filtered with a teflon filter with pores of 0.45 μm . Linear poly(methyl methacrylate) standards were used for calibration ($M_p=2500\text{-}270,000$ g/mol).

4.4.4. Ion Exchange Capacity (IEC) Analysis

Ion exchange capacity (IEC) of the membranes was determined by titration method. Around 0.06g of the membrane film or 0.3g of the polymer in powder form was immersed in 50 mL of 1M NaCl solution and kept at 50 °C for 48 h to exchange H^+ ions with Na^+ ions. The solution was then titrated with a 0.1 M NaOH solution by using Phenolphthalein as an indicator to evaluate the released amount of H^+ . IEC value (meq g^{-1}) was calculated according to the following equation:

$$IEC = \frac{V_{\text{NaOH}} \times M_{\text{NaOH}}}{W_M} \quad (4.1)$$

where V_{NaOH} is the volume of the consumed NaOH solution (L) on titration, M_{NaOH} is the molarity of NaOH solution (0.1 M), and W_M is the dried membrane or polymer powder weight (g).

4.4.5. Swelling Tests

To measure the extent of swelling of the different membranes in water, they were first immersed in deionized water for 24 hrs to get rid of any unreacted monomer. And then, the films were dried in vacuum oven at 100°C for 4 hrs before immersing in deionized water at 25°C and 80°C for separate experiments. For the swelling experiments at 25°C, samples were weighed at 24hrs intervals for 400hrs, for the swelling experiments at 80°C samples were weighed only at the end of 24hrs. In each case, the excess water is wiped off gently with a tissue and the sample is weighed immediately. The membranes were again immersed in deionized water and the weighing procedure was repeated at the designated time intervals at 25°C. The weight percent change was calculated according to equation (4.2); where, m_f and m_i are the weights of the wet and dry membranes, respectively.

$$wt \% change = \frac{m_f - m_i}{m_i} \times 100 \quad (4.2)$$

4.4.6. Differential Scanning Calorimetry (DSC) Analysis

In this study, differential scanning calorimetry(DSC) was used to characterize the thermal transitions of the different polymer membranes. The DSC measurements were performed on a Perkin Elmer Differential Scanning Calorimeter in a nitrogen atmosphere. Up to 10mg of the samples in an aluminium pan covered with lids, together with the empty reference pan were scanned from 30°C to 300°C at a heating rate of 10°C/min. After the measurement, collected data was used to construct heat flow vs temperature plots which were then analyzed for the possible thermal transitions.

4.4.7. Dynamic Mechanical Analysis (DMA)

Dynamic mechanical analysis (DMA) was used to determine the thermo-mechanical properties of the different polymer membranes prepared in this study. For this purpose, the prepared polymer films were cut into rectangular pieces with dimensions of 25mm x 6mm x 0.15mm and scanned in a single frequency mode (1Hz) using a tension clamp with a temperature ramp from -50°C to 350°C at a heating rate of 5°C/min on a TAQ 800

Dynamic Mechanical Analyzer (TA Instruments LLC). The force applied was 0.01N. Two tests were performed for each sample. The collected data was used for the construction of storage modulus and loss modulus versus temperature plots.

4.4.8. Thermal Gravimetric Analysis (TGA)

The thermogravimetric analysis was conducted to investigate the thermal decomposition profiles of the prepared polymer membranes, using a Pyris 1 TGA (Perkin-Elmer) thermogravimetric analyzer. Samples of 5-10 mg were transferred into a nickel pan and heated under a nitrogen atmosphere from 30°C to 600°C with a heating rate of 10°C/min under N₂ (20 ml/min) flow. After measurements, weight% versus temperature (°C) graphs were plotted and analyzed.

4.4.9. Scanning Electron Microscopy (SEM) Analysis

The surface morphology of the polymer membranes was analyzed via scanning electron microscopy (SEM) using a Zeiss EVO 40 model instrument. In addition SEM was also used to examine if any phase separation occurred during the cure of the PESSGMA polymer with the co-monomers. The polymer membranes were all coated with Gold at a thickness of 15 nm, for 40 seconds as sputter coating time before analysis.

4.4.10. Proton Conductivity Measurements

The proton conductivities of the membranes were measured using an AC impedance spectrometer over the frequency range of 100mHz - 1MHz. A 5cm x 2.5cm membrane sample was placed between the plates in a temperature controlled cell open to air where the sample was equilibrated at 100% relative humidity. The membrane sample was sandwiched between the two voltage-sensing circular probes. A plate was mounted on the probes to keep the membrane under a constant pressure, thereby it provided good contact between the electrodes and the membrane. The conductivity cell was placed above liquid deionized water in the mid space of a sealed vessel as shown in Figure 4.12.

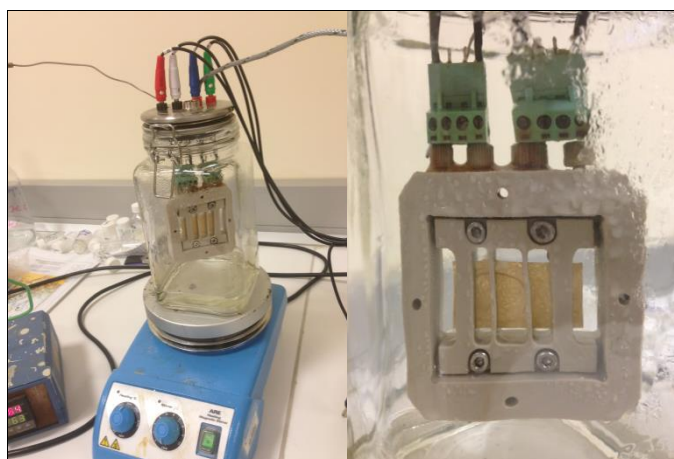


Figure 4.12. The proton conductivity measurement set-up (left) and the conductivity cell (right).

This experimental set-up allowed the membrane to equilibrate with saturated water vapor at desired temperature before the conductivity testing. The temperature was controlled by a feedback temperature controller. Proton conductivity measurements were conducted in 60°C and 80°C saturated water vapor for 48hrs. The resistance value that stabilized (at the end of around 48hrs) was recorded and the proton conductivity (σ) of the sample was calculated from equation(4.3), using the dimensions represented in Figure 4.13.

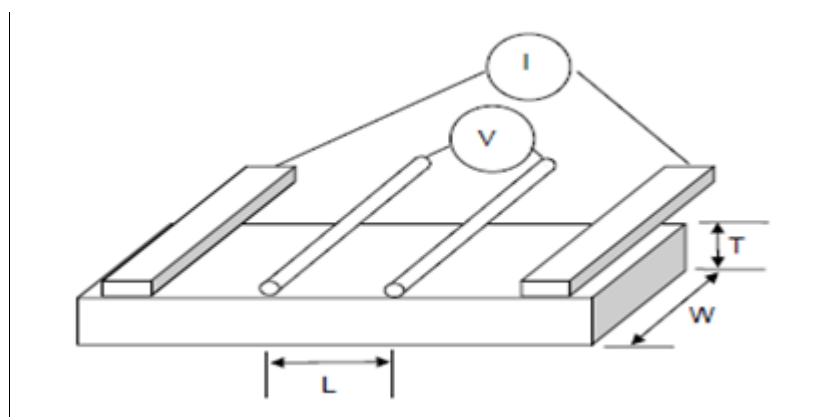


Figure 4.13. Representation of membrane dimensions for the proton conductivity measurement set up.

$$\sigma = \frac{L}{R * A} = \frac{L}{R * W * T} \quad (4.3)$$

$$\sigma(\text{mS}) = \frac{L(\text{mm}) * \left(\frac{1\text{cm}}{10\text{mm}}\right)}{R(\text{ohms}) * W(\text{mm}) * \left(\frac{1\text{cm}}{10\text{mm}}\right) * T(\text{microns}) * \left(\frac{1\text{cm}}{10,000\text{microns}}\right)} * \frac{1000\text{mS}}{1\text{S}}$$

where;

R: membrane bulk resistance (ohm),

L: thickness of two voltage-sensing probes in 4-probe (cm),

T: thickness of the membrane (cm),

W: width of the membrane (cm),

4.4.11. Methanol Permeability Measurements

The resistance to methanol crossover was evaluated by measuring the methanol permeability of the membranes. The methanol permeability of membranes was determined by using the Permagear horizontal side-by-side diffusion cell that consists of two-identical-compartments glass cell (A for feed and B for permeate) separated by a membrane. The membrane was placed between the two compartments and then clamped as shown in Figure 4.14. The effective membrane area was 1.8cm^2 . Compartment A was filled with 5M methanol (6mL) and compartment B with deionized water (6mL). Both the compartments having equal volume were kept under continuous stirring conditions by magnetic stirrers at 60°C during the measurement. To investigate the methanol permeability, liquid samples of $100\mu\text{L}$ were taken from the permeate side using a syringe at certain time intervals and analyzed by using gas chromatography. The methanol permeability was calculated by using Equation 4.4;

$$-\ln\left(1 - \frac{2C_B}{C_{A0}}\right) = \frac{2A_M DK}{V_o L} t \quad (4.4)$$

where $C_{A0}(\text{mol L}^{-1})$ is the initial methanol concentration (5M), $C_B(\text{mol L}^{-1})$ is the methanol concentration in B compartment at time t (s), V_o is the initial volume (6mL), A_M is the

effective membrane area (1.8cm^2), L is the membrane thickness (cm). There is a linear relationship between $\ln\left(1 - \frac{2C_B}{C_{A0}}\right)$ and time(t), thus, the methanol permeability ($P=DK(\text{cm}^2/\text{s})$) was obtained from the slope of the $\ln\left(1 - \frac{2C_B}{C_{A0}}\right)$ vs time plots.

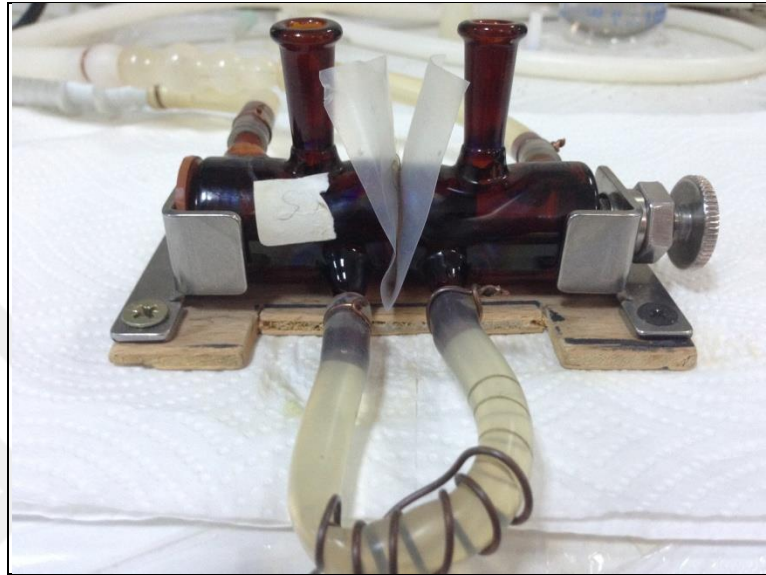


Figure 4.14. Two-compartment diffusion cell used in methanol permeability measurements.

5. POLY(ARYL ETHER SULFONE) (PESS) AND METHACRYLATED POLY (ARYL ETHER SULFONE) (PESSGMA) SYNTHESIS AND CHARACTERIZATION

In the first part of the synthesis, partially sulfonated polyarylether sulfone (PESS) polymer and its potassium salt PESS(K) were prepared. For this purpose, 20 mmol of 4-Fluorophenyl sulfone (FPS), 8.8 mmol of Bisphenol A (BPA), 12 mmol of hydroquinone 2- potassium sulfonate (HPS) and 40 mmol of potassium carbonate were reacted in a mixture of dimethyl acetamide(DMA), toluene and dimethyl sulfoxide (DMSO). Toluene was used for azeotropic distillation of water during reaction at 150°C. After 4 hours at 150°C, the temperature was raised to 180°C and the reaction was continued at this temperature for 10 hours to complete the polymerization. At the end of the reaction time, the PESS product was precipitated and the purification steps were performed. Although last steps of purification which were precipitation of the polymer in HCl solution and methanol and then extraction of inorganic compounds were performed for synthesis of PESS to obtain the polymer in acidic form with SO₃H substituents, these steps were not performed for synthesis of PESS(K) to get the potassium salt of sulfonate groups. Additionally, as explained in the experimental section, in an effort to decrease the inhibition effects of sulfonic acid groups on radical polymerization for the final product, a modified procedure for the PESS synthesis was also performed. In this procedure, PESS synthesis was carried out first in a slight excess of FPS under similar reaction conditions for 4 hours at 150°C and then for 10 hours at 180°C and then an additional amount of BPA was added and reaction was continued for an additional time of 4 hours at 180°C to ensure that the partially sulfonated polyarylether sulfone (PESS) chains were all BPA terminated. The chemical structures of all the synthesized PESS and PESS (K) polymers were confirmed by FT-IR and ¹H-NMR spectroscopy and molecular weight was determined via GPC. For the synthesis of the PESSGMA and PESSGMA(K) polymers, the PESS or PESS(K) polymer was reacted with glycidyl methacrylate under similar reaction conditions (6 hours at 60°C with DABCO as catalyst) to convert the aromatic hydroxylends of the PESS or PESS(K) polymer to glycidyl methacrylate esters. The chemical structures of all the synthesized PESSGMA and PESSGMA(K) polymers were also characterized via FT-

IR and $^1\text{H-NMR}$ spectroscopic techniques and molecular weight of these polymers was determined via GPC.

5.1. CHARACTERIZATION OF THE PESS AND PESSGMA POLYMERS VIA FT-IR SPECTROSCOPY

The FT-IR spectrum of the synthesized PESS polymer is shown in Figure 5.1. The broad absorption band in the 3441 cm^{-1} region shows the aromatic hydroxyl end groups. The several peaks in the $2900\text{-}3000\text{cm}^{-1}$ region seen on the broad hydroxyl band can be attributed to the sulfonic acid groups ($-\text{SO}_3\text{H}$) on the polymer chain. The sharp peaks at 1586 , 1489 and 1472 cm^{-1} correspond to vibrations of the aromatic rings on the polymer backbone. The characteristic peaks of the various aryl oxides (Ar-O-Ar) appears as a broad band at 1247 cm^{-1} and the characteristic absorption of the aromatic sulfone (Ar-(S=O)=O-Ar) occurs at 1149cm^{-1} . The two peaks at 1074 and at 1013 cm^{-1} are attributed to the aromatic sulfonate group ($-\text{SO}_3$) stretching vibrations. The presence of the characteristic functional groups of the PESS polymer in this spectrum is an indication of the successful synthesis of the PESS polymer. PESS polymer synthesized from both of the procedures described in the experimental section exhibited similar spectra.

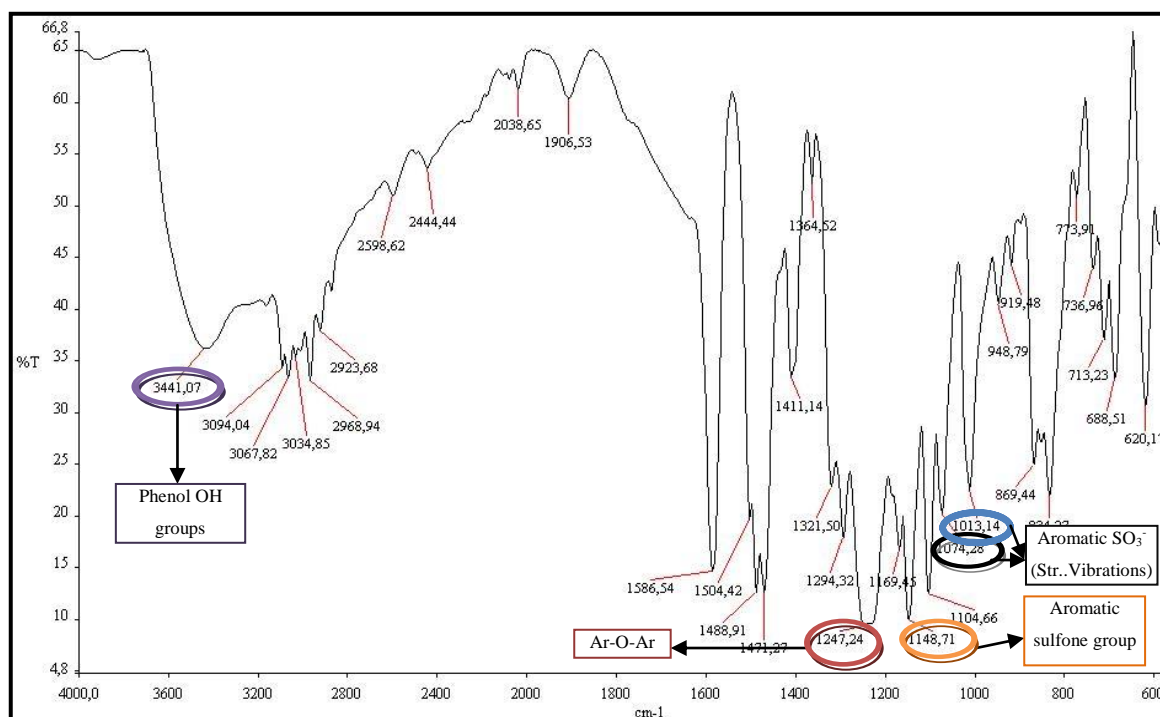


Figure 5.1. FT-IR spectrum of the PESS polymer.

For the synthesis of the PESSGMA, the PESS polymer was reacted with glycidyl methacrylate to convert the aromatic hydroxyls of the PESS polymer to glycidyl methacrylate esters. The FT-IR spectrum of the PESSGMA polymer is shown in Figure 5.2. As can be seen, in addition to the characteristic peaks listed for the FT-IR spectrum of the PESS polymer, this spectrum also shows the 1716 cm⁻¹ peak which is attributed to the carbonyl stretching vibration (C=O) and the 1638cm⁻¹ peak which should belong to the CH₂=C< double bond stretching vibration of the GMA moiety. In addition the absence of the epoxide peak of the GMA which should appear at around 917cm⁻¹ confirms the conversion of GMA to its ester (PESSGMA). The broad hydroxyl band this time at 3434cm⁻¹ is still present in this spectrum since although the aromatic hydroxyls should be consumed through reaction with GMA, a new aliphatic hydroxyl (>CH-OH) is produced for the PESSGMA product as shown in Figure 4.5. All this data confirms the formation of the PESSGMA polymer. The PESSGMA obtained from both of the procedures described in the experimental section again exhibited similar spectra.

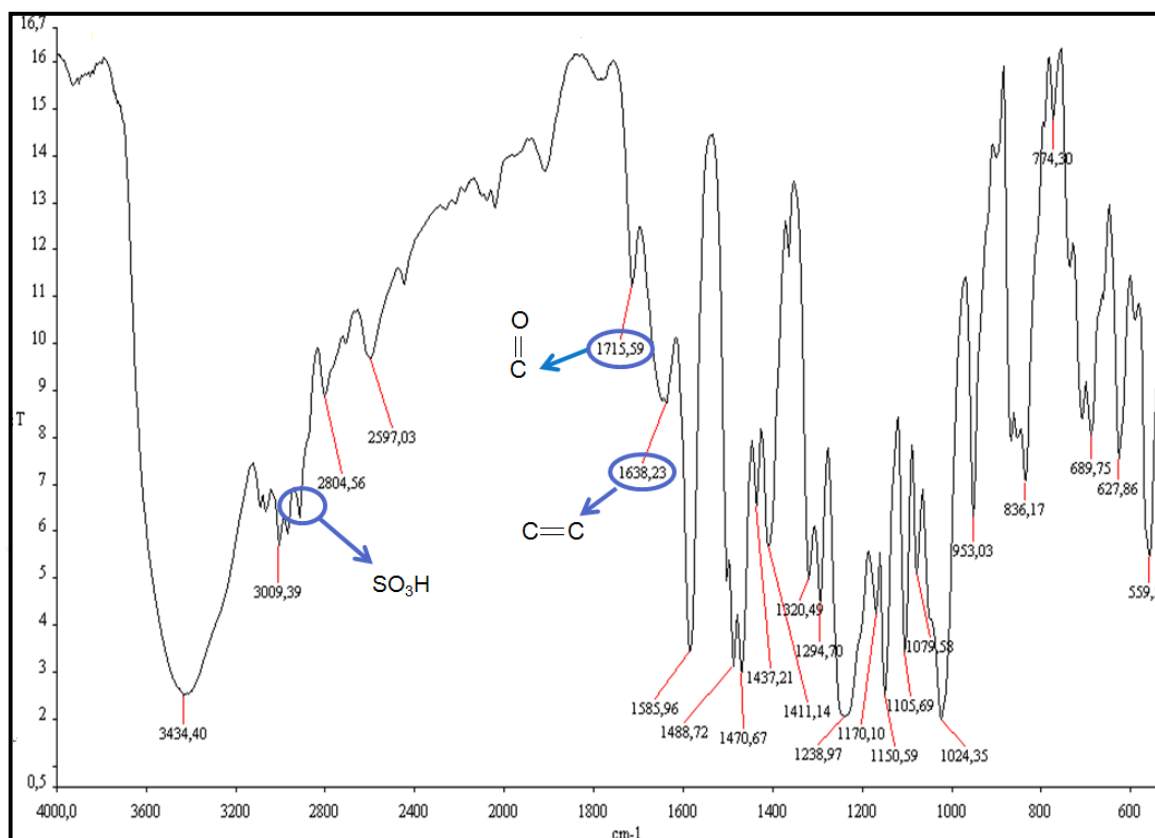


Figure 5.2. FT-IR spectrum of the PESSGMA polymer.

5.2. CHARACTERIZATION OF THE PESS AND PESSGMA POLYMERS VIA ^1H -NMR SPECTROSCOPY

The ^1H -NMR spectrum of the PESS polymer (synthesized with the first procedure) is presented in Figure 5.3. The peak at 1.65 ppm represents the methyl protons of the Bisphenol A in the polymer backbone. The peaks in the 6.95 to 7.20 ppm region show the aromatic protons that are in ortho (*-o*) position to the oxide and sulfone groups on the polymer chain. The 7.25 ppm peak should show the aromatic protons that are in *o*- position to the tert- butyl group of the BPA. The peak at 7.45 ppm is attributed to the aromatic sulfone proton that is in *-o* position to the hydroquinone sulfonic acid oxide as shown in the figure. The multiple peaks in the 7.80-8.00 ppm region on the other hand, should denote the hydroquinone sulfonic acid aromatic protons and the aromatic sulfone protons in *o*-position to the hydroquinone sulfonic acid structure. While the strong peak at 2.5 ppm shows the residual protons of the NMR solvent (dimethyl sulfoxide d_6), the strong peak at 3.7 ppm represents the residual methanol or water protons. The copolymer composition was

also confirmed via $^1\text{H-NMR}$ analysis. For the PESS synthesis the sulfonated and non-sulfonated diols were used in a ratio of 0.6 :0.44. The resulting copolymer composition of the PESS polymer was also confirmed via $^1\text{H-NMR}$ analysis through integration of the necessary proton peaks.

Theoretically for the PESS polymer, the peak integration ratio of the aromatic hydrogen peak at 7.45ppm labeled as A and the methyl protons peak at 1.65 ppm labeled as B in Figure 5.3, (A/B) should give the copolymer composition. The peak integration of the two peaks in this spectrum gives a ratio ($0.60/2.40=0.25$). This ratio gives the sulfonated repeating unit to non sulfonated repeating unit mol ratio of 0.60:0.40 for this product. Thus according to the $^1\text{H-NMR}$ analysis, the PESS polymer contains about 60% mole of sulfonated repeating unit.

All these data confirm that the PESS polymer was successfully prepared. The PESS product synthesized with the second procedure, exhibited a similar spectrum with the same characteristic peaks and therefore not shown. A similar quantitative analysis of this product's spectrum gave the sulfonated repeating unit to non sulfonated repeating unit mol ratio of around 0.60:0.40. In addition the analysis of the $^1\text{H-NMR}$ spectra of other PESS products produced with the same method all indicated that the sulfonated repeating unit to non sulfonated repeating unit mol ratio was around 0.60:0.40 as well.

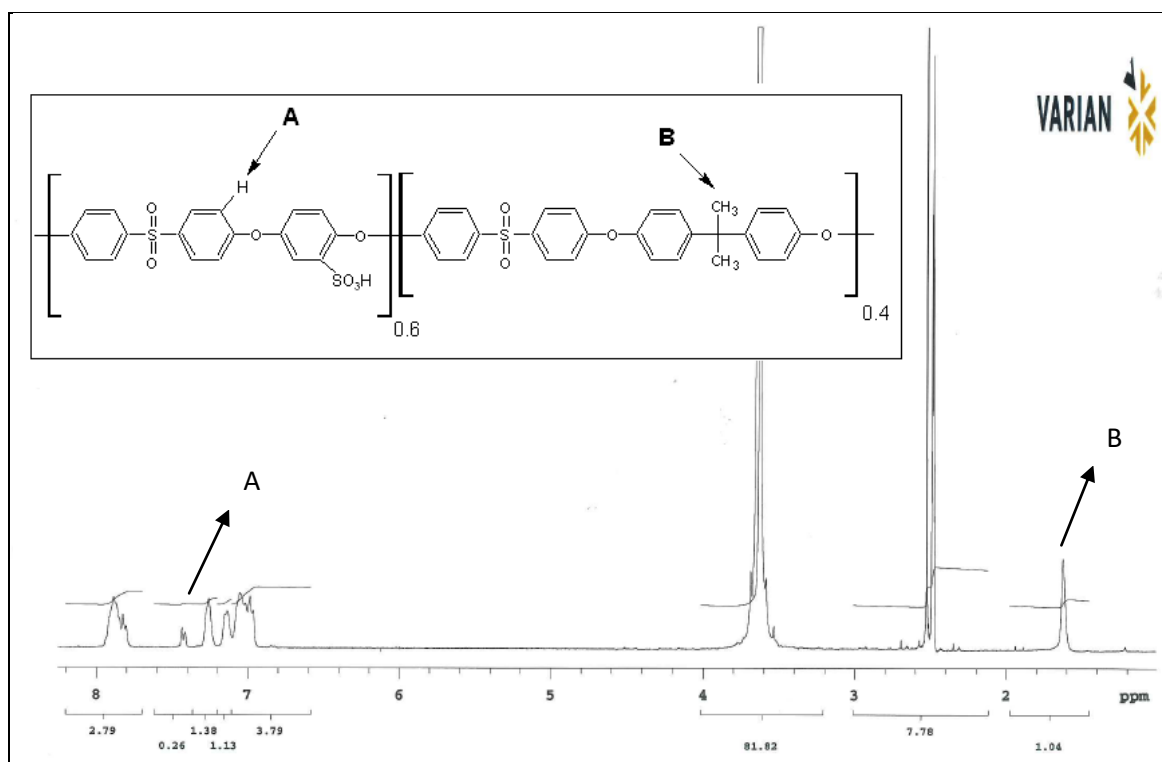


Figure 5.3. The $^1\text{H-NMR}$ spectrum of the PESS polymer.

The $^1\text{H-NMR}$ spectrum of the PESSGMA polymer (synthesized with the first procedure) is presented in Figure 5.4. (a). This spectrum has some additional peaks that are characteristic of the GMA moiety at 1.9, 3.9, 4.1, 5.65 and 6.1 ppm respectively. These peaks have a lower intensity than the peaks of the polymer backbone since the GMA is attached only to the ends of the main polymer chain. Therefore a magnified version of this spectrum is given in Figure 5.4.(b) with the peak assignments for the various protons of the GMA moiety. Thus the $^1\text{H-NMR}$ analysis in addition to the FT-IR data confirms the successful synthesis of the PESSGMA polymer. The $^1\text{H-NMR}$ spectrum of the PESSGMA polymer synthesized with the second procedure also exhibited a similar spectrum with the same characteristic peaks and therefore not shown.

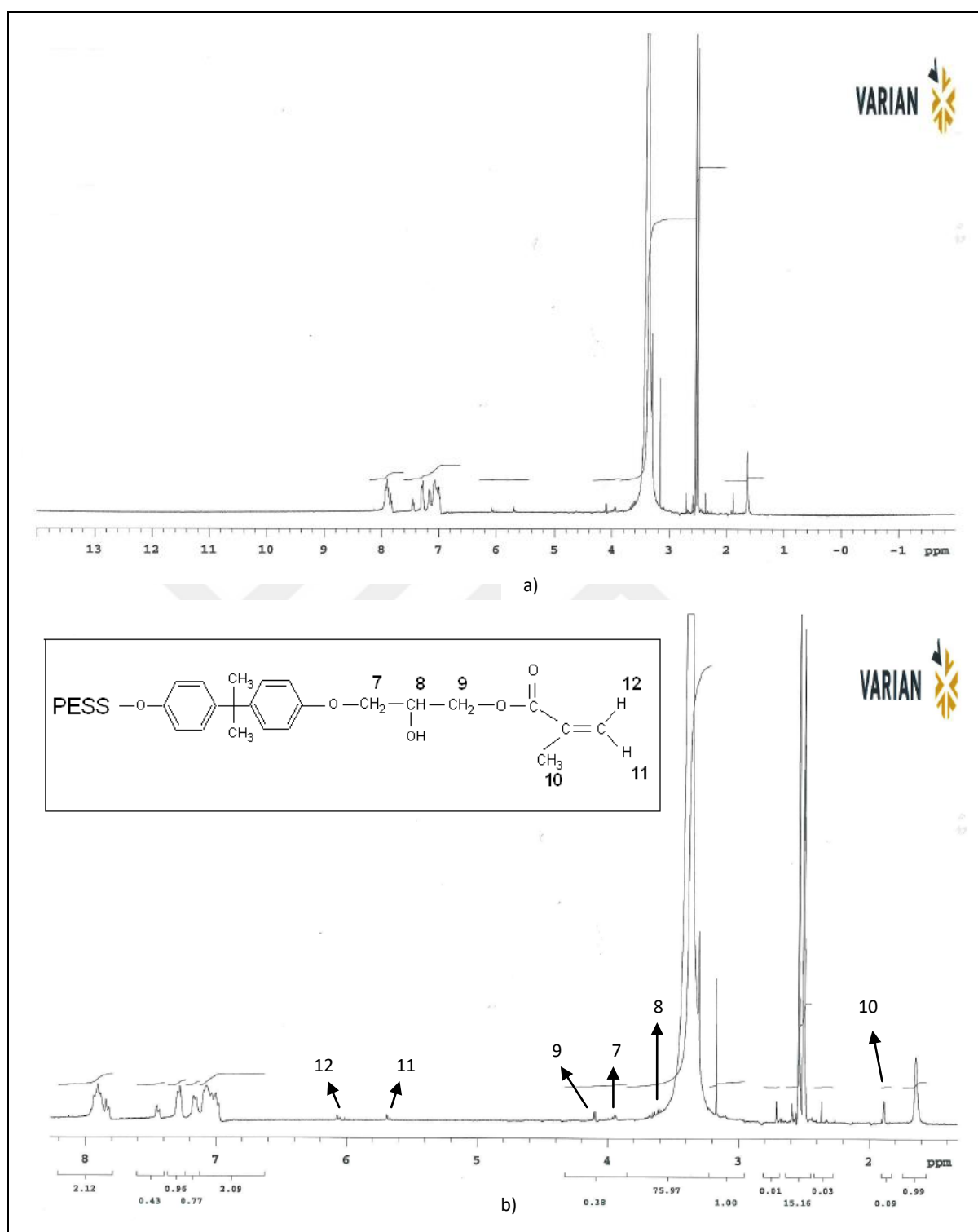


Figure 5.4. The $^1\text{H-NMR}$ spectrum of (a) the PESSGMA polymer and (b) its magnified version.

5.3. CHARACTERIZATION OF THE PESS(K⁺) AND PESSGMA(K⁺) POLYMERS VIA FT-IR AND ¹H-NMR SPECTROSCOPY

The FT-IR spectrum of the synthesized PESS(K) polymer is shown in Figure 5.5. Although, the characteristic functional groups of the PESS(K) polymer indicate absorbance at approximately similar wavelengths as those of the PESS polymer, an absorption peak at 1635 cm⁻¹ is more obvious in the PESS(K) spectrum. This peak may show an aromatic C=C stretching vibration shifted to higher wavelength due to the presence of SO₃K group.

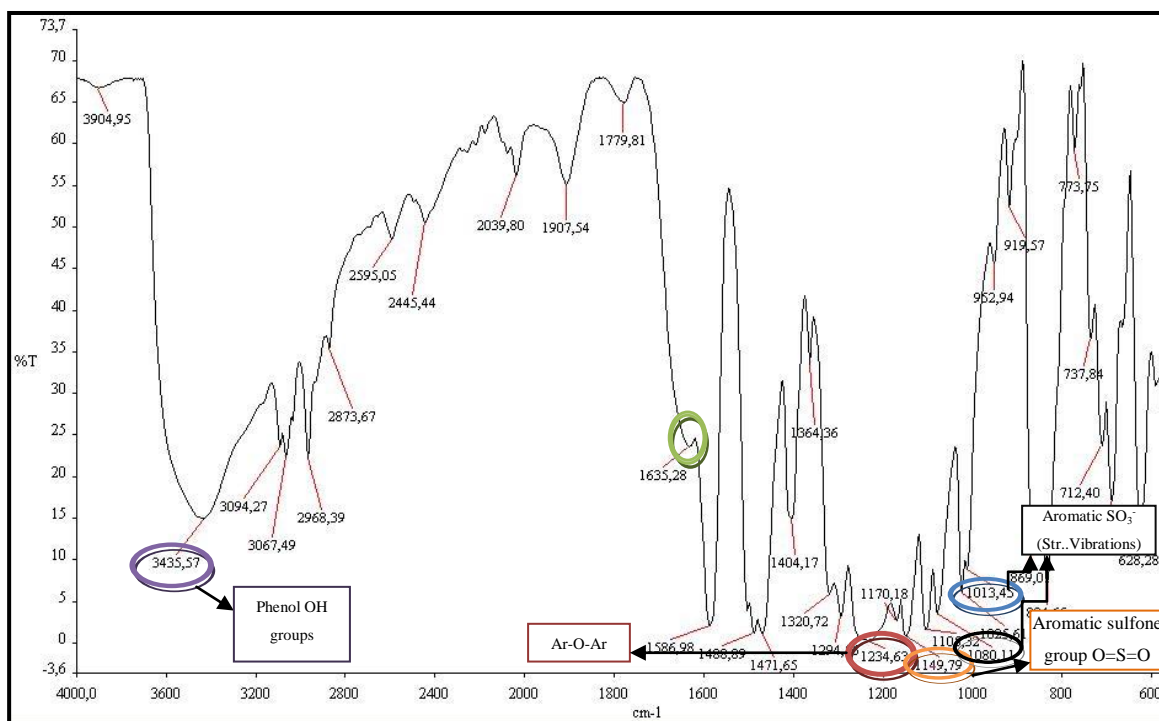


Figure 5.5. The FT-IR spectrum of the PESS (K) polymer.

The ¹H-NMR spectrum of the PESS(K) polymer is presented in Figure 5.6. As shown in Figure 5.6, the spectrum of the PESS(K) polymer is identical to that of the PESS polymer with the same peak assignments and similar integral ratios.

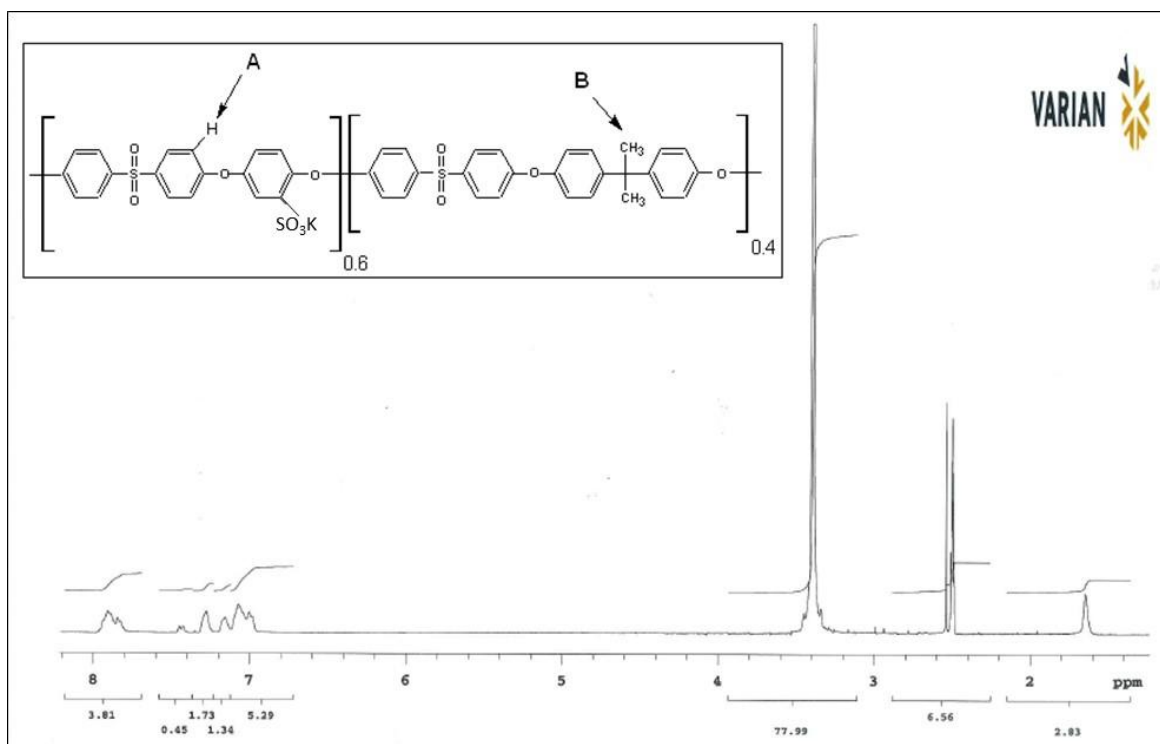


Figure 5.6. The ¹H-NMR spectrum of the PESS(K) polymer.

The FT-IR spectrum of the PESSGMA(K) polymer is shown in Figure 5.7. When the spectrum of PESSGMA (K) is analyzed, the characteristic peaks are rather broad and it is seen that the peak at around 1630 cm^{-1} is more intense than the 1638 cm^{-1} peak of the PESSGMA polymer which shows the C=C stretching vibration of the GMA moiety. As mentioned above, a peak at 1635 cm^{-1} was also present in the PESS(K) spectrum which was attributed to the C=C stretching vibration of an aromatic ring containing the SO₃K groups. Thus the appearance of these two peaks in the 1630 cm^{-1} region for the PESSGMA(K) polymer results in a broad and intense peak at this wavelength. Therefore, the peak of carbonyl (C=O) stretching vibration occurs only as a shoulder on the 1635 cm^{-1} peak. Other peak assignments can be made in a similar manner to that of the PESSGMA IR spectrum. The absence of the epoxide peak of GMA which should appear at around 917 cm^{-1} in this spectrum also confirms the conversion of GMA to its ester.

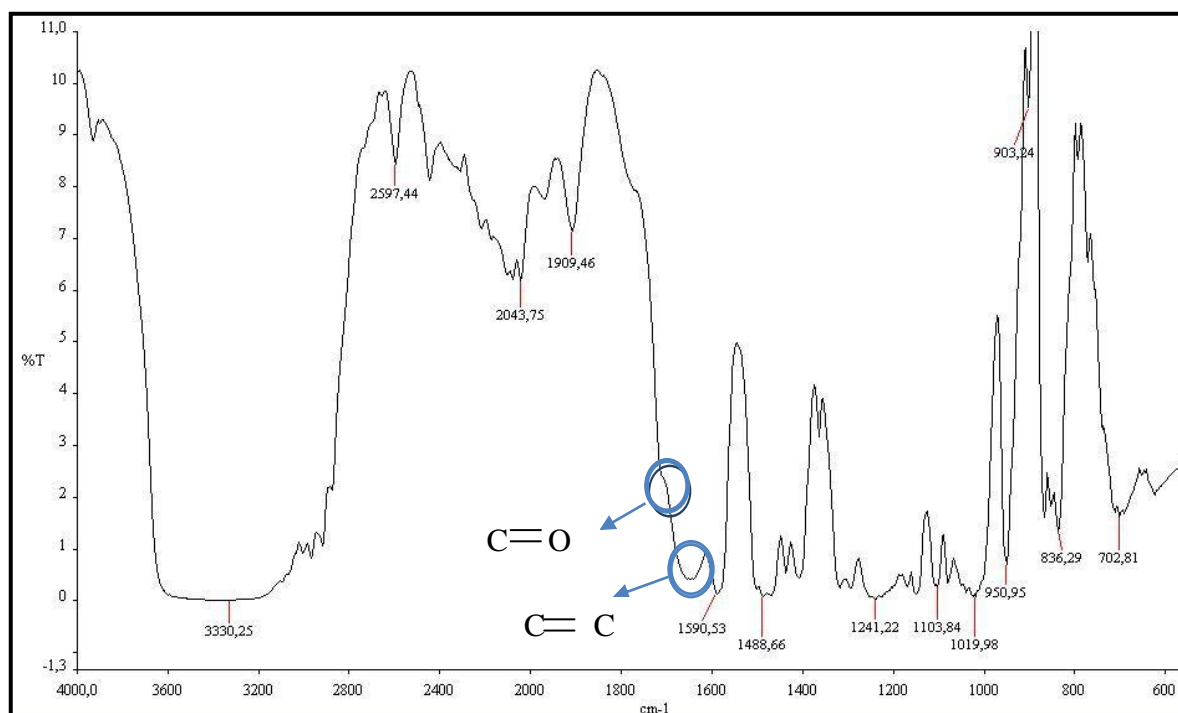


Figure 5.7. FT-IR spectrum of the PESSGMA (K) polymer.

The $^1\text{H-NMR}$ spectrum of the PESSGMA(K) polymer is presented in Figure 5.8. When the spectrum was investigated, it was seen that while the peak at 3.9 ppm present in the PESSGMA spectrum, showing the $-\text{CH}_2-$ protons attached to the Bisphenol A or hydroquinone potassium sulfonate phenol O atom is considerably weakened, a new peak at 4.5 ppm is present in the PESSGMA(K) spectrum. It is believed that in the reaction of the PESS(K) polymer with GMA, instead of the phenol OH end groups of the PESS(K) polymer, the $\text{SO}_3(\text{K})$ groups have reacted with GMA via an addition reaction to form the glycidyl methacrylate esters (where the SO_3^- group acted as a stronger nucleophile than the phenol OHs.). Thus the peak at 4.5 ppm should show the $-\text{CH}_2-$ protons attached to the SO_3 groups present on the polymer chain. The possible structure of the PESSGMA(K) polymer with the peak assignments is shown in Figure 5.8. The presence of the weak peak in the 3.9- 4.0 ppm region peak shows that product formed via the addition of the GMA to the phenol OHs occurred to a very limited extent.

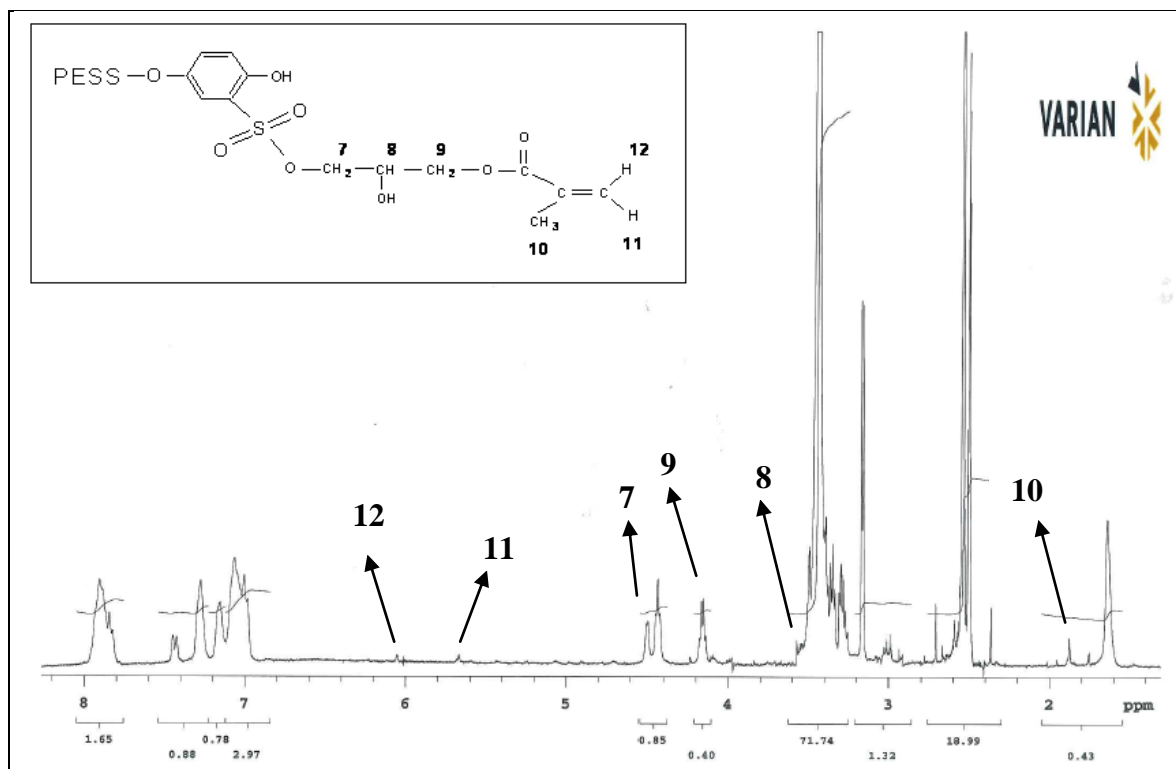


Figure 5.8. The ^1H -NMR spectrum of the PESSGMA(K) polymer.

5.4. GPC ANALYSIS OF THE PESS AND PESSGMA POLYMERS

The molecular weight data as determined from GPC analysis for the PESS and PESSGMA polymers synthesized by the two methods described in the experimental section, is given in Table 5.1. As can be seen the BPA terminated PESS polymer synthesized with the second method (PESS(2)) exhibited a lower molecular weight than the PESS polymer synthesized in an excess of the diol monomers with the first method (PESS(1)). If only the first part of the reaction between FPS and the diol monomers (BPA and HPS) carried out at 150°C for 4 hours then at 180°C for 10 hours was considered, as long as conversions are similar one may expect a higher molecular weight for the polymer synthesized for the 2nd method according to Carother's Equation, as the stoichiometric excess of one monomer of the 2nd method is less than that of the 1st method. The lower molecular weight of the PESS polymer synthesized with the second method may be attributed to the effect of BPA addition to FPS terminated polymer chains especially to lower molecular weight chains (for reaction of an additional time of 4 hours at 180°C) which may have changed the molecular weight distribution and decreased the number average molecular weight.

Interestingly the addition of GMA to the PESS polymers synthesized by the two methods both led to a larger molecular weight increase than would be expected for GMA addition to only chain ends (eg +12,518g/mol for PESS(1) and 35,023g/mol for PESS(2)). In addition for the PESS polymer synthesized by the second method the molecular weight is nearly doubled when reacted with GMA to form the PESSGMA product. Some radical reactions through methacrylate double bonds, such as di-merization may be responsible for the increase of molecular weight as polycondensation reaction at 60°C (the temperature of the reaction between PESS and GMA) is not possible. However as discussed earlier, the methacrylate functionality of the PESSGMA pre-polymer is still present as demonstrated by FT-IR and ¹H-NMR spectroscopy. Further analysis is necessary for the exact structural identification of the PESSGMA pre-polymer and the structures depicted in Figure 2.16(b) and Figure 4.5 are idealized structures. The molecular weight of the PESSGMA(K) synthesized with the 1st method on the other hand was lower than the molecular weight of both PESSGMA(1) and PESSGMA(2).

Table 5.1. The molecular weight data of the PESS and PESSGMA polymers as determined from GPC analysis. (\bar{M}_n is number average molecular weight, \bar{M}_w is weight average molecular weight and \bar{D} is the polydispersity index)

Polymer	\bar{M}_n (g/mol)	\bar{M}_w (g/mol)	\bar{D}
PESS(1)	50642	74956	1.480
PESSGMA(1)	62980	88200	1.400
PESSGMA(K)(1)	28667	39839	1.390
PESS(2)	35342	54310	1.537
PESSGMA(2)	70365	98946	1.406

(1): 1st method of PESS synthesis, (2): 2nd method of PESS synthesis

6. STRUCTURAL CHARACTERIZATION OF CROSS-LINKED PESSGMA POLYMERS

In this study in addition to the structural characterization of the PESS and PESSGMA polymers, FT-IR spectroscopy was also used to confirm the polymerization of the PESSGMA polymer after self cure or cure with styrene and vinyl phosphonic acid by following the intensity of the peaks that correspond to vinyl stretching vibrations of both glycidyl methacrylate moiety of the PESSGMA polymer and the co-monomers. In addition, FT-IR spectroscopy was also used to confirm the condensation reactions that occurred between the hydroxyl groups of PESSGMA and VPA for the PESSGMA/VPA or PESSGMA/STY/VPA polymers. In this section, first a detailed analysis of the FT-IR spectra of the PESSGMA and PESSGMA(K) samples cured under the conditions listed in initial trials will be presented, then FT-IR spectroscopic analysis of the PESSGMA polymers (synthesized with the second procedure) cured under optimized conditions will also be discussed. In addition the Ion Exchange Capacity (IEC) of the PESS and PESSGMA polymers which give additional information about the structure of these polymers will also be presented. Finally results of swelling in water both at room temperature and at 80°C for the PESS and PESSGMA polymers cured under optimized conditions will be given and discussed. The swelling results will be used to both confirm the cross-linked structures of the PESSGMA polymers and compare the degree of cross-linking for the different PESSGMA polymers.

6.1. FT-IR ANALYSIS

To polymerize the PESSGMA and PESSGMA(K) pre-polymers via radical polymerization through the GMA functionality attached to the polymer chains, DMSO solutions of monomers (PESSGMA or PESSGMA(K) with or without co-monomers) were cast into films in the presence of a radical initiator into petri dishes and dried under vacuum at the specified conditions as explained in the experimental section. Also as discussed in the experimental section, the potassium salt form of the PESS polymer was reacted with glycidyl methacrylate and PESSGMA(K) polymer was prepared and self-polymerized and copolymerized with styrene and vinyl phosphonic acid in an effort to examine and prevent the possible inhibiting effect of sulfonic acid groups on radical polymerization.

However, as the addition of GMA to the potassium salt of the PESS polymer led to glycidyl methacrylate addition to sulfonate groups that is undesirable, this route was not explored further for preparation of membranes. But still, the FT-IR spectroscopic analysis of both the polymerized PESSGMA and PESSGMA(K) polymers and copolymers will be presented with comparisons of the spectra of the different polymer membranes.

The pre-polymer, comonomer and initiator concentrations as well as the cure conditions examined in the initial trials for the cure of the PESSGMA and PESSGMA(K) pre-polymers were given in Table 4.1 and Table 4.2 respectively in the Experimental Section. The compositions of the PESSGMA films prepared and the optimized cure conditions applied were presented later in Table 4.3. During the drying process, the reactive groups of pre-polymers and monomers reacted in the presence of a radical initiator by thermal initiation via radical polymerization. The radical polymerization of the pre-polymers in the absence or presence of comonomers was demonstrated via FT-IR spectroscopy and the extent of polymerization was compared for different compositions and cure conditions as will be presented in the following sections.

6.1.1. Self Polymerization of PESSGMA and PESSGMA(K)

All self polymerizations of pre-polymers PESSGMA and PESSGMA (K) were performed in presence tert-butyl peroxy benzoate initiator, but percent of initiator used was changed. In addition to changing percent of initiator, drying conditions were also varied as listed in Table 4.1.

Firstly 0.5 g PESSGMA was self-polymerized with 4% tert-butyl peroxy benzoate by drying under vacuum at 100°C for 3 hours and then 130°C for 3 hours. The FT-IR spectrum of the self-polymerized PESSGMA with 4% of initiator under these conditions is shown in Figure 6.1. The functional groups of the PESSGMA polymer are seen in this spectrum. However, when compared to the FT-IR spectrum of the PESSGMA product (Figure 5.2) a considerable decrease in intensity of the 1638 cm⁻¹ peak which indicates CH₂ = C< double bond stretching vibration is analyzed. The loss of intensity of this peak is expected because during the polymerization reaction of the pre-polymer, the double bond (CH₂ = C<) of the GMA moiety is consumed and become saturated. However due to

the presence of the residual peak in the 1630cm^{-1} region, it can be said that the complete polymerization was not achieved.

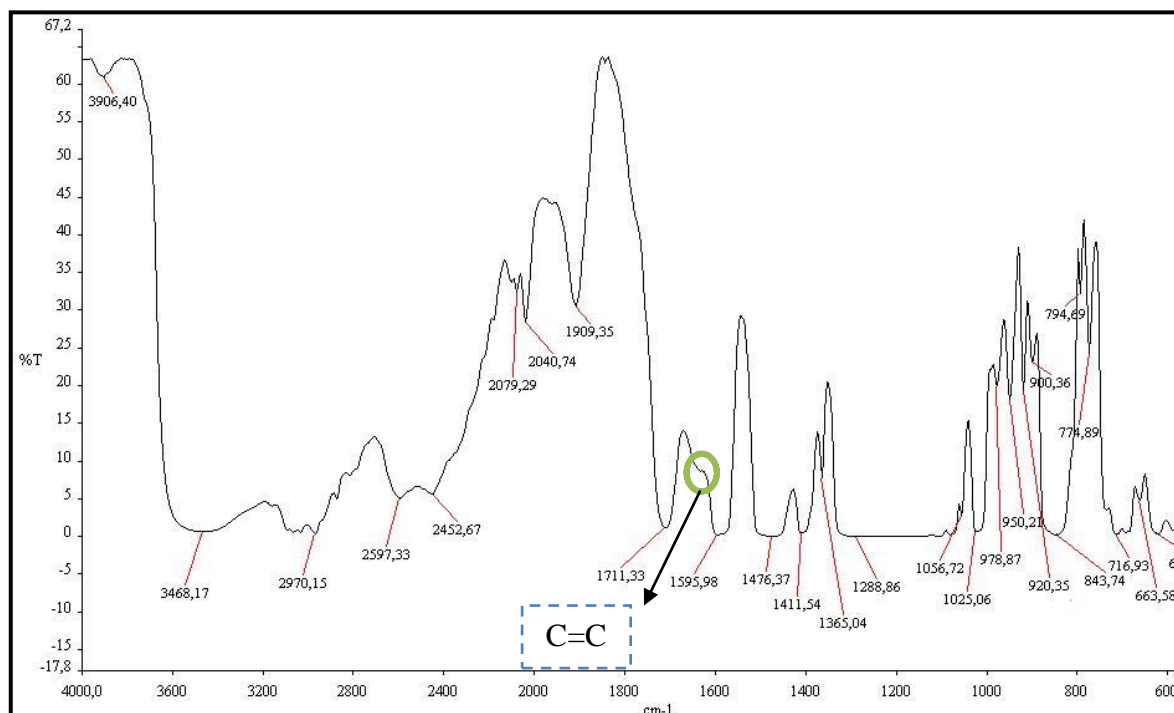


Figure 6.1. The FT-IR spectrum of PESSGMA polymerized with 4% of tert-butyl peroxy benzoate (100°C for 3 hours, 130°C for 3 hours).

Secondly, self polymerization of 0.5 g of PESSGMA(K) with 4% of tert-butyl peroxy benzoate was performed at the same drying conditions of self polymerization of PESSGMA with 4% of initiator. The FT-IR spectrum of the PESSGMA (K) polymerized with 4% of initiator is shown in Figure 6.2. The spectrum shows that the 1630cm^{-1} peak intensity is considerably decreased as compared to the spectrum of the PESSGMA (K) polymer (Figure 5.7), and is seen as a shoulder on the 1593cm^{-1} peak, however a comparison for the consumption of this peak for the radical polymerized PESSGMA and PESSGMA(K) polymers is not possible, since the peaks in the region are quite broad.

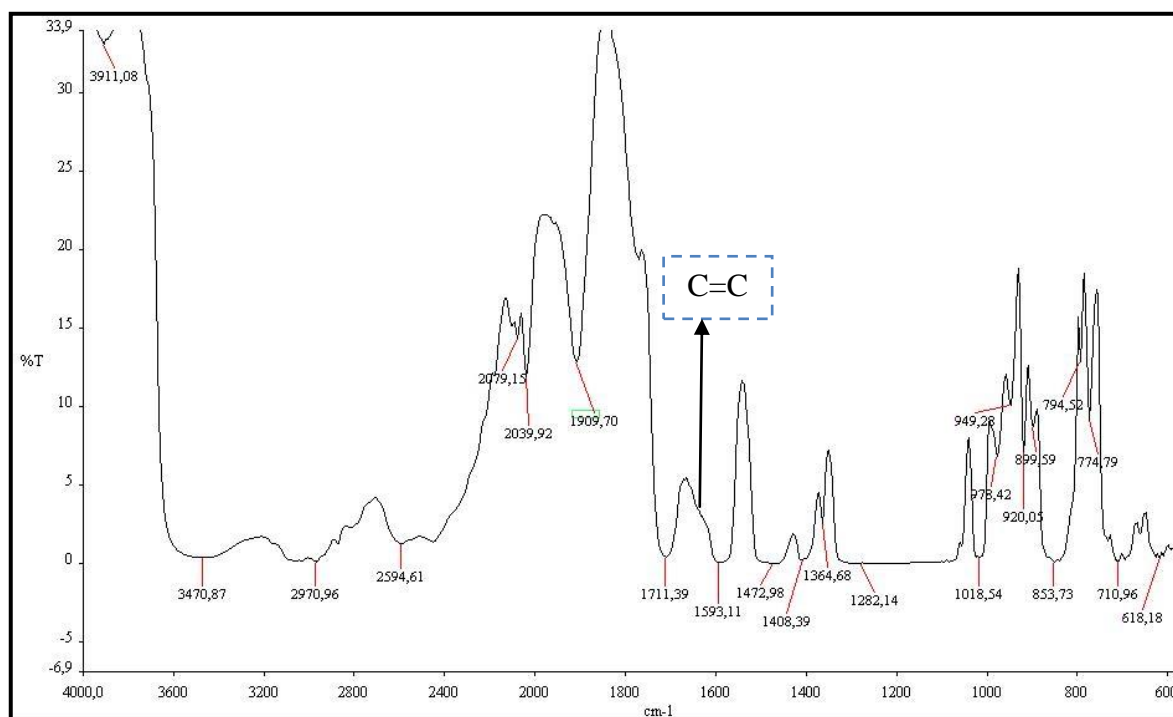


Figure 6.2. The FT-IR spectrum of PESSGMA(K) polymerized with 4% of tert-butyl peroxy benzoate (100°C for 3 hours, 130°C for 3 hours).

The self-polymerized PESSGMA (K) sample was kept at 130°C for an additional time of 3 hours for further polymerization. The FT-IR spectrum of the PESSGMA(K) polymerized with 4% Tert-butyl peroxy benzoate and dried for 3 hours at 100°C and 6 hours at 130°C is shown in Figure 6.3. The residual peak in the 1630 cm⁻¹ region is still present in this spectrum indicating that cross-linking of the PESSGMA(K) pre-polymer is incomplete. The presence of a new peak at 1754 cm⁻¹ in addition to the 1712cm⁻¹ peak may indicate the formation of different conjugated forms glycidyl methacrylate carbonyl in the polymerized PESSGMA(K) product.

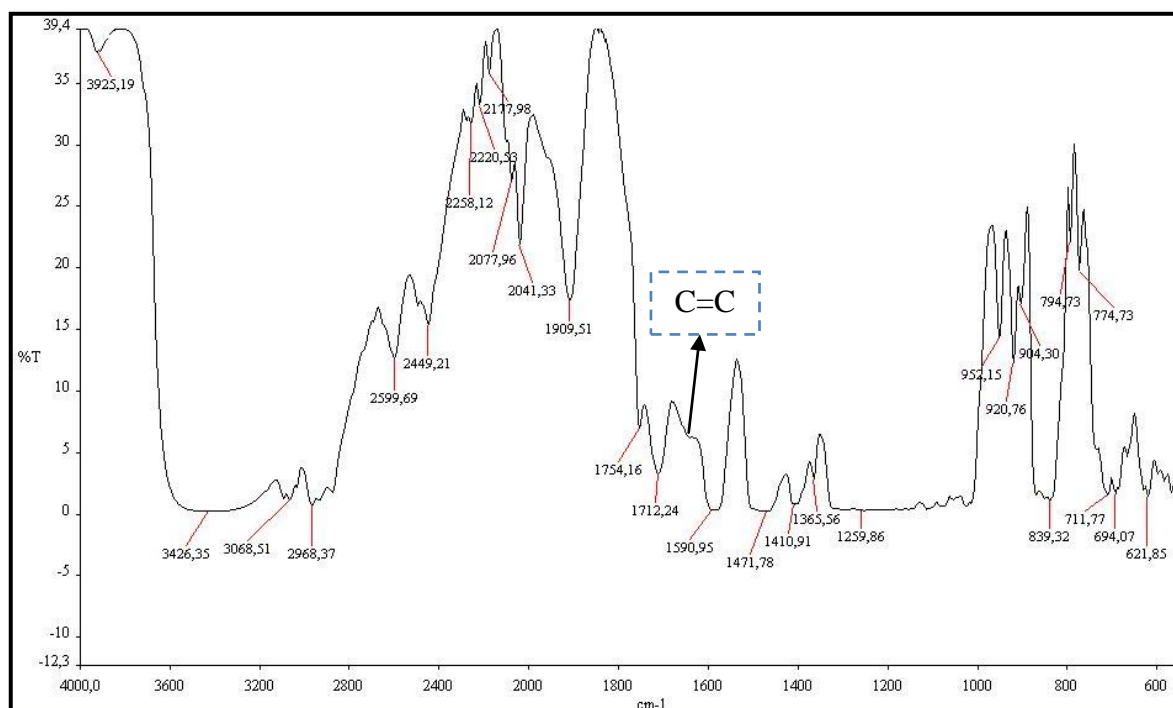


Figure 6.3. The FT-IR spectrum of PESSGMA (K) polymerized with 4% of tert-butyl peroxy benzoate (100°C for 3 hours, 130°C for 6 hours).

Afterwards, self-polymerization of PESSGMA was performed by increasing the weight percent of the tert-butyl peroxy benzoate initiator to 6%. The cure conditions were again 100°C for 3 hours, 130°C for 6 hours under vacuum. The FT-IR spectrum of the PESSGMA polymerized with 6% initiator is shown in Figure 6.4. There is a slight decrease in the intensity of the 1638 cm^{-1} peak as compared to the same sample cured with 4% initiator (100°C for 3 hours, 130°C for 3 hours) due to both increase in initiator content and duration of heating. The 1754 cm^{-1} peak in addition to the 1709 cm^{-1} peak that must correspond to the different conjugated forms glycidyl methacrylate carbonyl stretching vibration is again present in this spectrum.

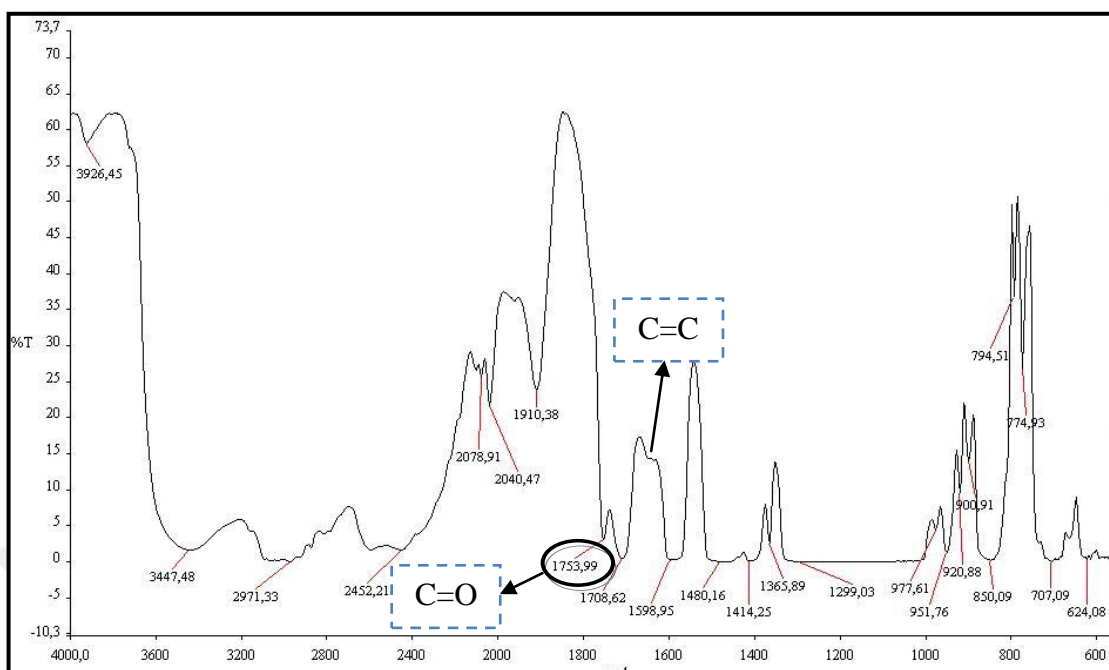


Figure 6.4. The FT-IR spectrum of PESSGMA polymerized with 6% of tert-butyl peroxy benzoate (100°C for 3 hours, 130°C for 6 hours).

The FT-IR spectrum of this PESSGMA (K) polymerized with 6% of tert-butyl peroxy benzoate at 100°C for 3 hours and 130°C for 6 hours is shown in Figure 6.5. This spectrum shows that the 1630 cm^{-1} unsaturation peak was nearly completely consumed. In addition both the 1754 cm^{-1} and the 1712 cm^{-1} peaks that show the different conjugated forms of carbonyl stretching vibrations are also present in this spectrum.

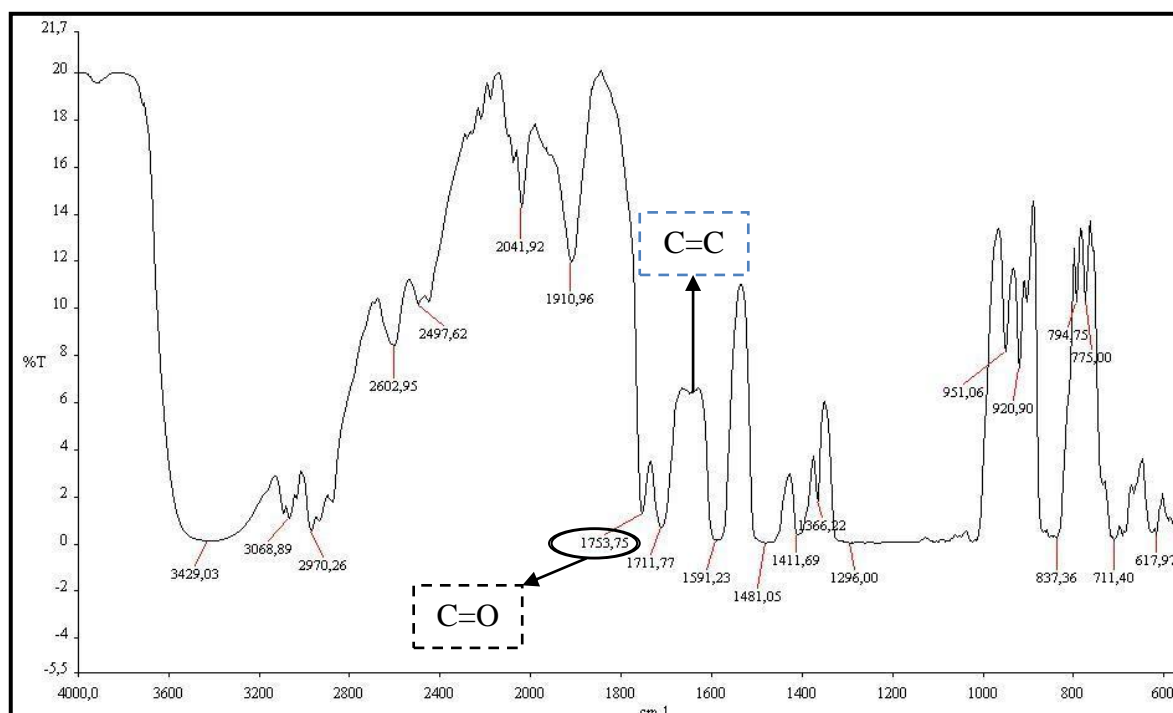


Figure 6.5. The FT-IR spectrum of PESSGMA (K) polymerized with 6% of tert-butyl peroxy benzoate (100°C for 3 hours, 130°C for 6 hours).

Finally, since none of the studied samples gave a complete consumption of the GMA methacrylate functionality through radical polymerization, an initiator concentration of 10wt% which is much higher than the common radical polymerization processes was employed. The FT-IR spectrum of the PESSGMA self polymerized with 10% Tert-butyl peroxy benzoate at 100°C for 3 hours, and then at 130°C for 6 hours, is shown in Figure 6.6. Even though, the peak at 1638 cm^{-1} lost intensity considerably as compared to the PESSGMA FT-IR spectrum shown in Figure 5.2, there is no considerable reduction in 1638 cm^{-1} unsaturation peak intensity when compared to the FT-IR spectrum of the PESSGMA polymerized with 6% Tert-butyl peroxy benzoate under similar conditions shown in Figure 6.4. Thus an initiator concentration above 6wt% is ineffective in increasing the extent of radical polymerization of the PESSGMA pre-polymers.

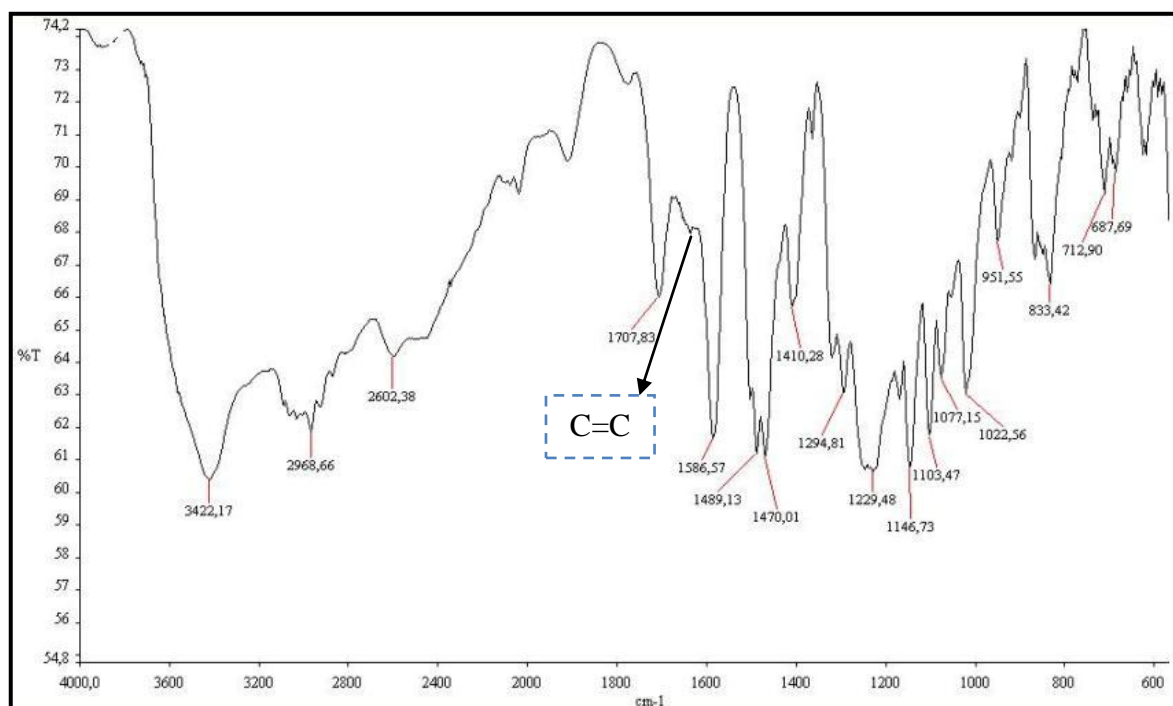


Figure 6.6. The FT-IR spectrum of PESSGMA polymerized with 10% of tert- butyl peroxy benzoate (100°C for 3 hours, 130°C for 6 hours).

The FT-IR spectrum of the PESSGMA (K) polymerized with 10wt % of tert- butyl peroxy benzoate under the same conditions applied for PESSGMA (100°C for 3 hours, 130°C for 6 hours) is shown in Figure 6.7. Although the characteristic bands are rather broad in this spectrum, a comparison of this spectrum to the FT-IR spectrum of PESSGMA (K) polymerized with 6% tert- butyl peroxy benzoate under similar conditions which is shown in Figure 6.5 shows no decrease in the intensity of the 1630 cm⁻¹ peak for the 10% initiator sample again showing that initiator concentrations above 6% is not effective in increasing the extent of radical polymerization of the PESSGMA(K) polymers.

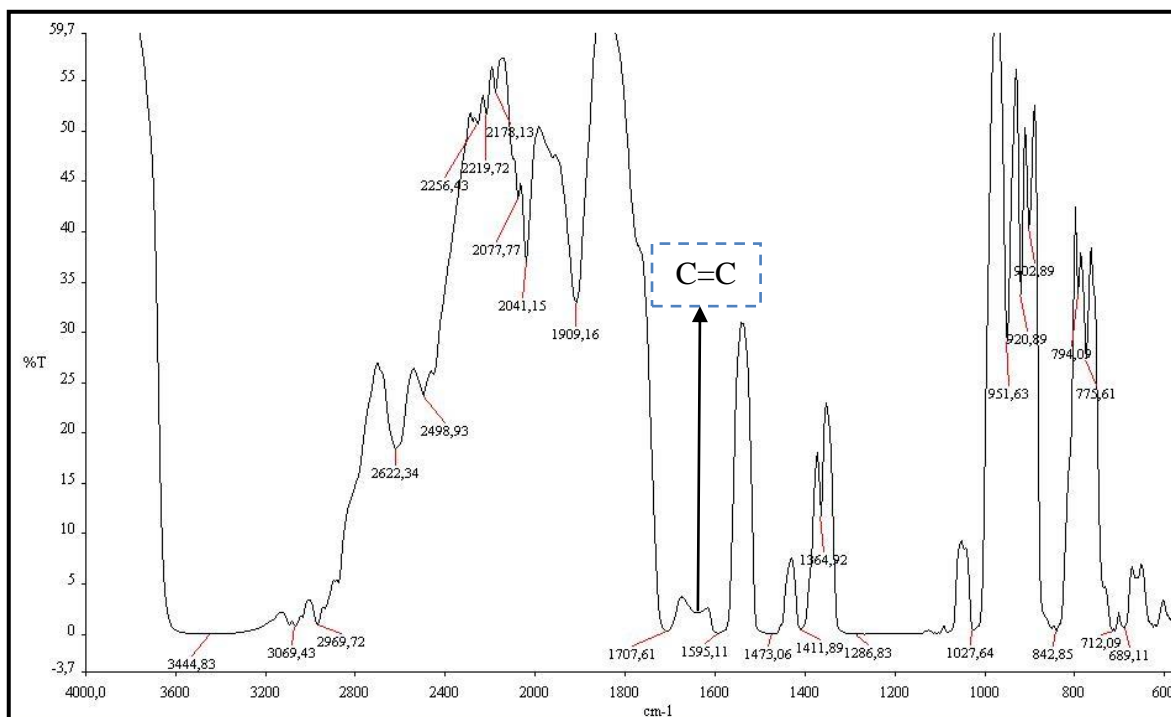


Figure 6.7. The FT-IR spectrum of PESSGMA(K) polymerized with 10% of tert-butyl peroxy benzoate (100°C for 3 hours, 130°C for 6 hours).

6.1.2. Polymerization of PESSGMA(K) with Styrene

The co-polymerization of PESSGMA (K) with co-monomer styrene (30wt%) was performed in presence of 4wt% benzoyl peroxide via solution casting method since styrene is known to be reactive in copolymerization with methacrylates. The sample was dried under vacuum at 90°C for 5 hours then at 130°C for 3 hours. Thus, a different cure cycle was applied in order to prevent the loss of the volatile styrene through evaporation. The FT-IR spectrum of the PESSGMA(K)/STY polymer is shown in Figure 6.8. The characteristic peaks for the functional groups of the PESSGMA(K) polymer and styrene (which has some similar structural units as the PESSGMA(K) polymer: eg an aromatic ring and a vinyl group) are present in this spectrum. However, considerable loss of the intensity of 1630 cm^{-1} peak which shows the $\text{CH}_2=\text{C}<$ double bond stretching vibration is observed as compared to 1630 cm^{-1} peak of the PESSGMA (K) FT-IR spectrum shown in Figure 5.7. Since styrene C=C stretching vibration occurs in the same region this shows that PESSGMA(K) was successfully polymerized with styrene, however since this peak is

still present as a shoulder on the 1595cm^{-1} peak, the copolymerization or the cure reaction was incomplete.

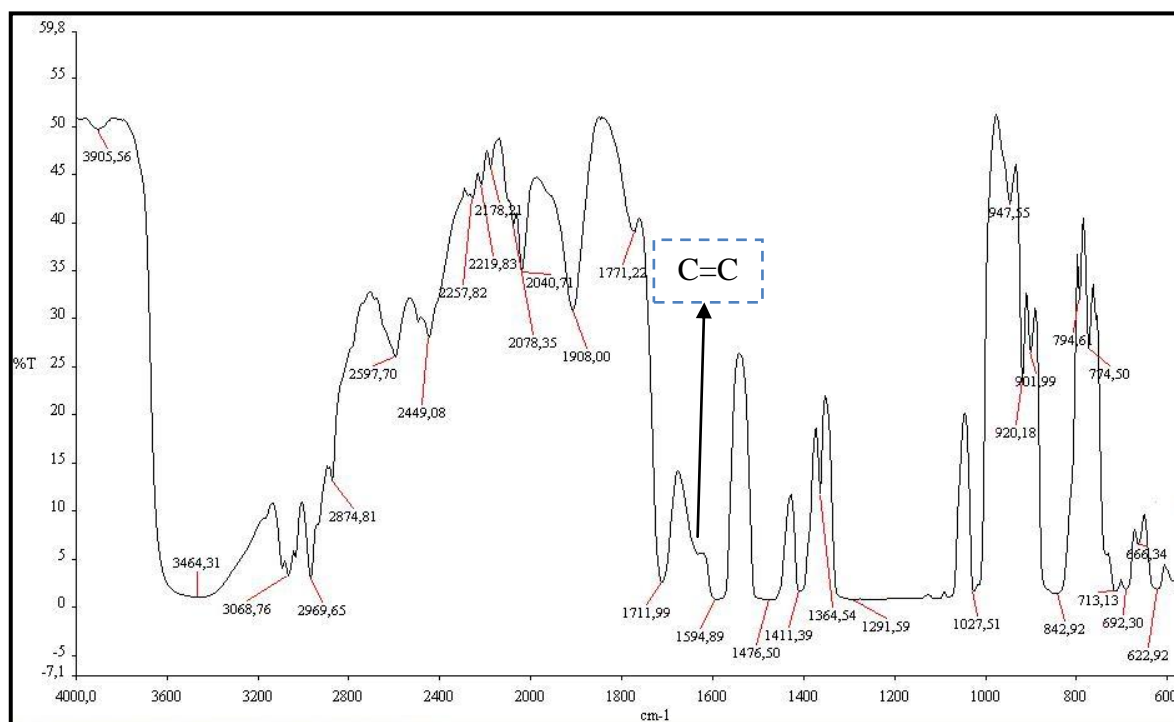


Figure 6.8. FT-IR spectrum of PESSGMA (K) -styrene polymerized with 4% benzoyl peroxide (90°C for 5 hours, 130°C for 3 hours).

6.1.3. Polymerization of PESSGMA(K) with Sulfonated Styrene (Sodium 4-vinyl benzene sulfonate)

Sulfonated styrene monomer (sodium 4-vinyl benzene sulfonate) was also intended to be used for the cure of both the PESSGMA(K) and PESSGMA polymers in order to introduce additional $-\text{SO}_3\text{H}$ groups to the polymer matrix (after the acidification of the final polymers) which is expected to increase the proton conductivity of the final polymers. Thus the PESSGMA(K) polymer and the sodium 4-vinyl benzene sulfonate monomer in the presence of 4% benzoyl peroxide was solution cast and dried under vacuum at 90°C for 5 hours then 130°C for 3 hours. However, at the end of the cure cycle, the sulfonated styrene monomer (sodium 4-vinyl benzene sulfonate) was found to phase separate in the film as shown in Figure 6.9 and the film formed had no mechanical integrity.

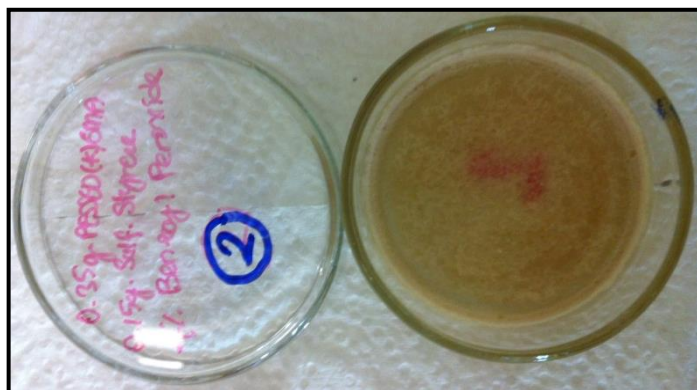


Figure 6.9. The PESSGMA(K)- sulfonated styrene film prepared with 4% benzoyl peroxide (90°C for 5 hours, 130°C for 3 hours).

6.1.4. Polymerization of PESSGMA(K) with Vinyl Phosphonic Acid

Vinyl phosphonic acid is another monomer that is introduced to the PESSGMA polymer to both act as a comonomer for the cross-linking of the PESSGMA polymer and to increase the proton conductivity of the resulting polymers. Thus initially, the PESSGMA(K) polymer and vinyl phosphonic acid (30wt%) mixtures in the presence of 4% benzoyl peroxide were solution cast and dried under vacuum at 90°C for 5 hours then 130°C for 3 hours. The FT-IR spectrum of the PESSGMA(K)/VPA polymer is shown in Figure 6.10. The FT-IR spectrum of this sample shows a significant difference from FT-IR spectrum of the PESSGMA (K) polymer (Fig. 5.7.) and the FT-IR spectra of all the PESSGMA(K) polymers presented so far. This difference is that the broad band at 3430 cm^{-1} region which belongs to the -OH group of the GMA moiety of the PESSGMA(K) polymer which is present in all other spectra of the PESSGMA(K) polymers is absent in this FT-IR spectrum. This may indicate that the -OH groups of the of GMA moiety on the PESSGMA (K) polymer chain ends reacted with the -OH groups of vinyl phosphonic acid via a condensation reaction. However, the presence of a broad band in the 2850 cm^{-1} region which must belong to the -OH groups of vinyl phosphonic acid units indicates that not all VPA OH's are consumed in the reaction with OH's of the PESSGMA(K) polymer. The 1630 cm^{-1} unsaturation peak of the PESSGMA (K) polymer is not visible in this IR spectrum, however the peak at 1615 cm^{-1} showing the VPA C=C stretching vibrations is present as a weak peak, which may indicate that the radical polymerization of the

metahcrylate of the PESSGMA(K) polymer and vinyl group of the VPA took place to a certain extent.

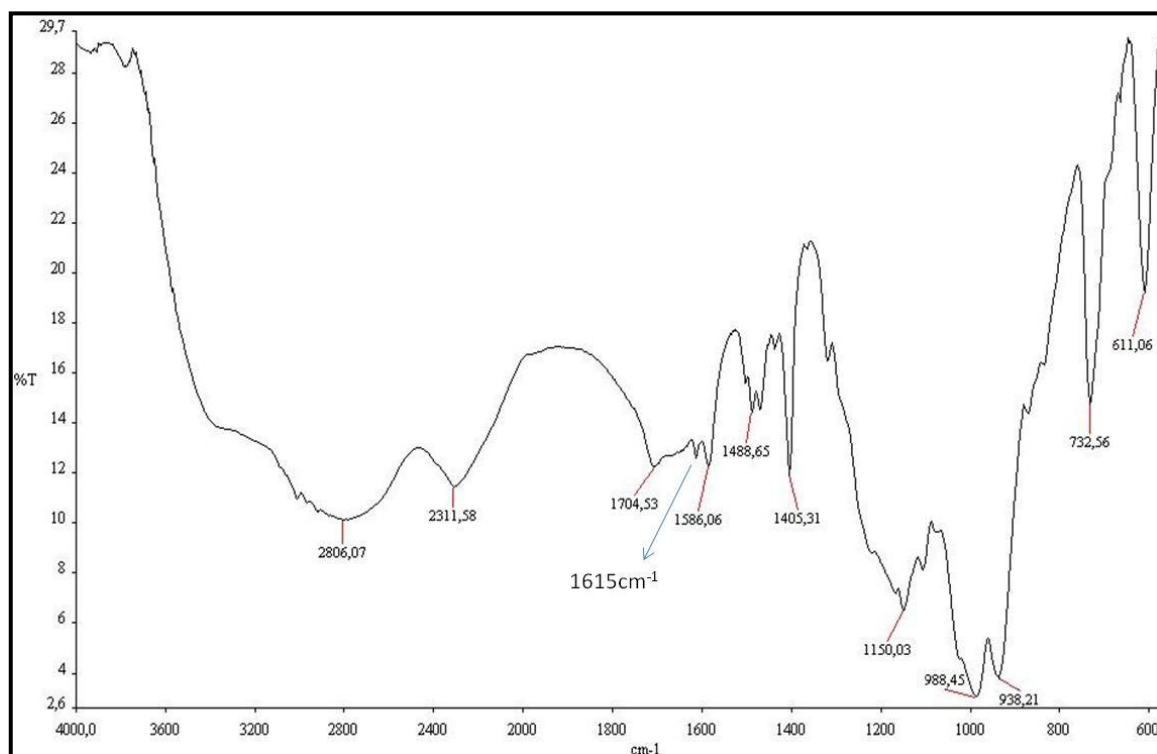


Figure 6.10. FT-IR spectrum of PESSGMA (K) and vinyl phosphonic acid polymerized with 4% benzoyl peroxide (90°C for 5 hours, 130°C for 3 hours).

6.1.5. Polymerization of PESSGMA with Styrene

PESSGMA was polymerized with 30wt% co-monomer styrene by drying under vacuum at 100°C for 5 hours, 130°C for 3 hours and then at 150°C for 12 hours in the presence of 4wt % benzoyl peroxide. The FT-IR spectrum of the PESSGMA/STY copolymer cured with 4% benzoyl peroxide under these conditions is shown in Figure 6.11. As this spectrum is compared to the FT-IR spectrum of the PESSGMA pre-polymer (Figure 5.2) again a considerable decrease in intensity of the 1638 cm⁻¹ peak which indicates CH₂ = C< double bond stretching vibration is analyzed due to radical polymerization of the double bond of the GMA moiety with styrene, whereas all other characteristic peaks of the PESSGMA pre-polymer are still present. However since this unsaturation peak is not completely consumed, it can be said that complete polymerization of vinyl groups was not achieved.

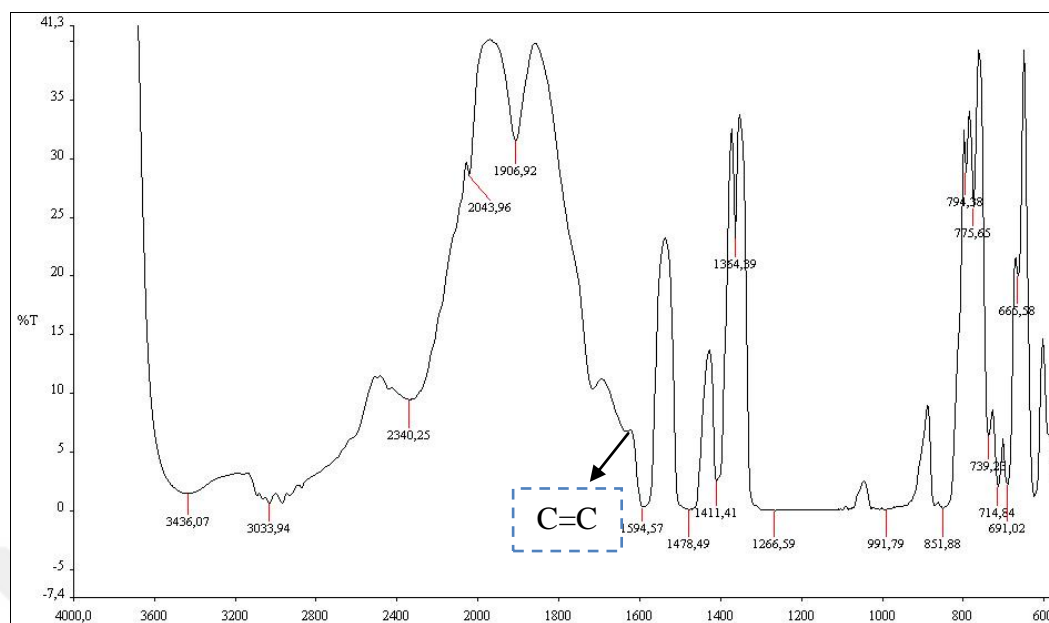


Figure 6.11. FT-IR spectrum of PESSGMA and styrene polymerized with 4% benzoyl peroxide (100°C for 5 hours, 130°C for 3 hours, 150°C for 12 hours).

6.1.6. Polymerization of PESSGMA with Sulfonated Styrene (Sodium 4-vinyl benzene sulfonate)

Sulfonated styrene monomer (sodium 4-vinyl benzene sulfonate) was also used for the cure of the PESSGMA polymer using similar cure conditions as applied for the cure of the PESSGMA(K) polymer with the same monomer. Hence, PESSGMA polymer and the sulfonated styrene monomer were solution cast in the presence of 4wt% benzoyl peroxide and dried under vacuum at 90°C for 5 hours then at 130°C for 3 hours. However, PESSGMA co-polymerization with sodium 4-vinyl benzene sulfonate did not occur and phase separation was observed as also observed for the cure of the PESSGMA(K) polymer with this monomer. Dai C.A.*et al.* similarly reported that sulfonated styrene induced phase separation when copolymerized with tetrabutylammonium[57]. Thus sodium 4-vinyl benzene sulfonate was found to be unreactive in radical copolymerization with PESSGMA and no further studies were performed with this co-monomer.

6.1.7. Polymerization of PESSGMA with Vinyl Phosphonic Acid

The copolymerization of PESSGMA with vinyl phosphonic acid was performed in presence of 4wt% benzoyl peroxide via solution casting method to increase the proton conductivity of the resulting polymers. The first sample was dried under vacuum at 100°C for 5 hours then 130°C for 9 hours. The FT-IR spectrum of this PESSGMA/VPA polymer cured under these conditions is shown in Figure 6.12. There is a considerable loss of the intensity of the 1638 cm⁻¹ peak which shows the CH₂=C< double bond stretching vibration as compared to 1638 cm⁻¹ peak of the PESSGMA FT-IR spectrum shown in Figure 5.2. However, due to the presence of the residual peak in the 1638 cm⁻¹ region, it can be said that the complete polymerization was not achieved. The 1715 cm⁻¹ peak which belongs to C=O carbonyl stretching vibration of the GMA methacrylate functionality occurs as a weak peak in this spectrum. In addition, the broad band at around 3445 cm⁻¹ that shows the hydroxyl band (OH) of the PESSGMA polymer did not lose intensity in this product which indicates that PESSGMA –VPA condensation reaction through the hydroxyl groups did not occur considerably in this product.

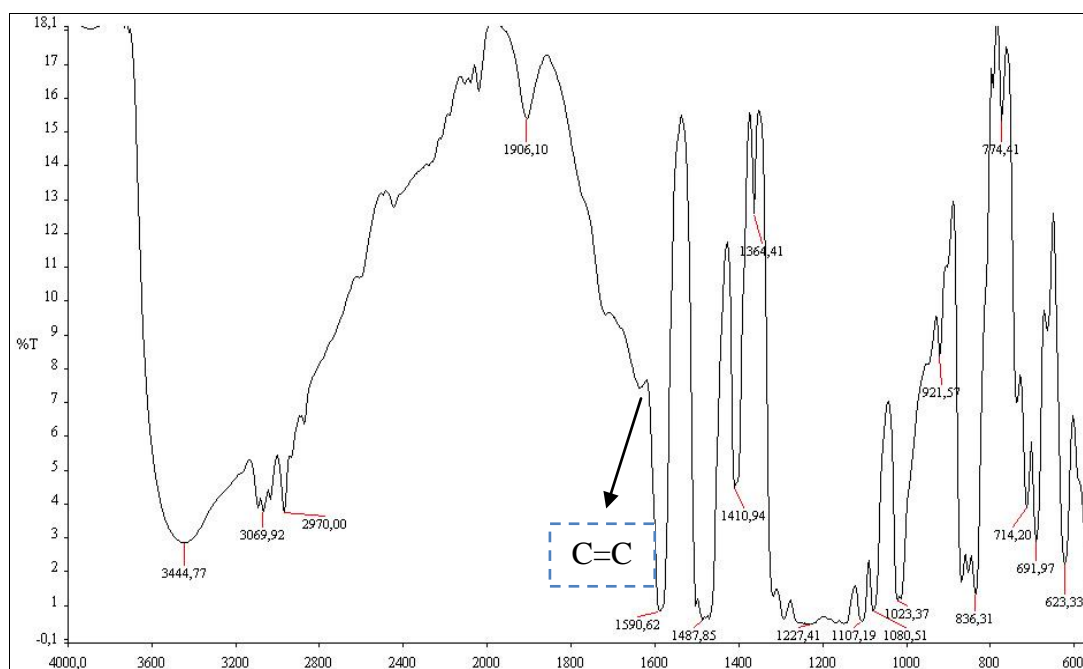


Figure 6.12. FT-IR spectrum of PESSGMA and vinyl phosphonic acid polymerized with 4% benzoyl peroxide (100°C for 5 hours, 130°C for 9 hours).

For a second sample, the post-cure temperature was increased from 130°C to 180°C. Thus PESSGMA was copolymerized with (30wt%) vinyl phosphonic acid in the presence 4wt% benzoyl peroxide by drying the same sample for 5 hours at 100°C then for 9 hours at 180°C under vacuum. The FT-IR spectrum of this product is shown in Figure 6.13. The spectrum shows well consumption of the 1638 cm⁻¹ unsaturation peak, also the carbonyl stretching peak can not be identified as the bands are quiet broad in this region. The disappearance of the hydroxyl band of the PESSGMA polymer in the 3400 cm⁻¹ region in this spectrum indicates that PESSGMA hydroxyls condensed with VPA hydroxyls in this product which must be an influence of the increase in the post-cure temperature. In addition, the presence of a broad band in the 2968 cm⁻¹ region which must belong to the –OH groups of vinyl phosphonic acid indicates that not all vinyl phosphonic acid –OH's are consumed in the reaction with –OH's of the PESSGMA polymer.

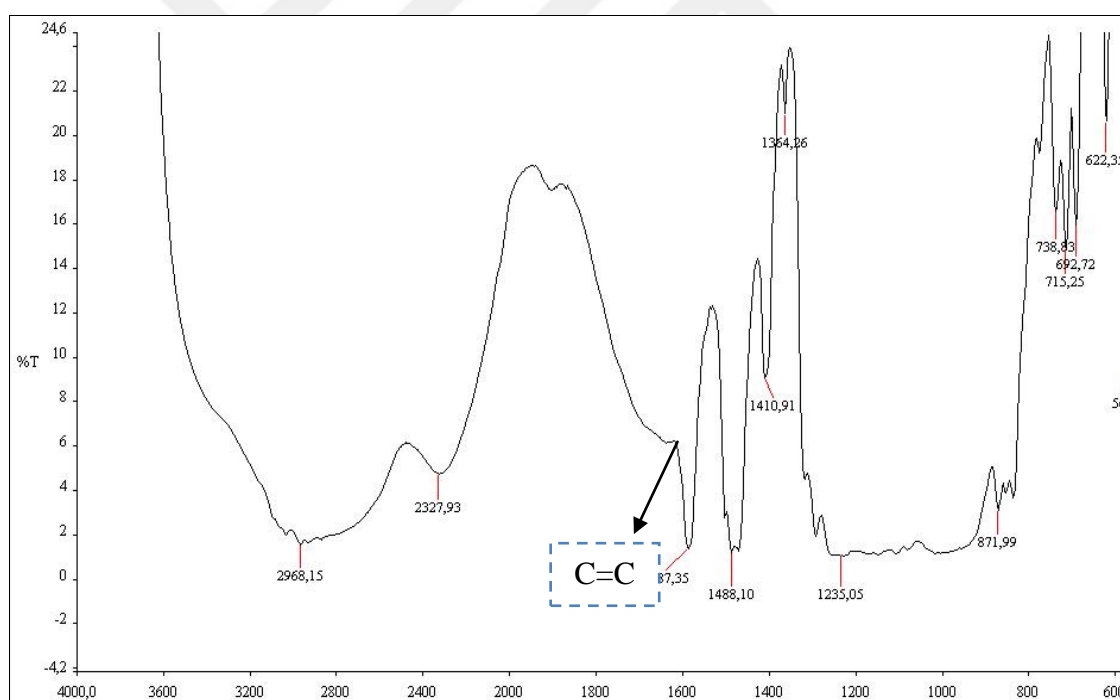


Figure 6.13. FT-IR spectrum of PESSGMA and vinyl phosphonic acid polymerized with 4wt% benzoyl peroxide (100°C for 5 hours, 180°C for 9 hours).

6.1.8. Polymerization of PESSGMA with Styrene and Vinyl Phosphonic Acid

Vinyl phosphonic acid and styrene are known as monomers that are both reactive in copolymerization with methacrylates. The PESSGMA, styrene (15 wt%) and vinyl phosphonic acid (15 wt%) mixture in the presence of 4wt% benzoyl peroxide was solution cast and dried under vacuum at 100°C for 5 hours then at 130°C for 9 hours. The FT-IR spectrum of this product is shown in Figure 6.14. The spectrum shows that the 1638 cm⁻¹ peak intensity is considerably decreased as compared to the spectrum of PESSGMA polymer in Figure 5.2, again indicating the consumption of double bonds through polymerization without complete conversion. Since CH₂=C< double bond stretching vibration lost intensity, the PESSGMA was successfully polymerized with styrene and vinyl phosphonic acid. However, as this peak still present in this spectrum, it can be said that the copolymerization was incomplete. In addition, the broad band in the 3400-3500 region is quiet intense in this product indicating that PESSGMA –VPA condensation reaction through the hydroxyl groups did not occur considerably in this product.

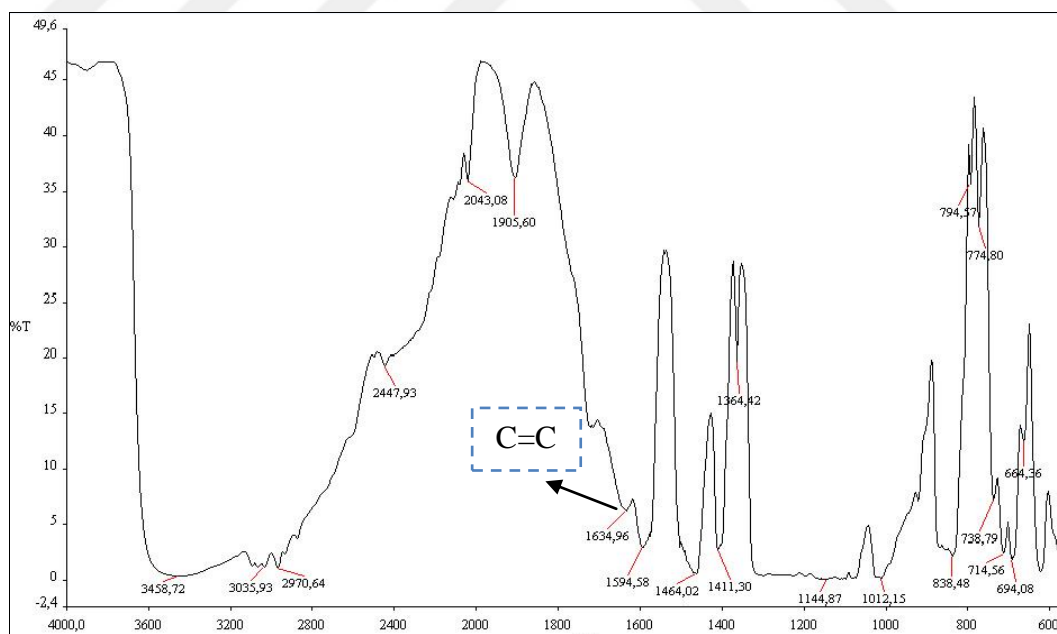


Figure 6.14. FT-IR spectrum of PESSGMA polymerized with styrene and vinyl phosphonic acid in the presence of 4wt% benzoyl peroxide (100°C for 5 hours, 130°C for 9 hours).

For analyzing the effect of the increase in post-cure temperature, the PESSGMA was similarly copolymerized with a mixture of styrene (15wt%) and vinyl phosphonic acid (15wt%) in the presence 4wt% benzoyl peroxide by drying the sample at 100°C for 5 hours then at 180°C for 9 hours. The FT-IR spectrum of this product is shown in Figure 6.15. This spectrum shows that the 1638 cm⁻¹ unsaturation peak was consumed to a higher extent as compared to the sample post-cured at 130°C. In addition, in this spectrum, the broad band in the 3400 cm⁻¹ region lost intensity as compared to that of the spectrum of the sample post-cured at 130°C (Figure 6.14). This result indicates that the increase of the post-cure temperature from 130°C to 180°C increases the extent of condensation reaction of the PESSGMA hydroxyls with VPA hydroxyls.

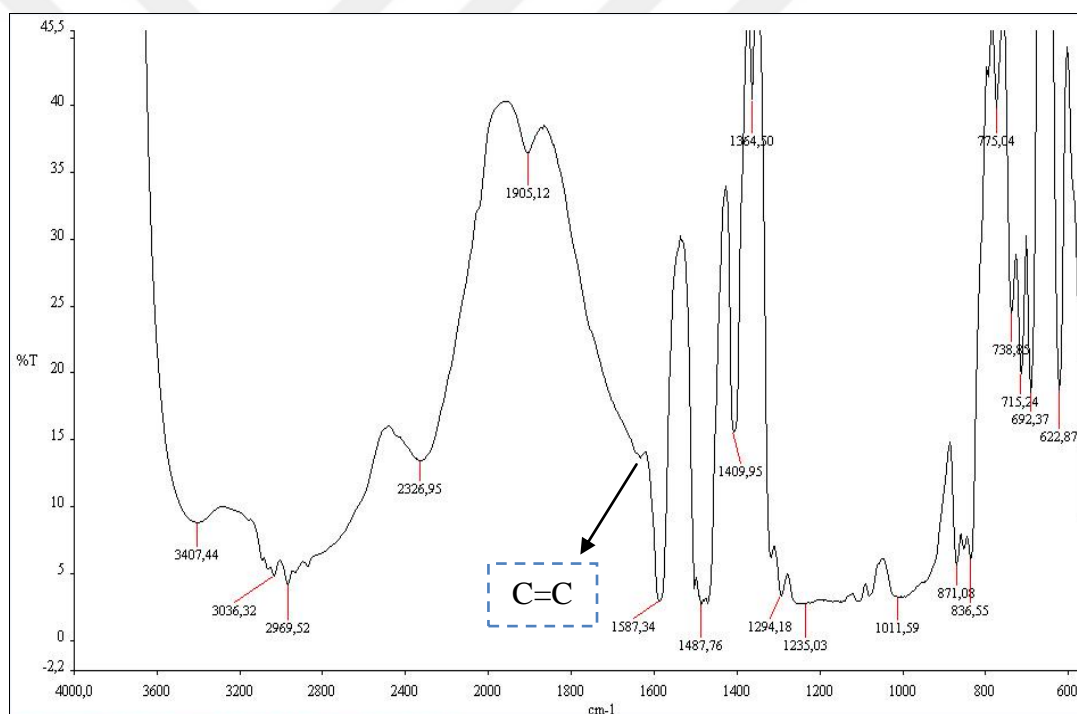


Figure 6.15. FT-IR spectrum of PESSGMA polymerized with styrene and vinyl phosphonic acid in the presence of 4wt% benzoyl peroxide (100°C for 5 hours, 180°C for 9 hours).

All the films obtained via radical polymerization of the PESSGMA and PESSGMA(K) pre-polymers with or without comonomers (applying the cure cycles tabulated in Table 4.1 and 4.2) with the exception of the samples prepared with sulfonated styrene resulted in rigid, strong films. The ones prepared with VPA were brittle. When these films were

placed in DMSO, samples cured for shorter times (eg. 100°C for 3 hours, 130°C for 3 or 6 hours) even at higher initiator contents were found to be soluble, which indicates that the PESSGMA and PESSGMA(K) pre-polymers were not cured completely to form a network structure. Samples cured for longer times and the samples with VPA post-cured at 180°C were insoluble in DMSO, however especially the samples postcured at 150 and 180°C had developed a dark brown color and became quite brittle. Thus in our next trials for the complete cure of the PESSGMA polymers, longer cure times and lower post-cure temperatures were applied as listed in Table 4.3. In addition the PESSGMA was prepared from BPA terminated PESS polymer according to procedure described in Experimental Section. In fact all the PESSGMA samples cured under these conditions were found to be insoluble in DMSO whereas the PESS polymer was soluble in the same solvent indicating the successful crosslinking of the PESSGMA polymers and network formation. The low reactivity of the PESSGMA polymers in the radical polymerization and therefore in the cure reactions can be attributed to a possible inhibition effect of the sulfonic acid groups.

As discussed in Section 5.4, the synthesis of the PESSGMA(K) polymer led to an undesirable product with the addition of glycidyl methacrylate moiety to the sulfonate groups which removed the possibility of converting sulfonate potassium salt to sulfonic acid groups after cure reactions. Therefore, no further studies were carried out with this polymer. In addition the cure of this polymer did not result in considerable improvement in reactivity of the methacrylate functionality towards radical polymerization. Thus all further analysis were carried out with PESSGMA polymers cured under the optimized conditions tabulated in Table 4.3. The FT-IR analysis of these samples will be described in following sections 6.1.9 to 6.1.12 and the IEC and the swelling in water results for these membranes will be discussed in sections 6.2 and 6.3 respectively. Analysis of physical properties of these PESSGMA polymer membranes for fuel cell applications will be presented in section 7.

6.1.9. Self Polymerization of PESSGMA After Cure Optimization

The PESSGMA polymer was homopolymerized in the presence of 4wt% tert-butyl peroxy benzoate by drying the sample at 100°C for 5 hours and then at 110°C for 15 hours, under vacuum. The FT-IR spectrum of this sample is shown in Figure 6.16. The characteristic

peaks for the functional groups of the PESSGMA polymer, such as the hydroxyl band in the 3400cm^{-1} region and the glycidyl methacrylate carbonyl peak at around 1710 cm^{-1} are also observed in this spectrum. However, when compared to the FT-IR spectrum of the PESSGMA product (Figure 5.2), the 1638 cm^{-1} peak which shows the glycidyl methacrylate, $\text{CH}_2 = \text{C}$ double bond stretching vibration is nearly completely consumed in this product which indicates that the polymerization of the PESSGMA was nearly complete.

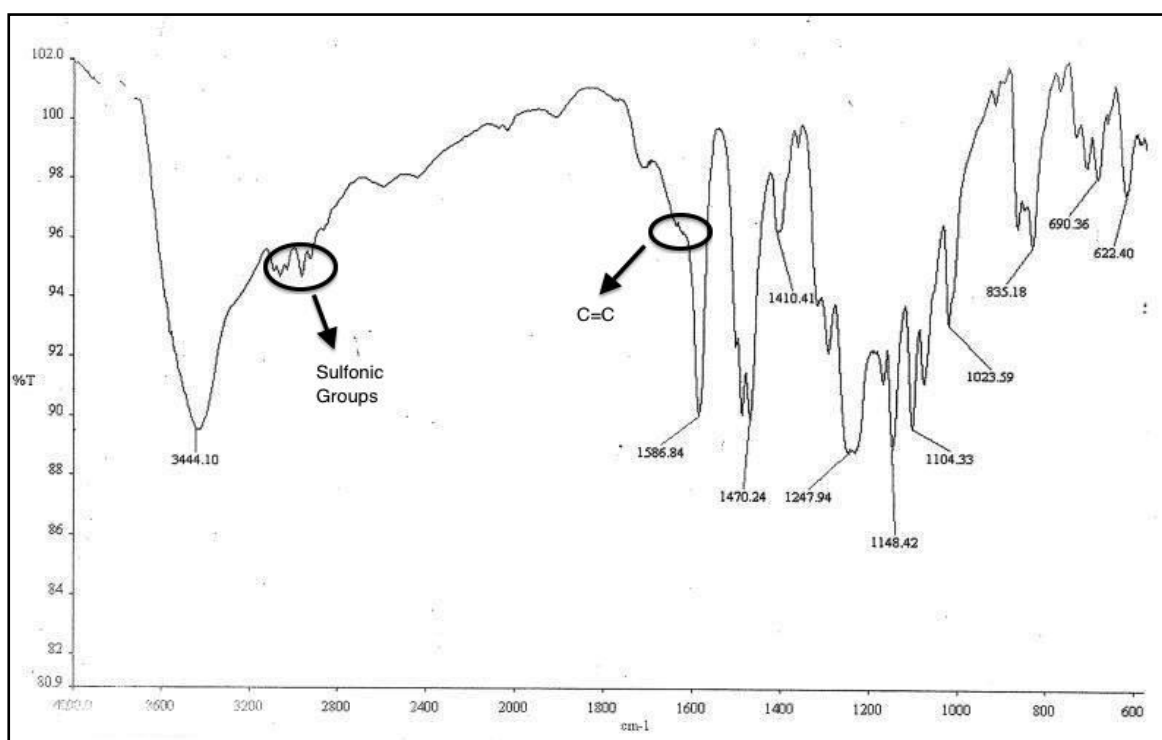


Figure 6.16. The FT-IR spectrum of PESSGMA self-polymerized in the presence of 4wt% of tert-butyl peroxy benzoate by drying sample at 100°C for 5 hours and then at 110°C for 15 hours under vacuum.

6.1.10. Polymerization of PESSGMA with Styrene After Cure Optimization

PESSGMA was copolymerized with 30wt% co-monomer, styrene in the presence of 4wt% benzoyl peroxide, by drying the sample at 100°C for 5 hours and then at 110°C for 15 hours, under vacuum. The FT-IR spectrum of the PESSGMA/STY polymer cured under these conditions is shown in Figure 6.17. As this spectrum is compared to the FT-IR spectrum of the PESSGMA pre-polymer (Figure 5.2) again a considerable decrease in

intensity of the 1638 cm^{-1} peak which indicates the $\text{CH}_2 = \text{C}<$ double bond stretching vibration is analyzed due to radical polymerization of the vinyl group of GMA moiety with styrene, whereas all other characteristic peaks of the PESSGMA pre-polymer are still present. However since this unsaturation peak is not completely consumed, it can be said that complete polymerization of vinyl groups was not achieved.

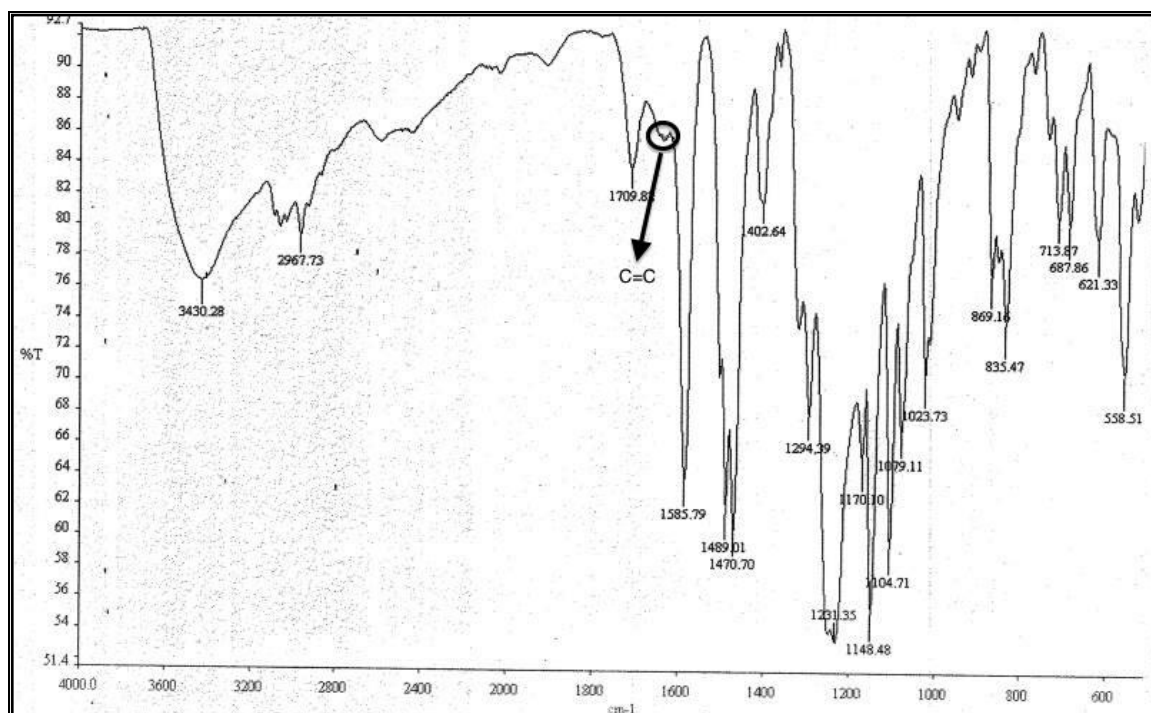


Figure 6.17. FT-IR Spectrum of PESSGMA/STY(70/30) sample polymerized in the presence of 4wt% of benzoyl peroxide by drying the sample at 100°C for 5 hours and then 110°C for 15 hours, under vacuum.

6.1.11. Polymerization of PESSGMA with Vinyl Phosphonic Acid After Cure Optimization

PESSGMA was copolymerized with 30wt% co-monomer, vinyl phosphonic acid in presence of 4wt% benzoyl peroxide by drying the sample at 100°C for 5 hours at 110°C for 5 hours and at 120°C for 10 hours, under vacuum via solution casting method. As mentioned in previous sections, copolymerization of PESSGMA with VPA was carried out to enhance the proton conductivity of the PESSGMA polymer. The FT-IR spectrum of PESSGMA/VPA polymer cured under these conditions is shown in Figure 6.18. This

spectrum shows again the considerable consumption of the 1638 cm^{-1} unsaturation peak of PESSGMA, however this peak is again not completely lost indicating conversion of all double bonds was not complete. In addition the 3440 cm^{-1} peak of the OH groups of PESSGMA prepolymer lost intensity considerably which as mentioned earlier may indicate a condensation reaction between the PESSGMA and vinyl phosphonic acid (VPA) hydroxyls. The presence of a broad band in 2970 cm^{-1} region which must belong to the –OH groups of vinyl phosphonic acid indicates that not all vinyl phosphonic acid –OH's are consumed in the reaction with –OH's of the PESSGMA prepolymer.

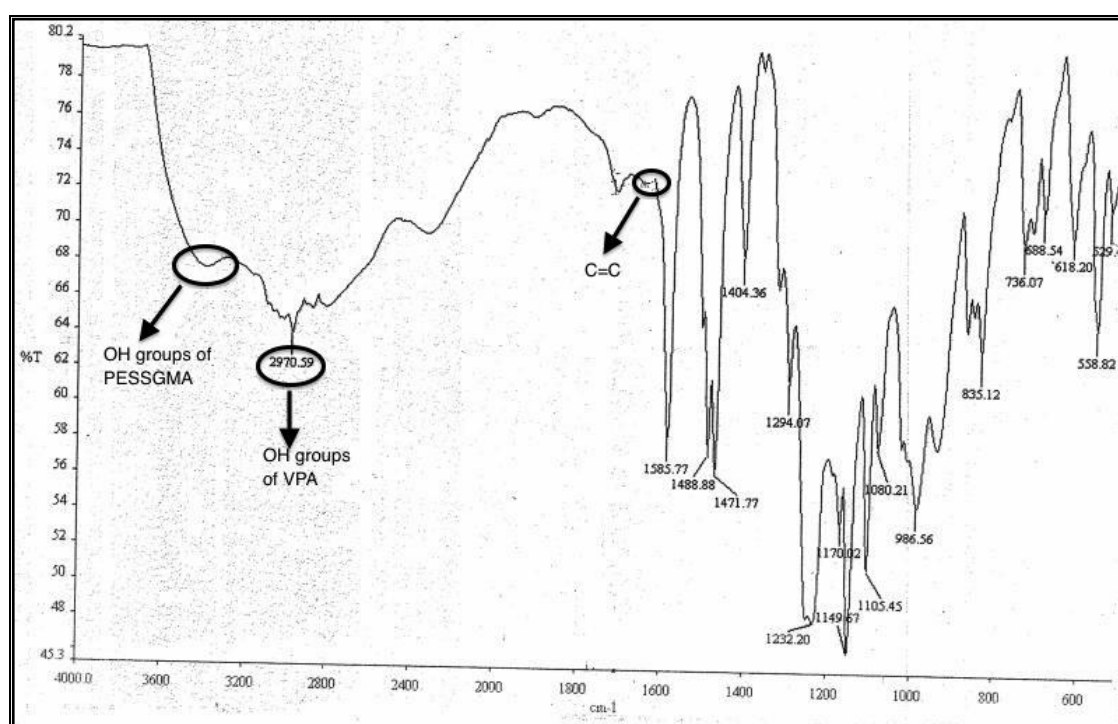


Figure 6.18. FT-IR spectrum of PESSGMA/VPA(70/30) sample polymerized in the presence of 4wt% of benzoyl peroxide by drying the sample at 100°C for 5 hours and then at 110°C for 5 hours and at 120°C for 10 hours, under vacuum.

6.1.12. Polymerization of PESSGMA with Styrene and Vinyl Phosphonic Acid After Cure Optimization

Styrene and vinyl phosphonic acid are monomers that are reactive in copolymerization with methacrylates. Thus, PESSGMA, styrene (15 wt%) and vinyl phosphonic acid (15 wt%) mixtures in the presence of 4wt% benzoyl peroxide were solution cast and dried

under vacuum at 100°C for 5 hours and then at 110°C for 5 hours and at 120°C for 10 hours. The FT-IR spectrum of this product is shown in Figure 6.19. This spectrum shows that the peak at 1638cm⁻¹ corresponding to CH=C< double bond stretching vibrations of the vinyl groups of the monomers again lost intensity considerably as compared to the spectrum of PESSGMA polymer shown in Figure 5.2, again indicating the consumption of double bonds through polymerization without complete conversion. In addition the 3426cm⁻¹ peak intensity is stronger as compared to the spectrum of the PESSGMA/VPA sample cured under the same conditions (Figure 6.18) due to the lower VPA content (15wt%) of the PESSGMA/STY/VPA sample. The condensation reaction between VPA hydroxyls and PESSGMA hydroxyls should occur to a less extent in this sample.

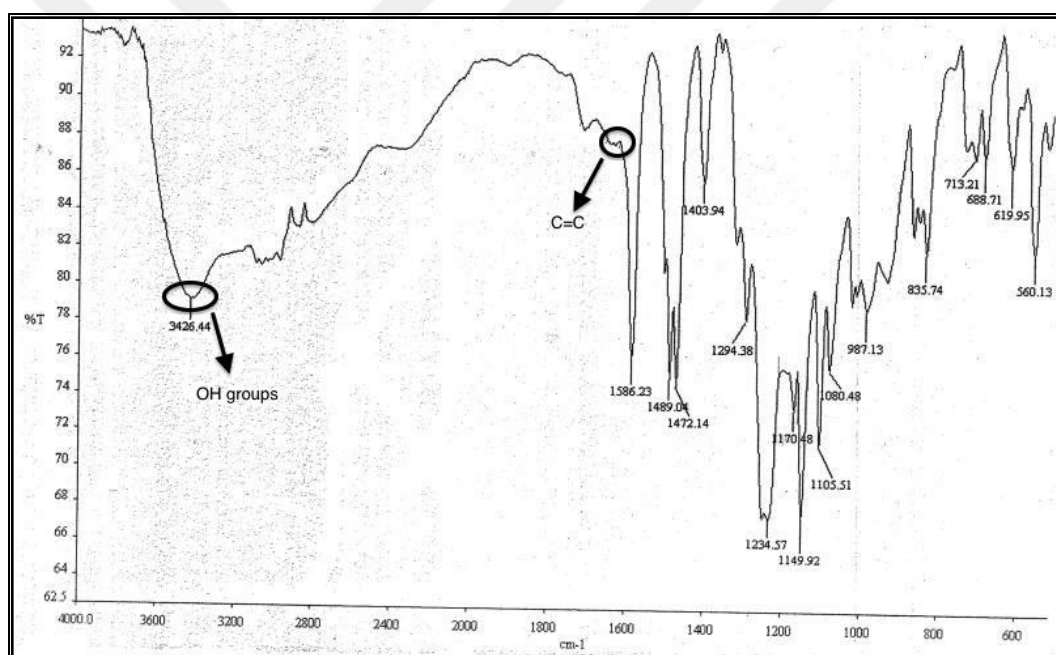


Figure 6.19. FT-IR spectrum of PESSGMA/STY/VPA(70/15/15) sample polymerized in the presence of 4wt% of benzoyl peroxide by drying the sample at 100°C for 5 hours and then at 110°C for 5 hours and at 120°C for 10 hours, under vacuum.

6.2. ION EXCHANGE CAPACITY (IEC) ANALYSIS

Ion exchange capacity (IEC), defined as the milliequivalents (meq) of conducting groups per gram of polymer, plays a crucial role in water uptake and conductivity of membranes. The IEC values of the bisphenol-A terminated PESS and PESSGMA polymers and

PESSGMA membranes prepared under optimized curing conditions were measured by titration method as described in Experimental Section 4.4.3. The results are listed in Table 6.1. Samples in powder form are the polymers as they are synthesized and purified, and the PESSGMA membranes are the cross-linked samples.

In general, proton conductivity relies heavily on the IEC values and water uptake of electrolyte membranes. Water uptake becomes a critical factor in proton conductivity for polymer electrolytes because water in a membrane acts as a transportation medium of protons. The membrane with high IEC usually contains fixed ionic groups in higher concentration. The membrane therefore has the tendency to dilute itself and its resulting swelling is more pronounced than the ones with lower capacity, leading to higher water uptake ability [61]. However a too high degree of swelling in water is not desirable for a membrane used in DMFC applications as it may lead to poor mechanical properties of the highly swollen membranes.

As shown in Table 6.1, PESS polymer has a measured IEC value of 1.88 meq g^{-1} (powdered polymer) and 2.17 meq g^{-1} (membrane) which is very close to its reported IEC values in the range of $1.8 - 2.2 \text{ meq g}^{-1}$ [58]. A decrease of IEC value was observed for the PESSGMA polymer for both un-crosslinked polymer as synthesized and its cross-linked film. This decrease in IEC for the PESSGMA polymer as compared to that of the PESS polymer can be attributed to both the increase in molecular weight of the polymer chains as determined from GPC analysis and to loss of the sulfonic acid groups to a certain extent upon possible side reaction with glycidyl methacrylate. For the crosslinked PESSGMA polymers we must expect a decrease in IEC as compared to the PESS polymer since it is known that with larger degrees of crosslinking, membranes have lower IEC values. The intermolecular crosslinking depresses the swelling of the polymer chain, which hinders the ion transport across them. Therefore, this decrement occurs due to the incomplete exchange of protons of sulfonic acid groups with Na^+ ions in the titration process. Although the cross-linked PESSGMA and PESSGMA/STY membranes show decreased IEC values as compared to that of PESS polymer, their IEC values are slightly higher than that of the un-cross-linked PESSGMA polymer in powder form. This increase may be related to the physical forms of the samples being titrated, the film samples may result in a better exposure of sulfonic acid groups to ion exchange and therefore may result in higher IEC values.

A different tendency was observed for the IEC of the PESSGMA/VPA membranes. The IEC values observed for PESSGMA/VPA membranes varied from 4.34 to 7.75 meq/g, which were gradually higher than the corresponding PESS, PESSGMA and PESSGMA/STY membranes which exhibited IEC values between 0.35-2.17 meq/g. PESSGMA/VPA membranes exhibited relatively higher ion-exchange capacity since additional acid groups were introduced to the system by the VPA comonomer, Interestingly, the IEC values decreased with increasing VPA content of the PESSGMA/VPA polymers. One explanation for this can be an increasing tendency of VPA –OH's to condensate at increasing VPA contents reducing the available protons from VPA for ion exchange. In addition, interestingly the presence of styrene in the composition of the membranes seems to lead to an increase in IEC. This can be seen in comparisons of the IEC values of the PESSGMA and PESSGMA/STY(70/30) membranes as well as the PESSGMA/STY/VPA(70/15/15) and PESSGMA/VPA(70/30) membranes. The higher IEC of the PESSGMA/STY sample as compared to that of the PESSGMA membrane can be attributed to a lower degree of crosslinking for the PESSGMA/STY polymer since PESSGMA is the cross-linker unit in this formulation. The higher IEC value of the PESSGMA/STY/VPA(70/15/15) sample as compared to that of the PESSGMA/VPA(70/30) sample on the other hand can again be explained by the increasing tendency of VPA –OH's to condensate at increasing VPA contents reducing the available protons from VPA for ion exchange.

Table 6.1. IEC values of the PESS, PESSGMA and PESSGMA copolymers at room temperature.

Polymer	IEC (meq/g)
*PESS	1.88 ± 0.05
*PESSGMA	0.28 ± 0.02
**PESS	2.17 ± 0.01
** ^c PESSGMA	0.35 ± 0.05
** ^c PESSGMA/STY(70/30)	0.75 ± 0.08
** ^c PESSGMA/STY/VPA(70/15/15)	7.75 ± 0.42
** ^c PESSGMA/VPA(70/30)	6.08 ± 0.25
** ^c PESSGMA/VPA(60/40)	5.58 ± 0.25
** ^c PESSGMA/VPA(50/50)	4.34 ± 0.17

*Powder **Membrane ^cCross-linked sample

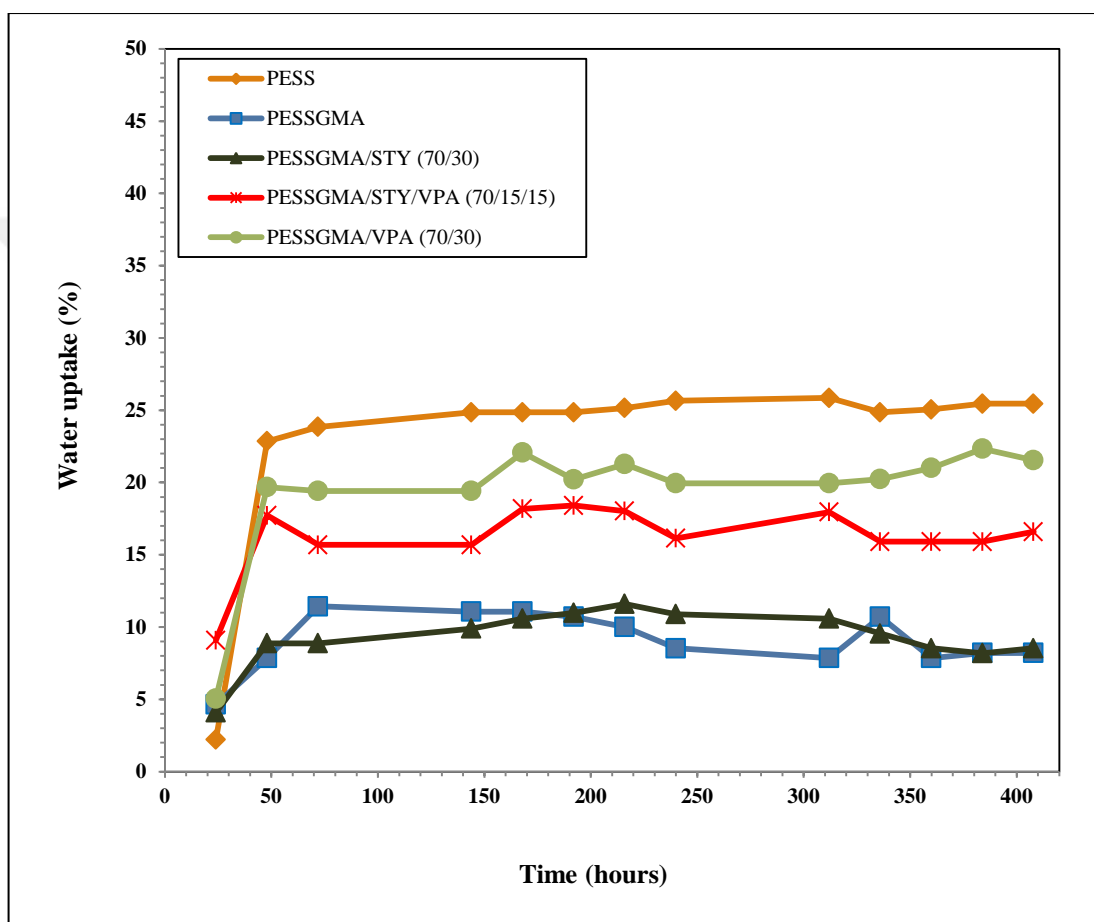
6.3. WATER SWELLING PROPERTIES

The water uptake and extent of swelling in water are important properties for polymer electrolyte membranes used for fuel cell applications. A too high water uptake value, especially at temperatures above 60°C, may lead to poor mechanical properties of the highly swollen membranes. Different approaches have been employed to enhance the dimensional stability and water swelling properties of polymer electrolyte membranes. One of these approaches is covalent cross-linking which has been used in this study for the sulfonated poly(arylether sulfone) polymer (PESS). Swelling experiments in water both at room temperature and at 80°C were performed to compare both the extent of swelling in water and the cross-linking densities of the different polymer membranes prepared in the study.

6.3.1. Swelling Experiments at Room Temperature

Figure 6.20 (a) shows the weight percentage change versus time plots of the PESS and PESSGMA films cured under optimized conditions (Table 4.3) for the swelling experiments at room temperature. Generally, the extent of swelling in a solvent for a polymer is strongly influenced by the degree of crosslinking of that polymer. As can be seen from Figure 6.20 (a), the weight percentage change values obtained for the PESSGMA membranes were lower than those observed for the PESS polymer membrane. The PESS polymer membrane swelled to the highest extent and exhibited about 25wt% water uptake at the end of 400 hours because of its linear structure followed by the PESSGMA/VPA and PESSGMA/STY/VPA polymers. The PESSGMA and PESSGMA/STY samples swelled the least and exhibited less than 10wt% water uptake at the end of 400 hrs. The higher extent of swelling for the PESSGMA/VPA and PESSGMA/STY/VPA polymers can be attributed to the more hydrophilic nature of the VPA monomer as compared to both the PESSGMA and styrene. The weight percentage change of the PESS and PESSGMA membranes at the end of 24 hrs at room temperature is also shown in Figure 6.20(b). As can be seen the water uptake of all the membranes were below 10wt% after 24 hrs in deionized water at room temperature. In contrary to the water uptake percentage data of the films at the end of 400 hours, the PESS polymer exhibited a lower uptake as compared to the cross-linked membranes. Also the PESSGMA/VPA

membrane exhibited lower water uptake than the PESSGMA/STY/VPA membrane. It can be seen that the membranes did not reach an equilibrium state at the end of 24 hours at room temperature. Thus the water uptake values obtained after the system reaches an equilibrium state is more appropriate for comparing the extent of swelling of the films in terms of structure and cross-link density.



(a)

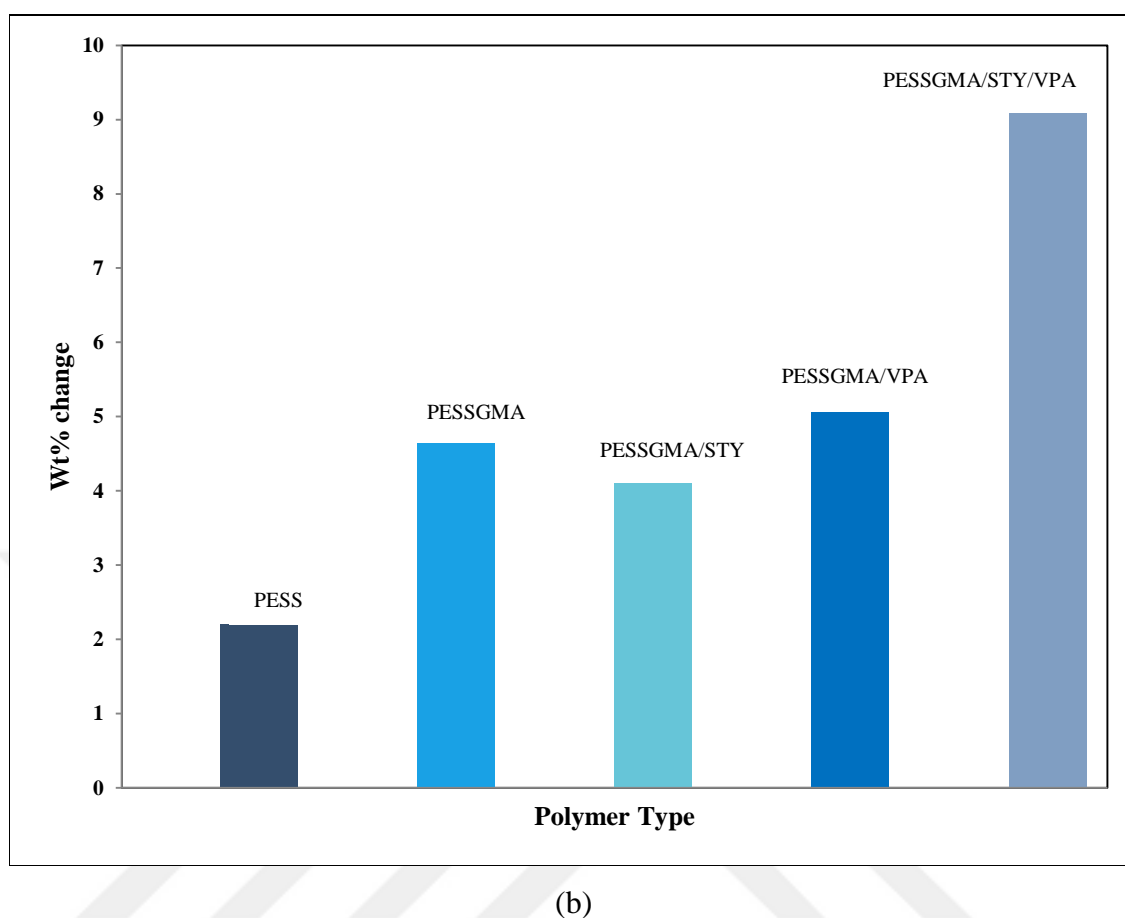


Figure 6.20 a) Weight % change data of the PESS and PESSGMA membranes in water for 400 hrs at room temperature b) weight % change values of the PESS and PESSGMA membranes after 24 hrs in water, at room temperature.

6.3.2. Swelling Experiments at 80°C

The weight percentage change of the PESS and PESSGMA membranes at the end of 24 hrs at 80°C is shown in Figure 6.21. It can be seen that after 24 hrs in deionized water at 80°C, the PESSGMA polymers exhibited considerably decreased swelling in water as compared to PESS polymer which can again be attributed to the cross-linked nature of the PESSGMA polymers. Swelling in water after 24 hrs at 80°C resulted in 55wt% weight change for the PESS polymer whereas the weight change was less than 10wt% for the PESSGMA and PESSGMA/STY polymers and approximately 30wt% for the PESSGMA/VPA polymer and nearly 20wt% for the PESSGMA/STY/VPA polymer. The extent of swelling was much higher at the end of 24 hrs at 80°C as compared to room

temperature. In addition, the extent of swelling changed for the different polymers in a similar trend with those observed at the end of 400 hours in water at room temperature. Here again, the higher extent of swelling observed for the PESSGMA/STY/VPA and PESSGMA/VPA copolymers as compared to the PESSGMA and PESSGMA/STY polymers can be attributed to the presence of the hydrophilic VPA monomer in these copolymers. Thus from both set of experiments, it can be said that the cross-linking of the PESS polymer led to a considerable decrease in the degree of swelling in water as expected, where the extent of swelling or water uptake can be tuned with the presence and concentration of a monomer with ionizable acid functionality such as vinyl phosphonic acid (VPA).

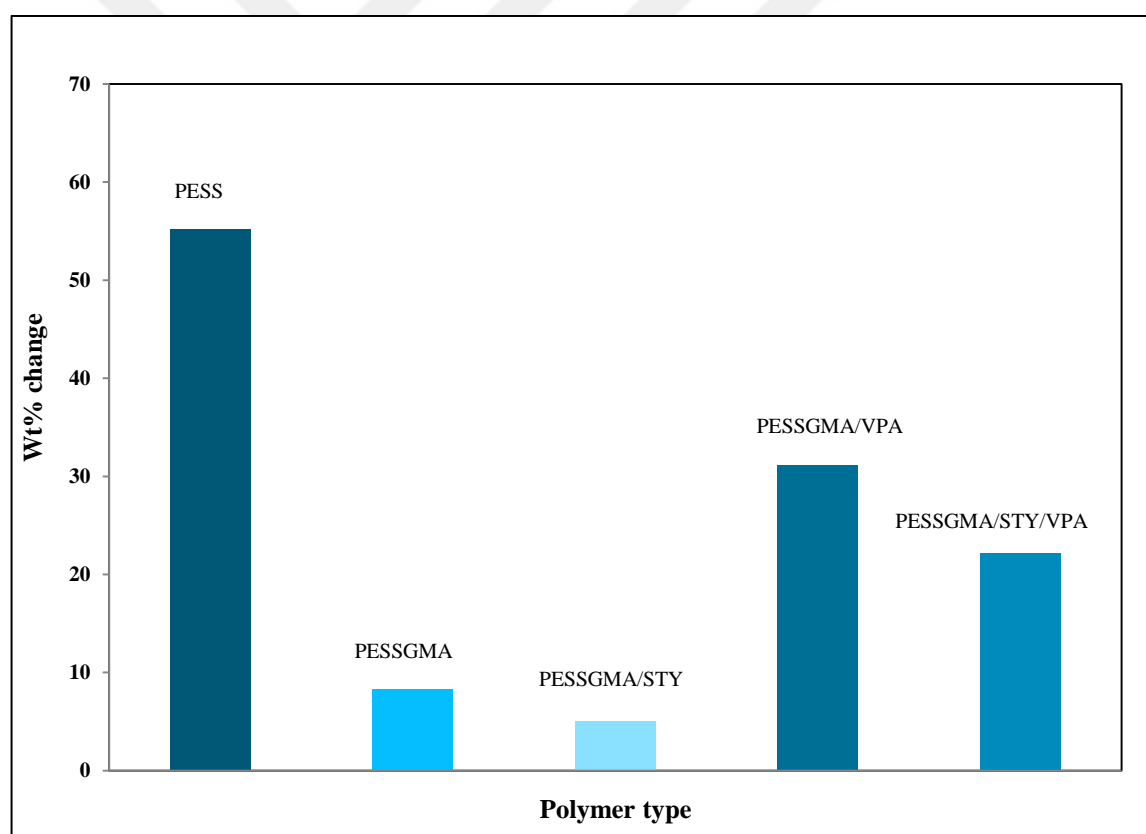


Figure 6.21. Weight % change values of the PESS and PESSGMA membranes after swelling in water for 24 hrs at 80°C.

7. ANALYSIS OF PROPERTIES OF PESS AND PESSGMA POLYMERS FOR FUEL CELL APPLICATIONS

In this chapter, properties like thermal transitions, thermomechanical properties, thermal degradation profiles, proton conductivity and methanol permeability of BPA terminated PESS membrane and the PESSGMA membranes cured under optimized conditions will be presented and will be evaluated with respect to the chemical structure and composition of the polymer membranes. In addition SEM analysis of the membranes will also be presented and discussed.

7.1. DSC ANALYSIS

The heat flow versus temperature plots of the different polymer membranes scanned from 30°C to 300°C at a heating rate of 10°C/min are shown in Figure 7.1. The DSC analysis showed a broad endothermic peak at around 105°C for the PESS and around 115°C for the PESSGMA and PESSGMA/STY polymers that stands for the transition of sulfonic acid groups into ionic clusters. For the PESSGMA/STY/VPA and PESSGMA/VPA polymers, these endo peaks shifted to around 125 °C and 130 °C respectively which may be explained by the presence phosphonic acid groups in addition to sulfonic acid groups. Thus the broad bands centered at around 125 °C for the PESSGMA/STY/VPA and at around 130 °C for the PESSGMA/VPA polymers may similarly be attributed to the transition of both sulfonic acid and phosphonic acid groups into ionic clusters, showing that this transition occurs at a higher temperature for the phosphonic acid groups. In a study on the thermal behavior of Nafion membranes by Almeida S.H. *et al.*[59], the DSC curves for the first heating, for both acid and salt forms of Nafion were reported to display two endothermic peaks, near 120 and 230°C. The high-temperature peak was assigned to the crystalline domains melting in Nafion, and the low-temperature peak was attributed to a transition into ionic clusters, and this transition was reported to exhibit significant changes depending on the nature of the counterion and the degree of hydration. Thus in our system the introduction of a cross-linked structure and phosphonic acid groups to the PESS polymer should both effect the hydration levels and the transition into ionic clusters as well as the temperature that this transition is observed. These peaks were all absent in the second scan indicating that the moisture absorbed in the membranes was lost in the first scan.

The second endo peaks observed for the PESS polymer at 204°C, at 219°C for the PESSGMA and at 215°C for the PESSGMA/STY/VPA copolymer may stand for the glass transition temperatures (T_g 's) of these polymers (despite T_g should be observed more like a step transition, the observation of an endo peak is also possible) although DMA showed lower T_g values for the corresponding polymers. In addition, DSC in general is not sensitive to the glass transition of cross-linked polymers and DMA is a more suitable method to measure the T_g for cross-linked polymers. Finally, the exo peaks observed at around 220 °C for PESS and at around 242 °C for the PESSGMA and PESSGMA/STY polymers may be attributed to the degradation of the side chain sulfonic acid groups. The exo peaks observed for the PESSGMA/VPA and PESSGMA/STY/VPA polymers at 215 °C and at 208 °C respectively can be assigned to the degradation of both the phosphonic and sulfonic acid groups.

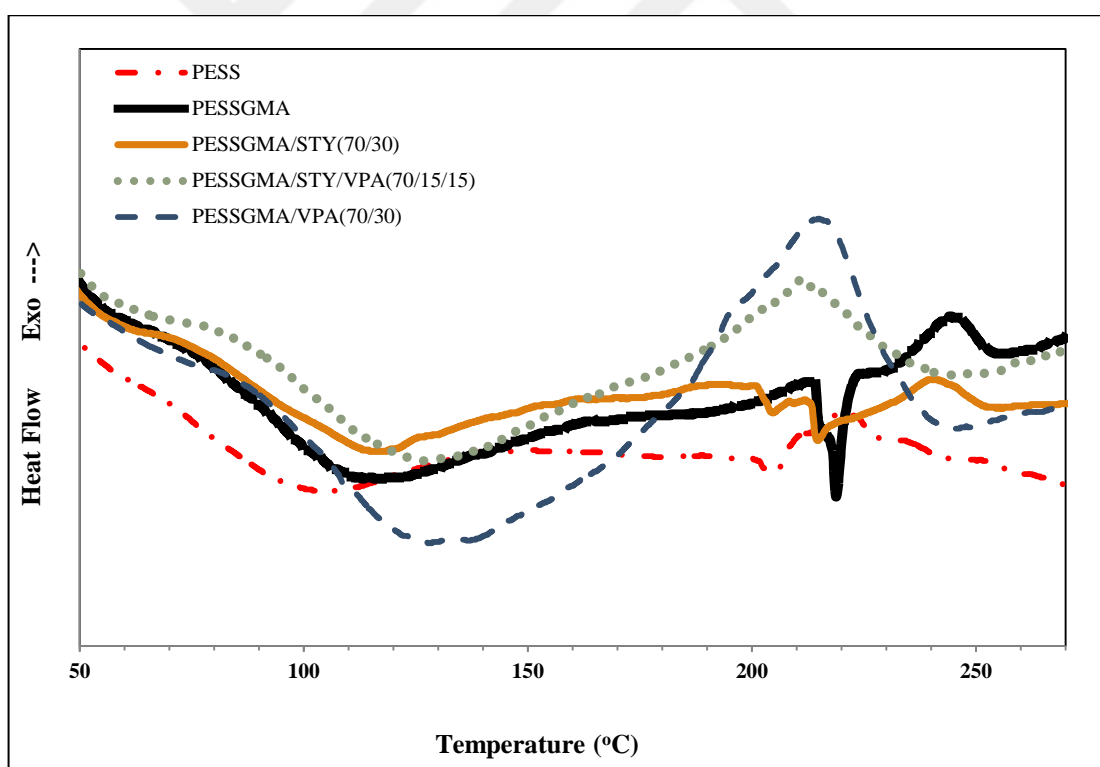


Figure 7.1. The DSC spectra of the PESS and PESSGMA polymer membranes.

The heat flow versus temperature plots of the PESSGMA/VPA(70/30), PESSGMA/VPA(60/40) and PESSGMA/VPA(50/50) polymer membranes scanned from

30°C to 300°C at a heating rate of 10 °C/min are shown in Figure 7.2. According to results of the DSC analysis, the broad endothermic band at around 130°C observed for the PESSGMA/VPA(70/30) polymer should correspond to the transition of both sulfonic acid and phosphonic acid groups into ionic clusters. As VPA content increases the endo peak at around 145°C for the PESSGMA/VPA(60/40) polymer and at around 150°C for the PESSGMA/VPA(50/50) polymer gains intensity on this broad band. These endo peaks can be associated with either the phosphonic acid transition into ionic clusters that can now be distinguished from the sulfonic acid groups or with the T_g 's of these polymers although they exhibited considerably lower T_g 's as determined from DMA data which will be presented in the following section. In addition, two exo peaks in the 185-220°C region are observed for the PESSGMA/VPA membranes. These exo peaks are more separated for the PESSGMA/VPA(60/40) and (50/50) films than the (70/30) film. The first exo peak of PESSGMA/VPA (60/40) and PESSGMA/VPA (50/50) at 186°C and 193°C respectively can be assigned to the degradation of the phosphonic acid groups and the second exo peak of the PESSGMA/VPA (60/40) and PESSGMA/VPA (50/50) at 218°C and 215°C respectively can be assigned to the degradation of the sulphonic acid groups.

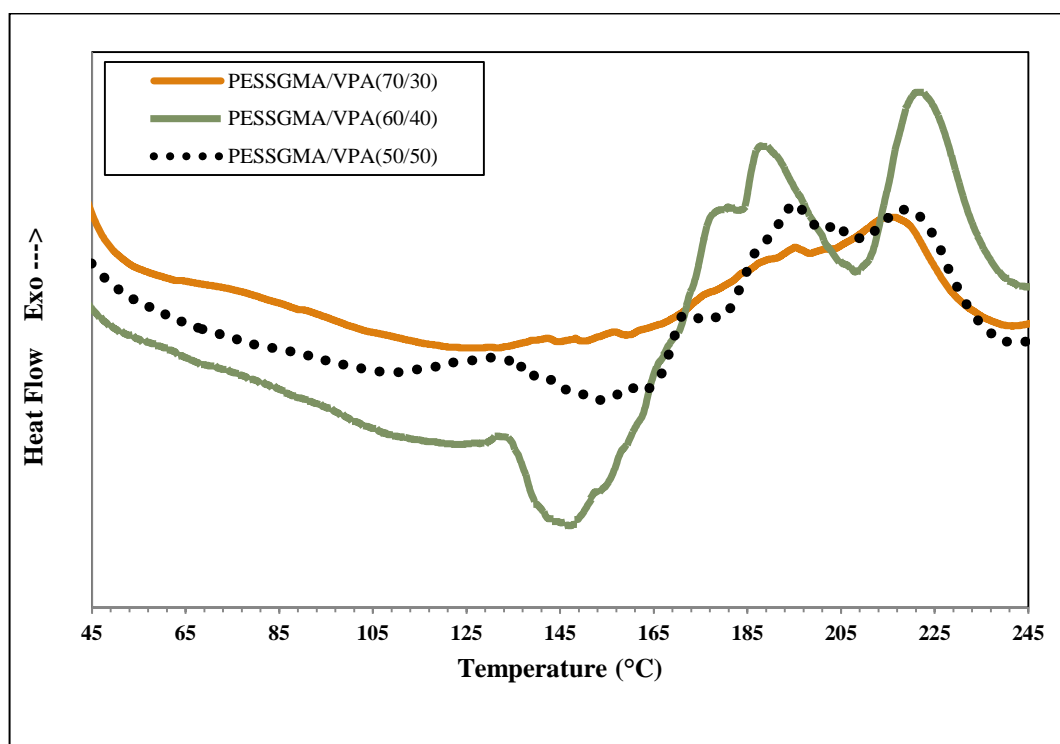


Figure 7.2. The DSC spectra of the PESSGMA/VPA polymer membranes.

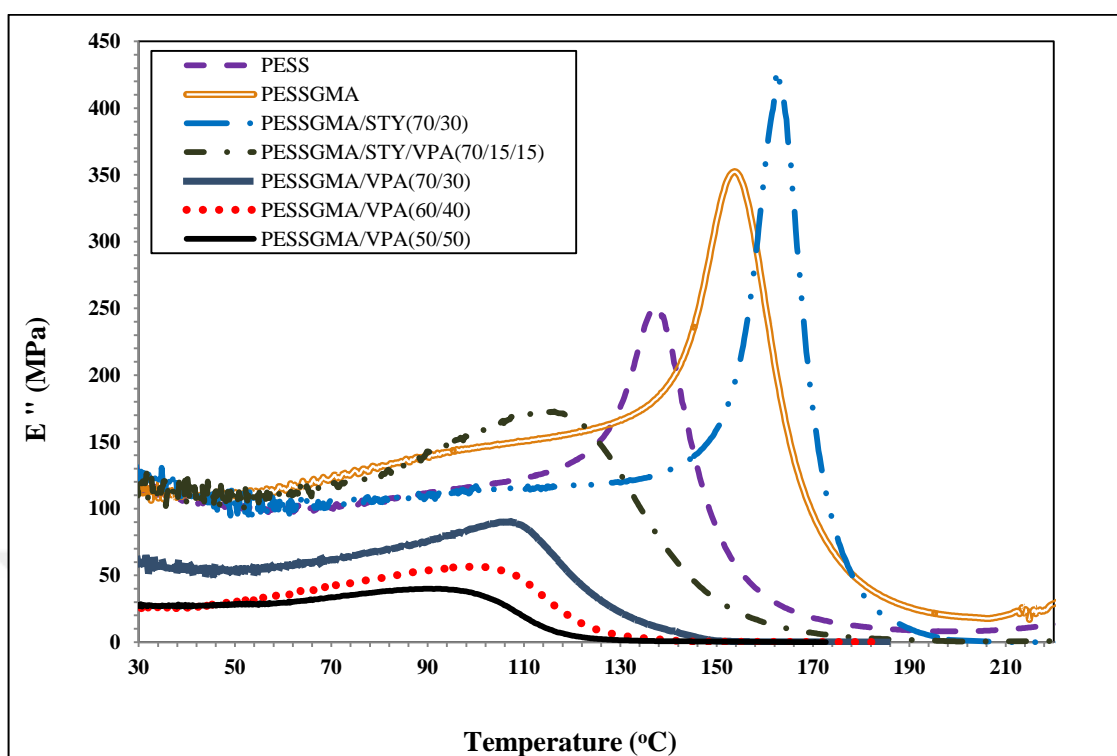
7.2. THERMOMECHANICAL PROPERTIES (DMA)

The thermomechanical properties of the PESS and PESSGMA polymer membranes were determined via DMA. Loss modulus (E'') and storage modulus (E') variations with respect to temperature for the PESS and PESSGMA polymer membranes are shown in Figure 7.3 (a) and (b) respectively. The maxima in the loss modulus (E'') curve corresponds to the state where the maximum energy is released and therefore the temperature at which the peak in the loss modulus occurred in the polymer was considered the glass transition temperature (T_g) of the material [60]. The loss modulus curves given in Figure 7.3(a) indicate that the T_g 's of these polymers range from 94 to 161°C and decrease in the following order; PESSGMA/STY(70/30) > PESSGMA > PESS > PESSGMA/STY/VPA(70/15/15) > PESSGMA/VPA(70/30) > PESSGMA/VPA(60/40) > PESSGMA/VPA(50/50). As expected, the crosslinking of PESS polymer results in an increase in T_g for the PESSGMA and PESSGMA/STY polymers. The higher glass transition temperature of the PESSGMA/STY polymer than that of the PESSGMA polymer can be as a result of the more efficient crosslinking of the PESSGMA methacrylate vinyl groups with styrene resulting in a higher cross-link density. The PESSGMA/VPA polymers on the other hand, although cross-linked exhibited lower T_g 's as compared to that of PESS polymer. This result may be attributed to the lower T_g of polyvinylphosphonic acid units that may have formed during the crosslinking of PESSGMA with VPA [45]. The T_g of polyvinylphosphonic acid homopolymer is reported to be around -234°C [42], therefore one must expect a decrease in the glass transition temperature with the introduction of this comonomer into the PESSGMA network structure. In fact, as will be discussed in the following section, SEM analysis of the PESSGMA/STY/VPA polymer indicated phase separation, thus some separate polyvinyl phosphonic acid unit may act to decrease the glass transition temperature although separate peaks in the loss modulus curves were not observed for this system.

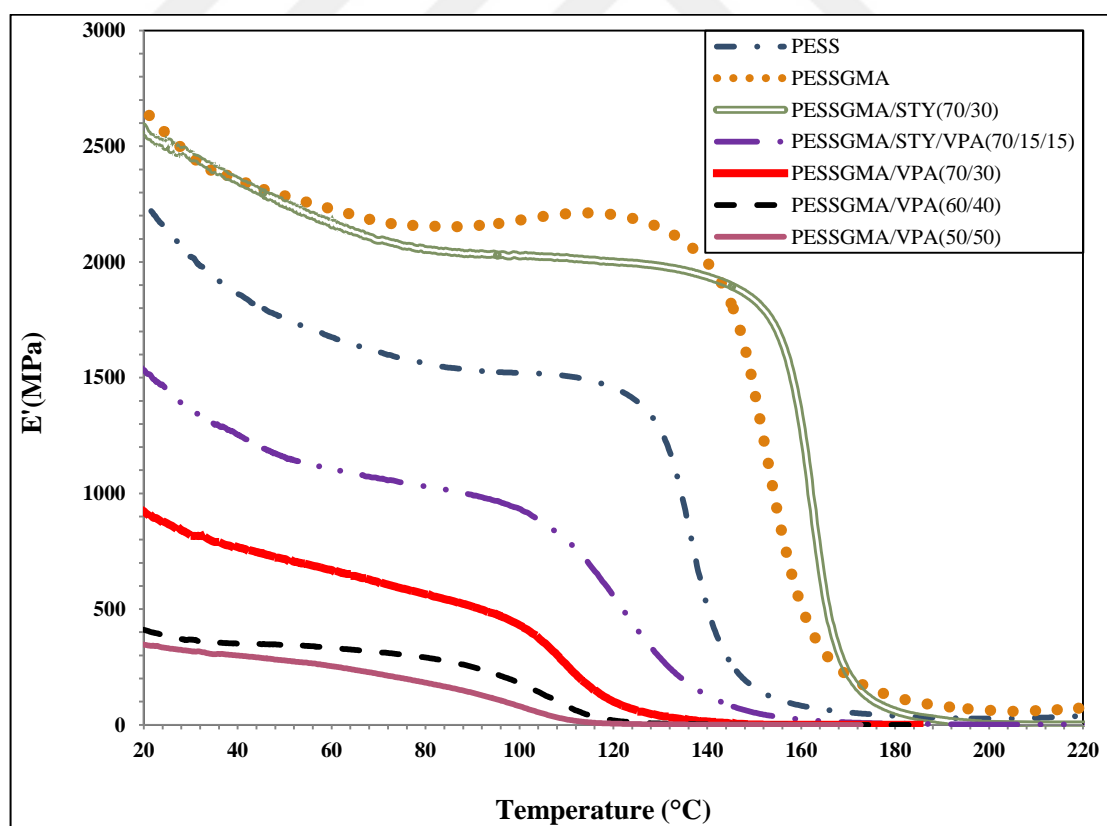
The higher T_g of the PESSGMA/STY/VPA(70/15/15) polymer as compared to that of PESSGMA/VPA polymers may again be attributed to the higher T_g of the polystyrene backbone as compared to that of the polyvinylphosphonic acid. The T_g 's of the PESSGMA/VPA polymers also decreased with increasing VPA content (from 30 to 50wt%). This result can be explained both by the lower T_g of polyvinyl phosphonic acid as

compared to the PESSGMA polymer and also to the expected decrease in crosslink density with decreasing content of the PESSGMA which is the cross-linker unit in the system.

An examination of storage modulus versus temperature plots in Figure 7.3(b) indicates that, at temperatures below the glass transition temperature (T_g) of PESS and PESSGMA polymers (thus in the temperature range where fuel cell membranes may be used), the storage modulus values decrease in the following order; PESSGMA > PESSGMA/STY(70/30) > PESS > PESSGMA/STY/VPA(70/15/15) > PESSGMA/VPA(70/30) > PESSGMA/VPA(60/40) > PESSGMA/VPA(50/50). Thus the cross-linked nature of PESSGMA and the introduction of the rigid aromatic styrene monomer to the system increased the modulus significantly as compared to the PESS polymer below the T_g of these polymers. In addition, the aromatic structure of the PESSGMA backbone and styrene gives rigidity to these polymers [61], thus the introduction of VPA monomer to the PESSGMA network seems to decrease the storage modulus. Also due to the lower reactivity of VPA monomer [62], as compared to styrene which is highly reactive in copolymerization with methacrylates, the PESSGMA/VPA polymers must exhibit lower crosslink densities, which was also confirmed with the higher swelling ratios of the PESSGMA/VPA polymers as compared PESSGMA/STY polymers. Thus, the lower crosslink density of the PESSGMA/VPA polymers may also act to decrease the modulus values. The increase in VPA content also seems to decrease the storage modulus values further due to both the lack of aromaticity of the VPA monomer in addition to the decreasing cross-link density of the system.



(a)



(b)

Figure 7.3. (a) Loss modulus versus temperature (b) storage modulus versus temperature plots for PESS, PESSGMA and PESSGMA co-polymer membranes.

For a direct comparison of the properties of the PESS and PESSGMA polymers, the storage modulus (E') values at room temperature and 60°C and the T_g 's as determined from the loss modulus maxima are presented in Table 7.1. In addition, the temperature of tan delta maxima for each polymer is also listed in this table. The temperature at which the tan delta is a maximum is also used for determining the T_g of a polymer and is always higher than the temperature corresponding to maximum loss modulus (E'') [63]. The T_g determined from tan delta maximum reflects the influence of the structural effects on the glass transition temperatures of cross-linked polymers when a peak can not be observed in the loss modulus curve. A quick examination of this table indicates that the storage modulus values of the PESS and PESSGMA polymers at 25°C range from 363 MPa to 2589 MPa. The introduction of the VPA comonomer to the PESSGMA network seems to decrease the storage modulus considerably due to the lack of aromaticity in its structure as well as an expected decrease in the cross-link density of the system, as discussed previously. The increase of the temperature from 25°C to 60°C results in about 11 to 21% decrease in the storage modulus values for the different types of the PESS and PESSGMA membranes. The storage modulus values of all the PESSGMA copolymers at 30wt% comonomer content range from 0.6GPa to 2.1GPa even at 60°C . The glass transition temperatures of all the membranes as determined from the loss modulus maxima are above 90°C which means that these membranes can be used below their T_g 's at $60\text{-}80^\circ\text{C}$ temperature range where they can be used in DMFC applications. The PESSGMA/STY(70/30) polymer exhibits the highest T_g at 161°C , whereas the PESSGMA/VPA(50/50) polymer exhibits the lowest T_g at 94°C . Similar trends are observed for the tan delta maximum temperatures.

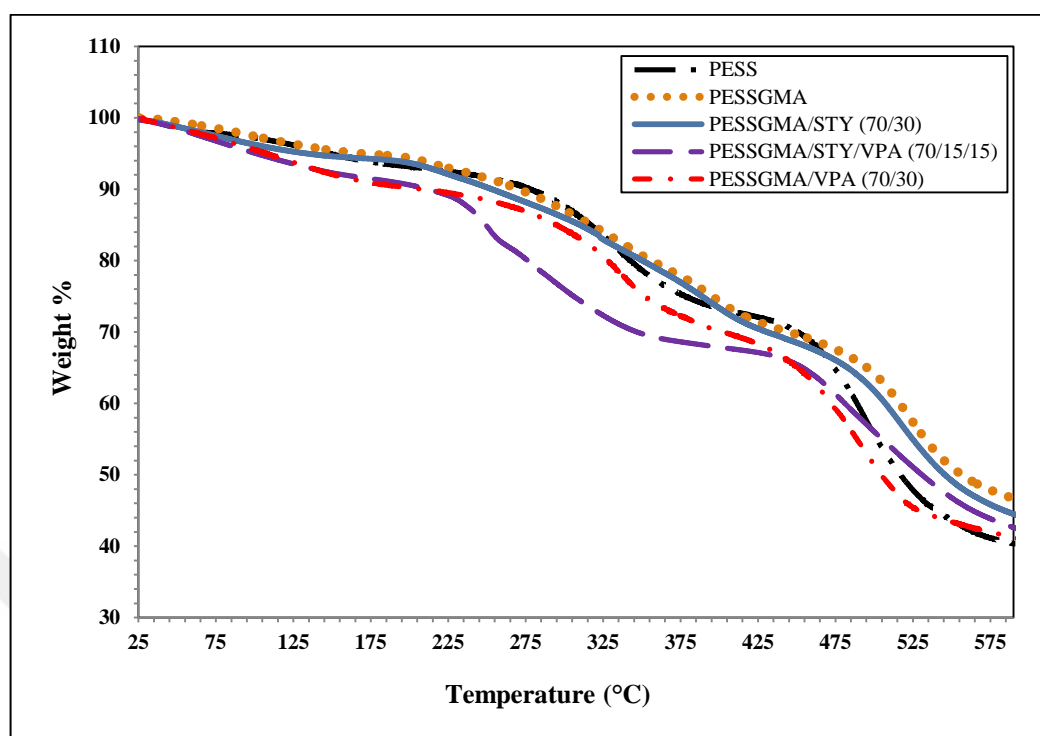
Table 7.1. Storage modulus (E') values at 25°C and 60°C and glass transition temperatures (T_g) for the PESS and PESSGMA polymers as determined by DMA.

Polymer	E'(25°C) (MPa)	E'(60°C) (MPa)	T_g (E'' Max) (°C)	T_g (Tan delta max) (°C)
PESS	1894±239	1674±130	139±1	160±14
PESSGMA	2589±40	2259±30	152±2	166±4
PESSGMA/STY(70/30)	2486±32	2129±30	161±2	172±2
PESSGMA/STY/VPA(70/15/15)	1066±374	931±435	112±4	144±26
PESSGMA/VPA(70/30)	739±131	583±84	114±6	146±14
PESSGMA/VPA(60/40)	420±35	352±112	104±4	125±2
PESSGMA/VPA(50/50)	363±32	289±36	94±4	118±0.3

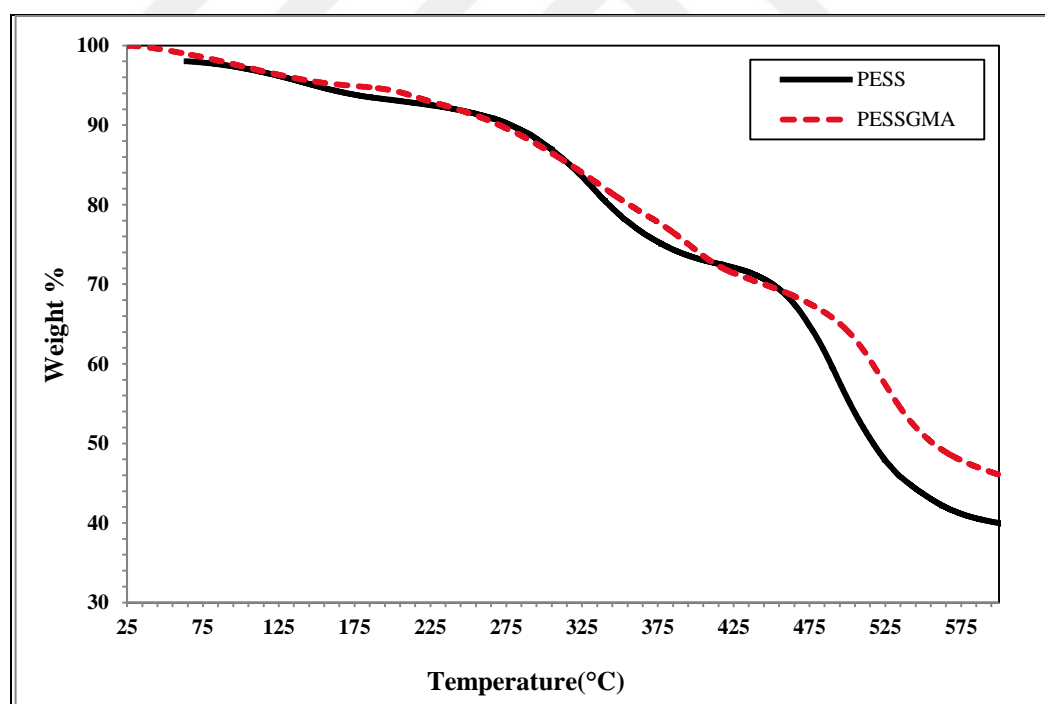
7.3. THERMAL GRAVIMETRIC ANALYSIS (TGA)

Thermogravimetric analysis (TGA) is used for determining a material's thermal stability and its fraction of volatile components by monitoring the percent weight change that occurs as a specimen is heated. The percentage weight versus temperature plots of the PESS, PESSGMA, PESSGMA/STY(70/30), PESSGMA/VPA(70/30) and PESSGMA/STY/VPA(70/15/15) polymer membranes scanned from 30°C to 600°C at a heating rate of 10°C/min are shown in figure 7.4(a), in addition percent weight versus temperature plots of the PESS and PESSGMA polymers are presented in figure 7.4 (b) for a better comparison. The plots shown in figure 7.4 (a) display two major weight loss stages at around 200–360 °C and 400–550 °C. The first weight loss stage can be ascribed to the removal of $-SO_3H$ groups and the second weight loss stage can be ascribed to the splitting of the poly(arylether sulfone) polymer main chain as noted for some other cross-linked poly(aryl ethersulfone) systems [64]. Thus the PESSGMA/VPA polymers must

exhibit a higher weight loss in this first degradation stage because of the loss of the phosphonic acid groups in addition to sulfonic acid groups. The slight weight loss under 200 °C observed for all samples on the other hand can be explained by the removal of water molecules from the polymer matrix or of moisture absorbed from the air. A quick examination of the percent weight versus temperature plots of the PESS and PESSGMA polymers shown in figure 7.4 (b) indicates that PESS and PESSGMA polymers exhibit similar degradation profiles in the 30-360°C temperature range. However, the second stage degradation starts at a higher temperature for the PESSGMA polymer (~ 480°C) as compared to the PESS polymer (~ 440°C) and the char residue at 600°C is also higher (46wt%) for the PESSGMA polymer as compared to that of PESS polymer (40wt%) due to the cross-linked structure of PESSGMA[65]. For the PESSGMA/STY polymer the degradation profile is quite similar to that of the PESSGMA polymer, thus the introduction of the styrene co-monomer or the change in cross-link density of the system does not seem to have a significant effect on the thermal stability of the PESSGMA network. For the PESSGMA/VPA polymer, there is a greater weight loss for the whole temperature range (30 to 600°C), and the second stage degradation starts at a lower temperature and the char residue is also lower than those of PESSGMA, PESSGMA/STY and PESSGMA/STY/VPA polymers. When the PESSGMA/STY/VPA polymer degradation profile is examined, the first stage degradation seems to start at the lowest temperature which may be attributed to the decrease in VPA content however the char yield after the second degradation is higher than both the PESSGMA/VPA and PESS polymer. This increased char yield for the PESSGMA/STY/VPA polymer as compared to that of the PESSGMA/VPA can be explained by the higher cross-link density of the PESSGMA/STY/VPA polymer as compared to that of the PESSGMA/VPA polymer as also observed from the swelling in water measurements.



(a)



(b)

Figure 7.4. The weight% vs temperature plots of (a) PESS, PESSGMA and PESSGMA copolymers (b) PESS and PESSGMA polymers.

The percent weight change versus temperature plots of the PESSGMA/VPA polymers at different VPA contents, (70/30), (60/40) and (50/50) are shown in Figure 7.5. Here, again two degradation stages can be observed for PESSGMA/VPA (70/30) polymer in the 30-600°C temperature range whereas three weight loss stages can be distinguished for the PESSGMA/VPA (60/40) and PESSGMA/VPA (50/50) polymers within the same temperature range. The two weight loss stages displayed by the PESSGMA/VPA (60/40) and PESSGMA/VPA (50/50) polymers in the 90-320°C temperature range may be attributed to the gradual degradation of sulfonic acid and phosphonic acid groups that can be distinguished in the presence of increasing amount of VPA. The last degradation stage which should correspond to the degradation of the main chain starts at nearly around 430°C for the PESSGMA/VPA (70/30) polymer and the main chain degradation starts at a lower temperature as the VPA content increases, at around 410°C for the PESSGMA/VPA (60/40) polymer and at around 390°C for the PESSGMA/VPA (50/50) polymer. The remaining char residue at 600°C also decreases with increasing VPA content as: 41wt% for PESSGMA/VPA (70/30), 35wt% for the PESSGMA/VPA (60/40) and 33wt% for the PESSGMA/VPA (50/50) polymer. Thus, it can be said that the temperatures at which the last stage degradation starts (corresponding to main chain and network degradation) shift to lower temperatures and the char residue at each temperature decreases as the VPA content increases for the PESSGMA/VPA polymers. This result may be explained by the decrease of PESSGMA content with increasing VPA content since PESSGMA is both cross-linker unit in the system and thermally more stable than the VPA co-monomer due to its aromatic structure [65]. Thus, the decrease in PESSGMA content and increasing VPA content decrease the cross-link density, the thermal stability and the char yield for the PESSGMA/VPA polymers.

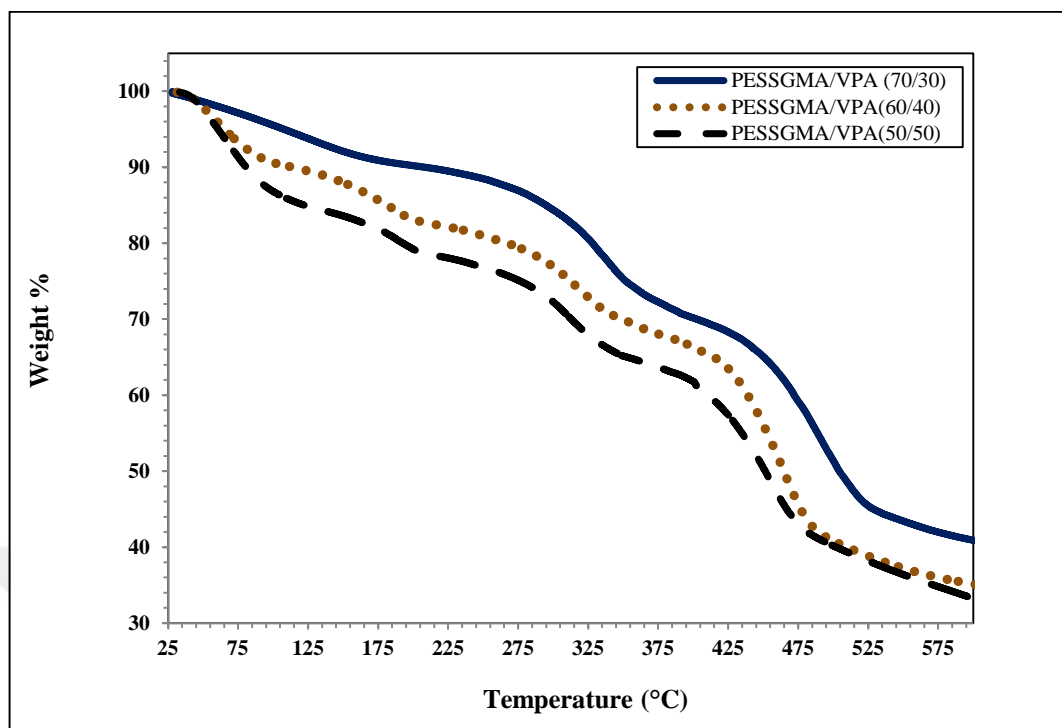


Figure 7.5. The weight% vs temperature plots of PESSGMA/VPA co-polymers.

The temperatures for 5, 10 and 20wt% loss for the PESS and PESSGMA polymer membranes are also listed in Table 7.2. Based on this data and above discussions we can conclude that the PESSGMA polymer exhibits slightly increased thermal stability as compared to the PESS polymer in the 30-400°C temperature range whereas the thermal stability in this temperature range decreases for the other PESSGMA copolymers although the char yield above 500°C are higher for all the PESSGMA polymers as compared to the PESS polymer due to their cross-linked nature. The decrease in the thermal stability of the PESSGMA/VPA polymers as compared to the PESS, PESSGMA and PESSGMA/STY polymers in the 30-400°C temperature range can be attributed to both more moisture absorption and the degradation of additional phosphonic acid groups in addition to the sulfonic acid groups in this temperature range. The temperature of 10wt% loss is above 200°C for all of the PESS and PESSGMA polymer membranes except for the PESSGMA/VPA(60/40) and PESSGMA/VPA(50/50) polymer membranes. The temperature of 20wt% loss is the lowest value at 192°C for the PESSGMA/VPA(50/50) and is the highest at 356°C for the PESSGMA membrane.

Table 7.2. The temperatures for 5,10 and 20wt% loss for the PESS and PESSGMA polymer membranes.

Polymer	Temperature of 5% weight loss (°C)	Temperature of 10% weight loss (°C)	Temperature of 20% weight loss (°C)
PESS	147	275	341
PESSGMA	168	272	356
PESSGMA/STY (70/30)	133	252	349
PESSGMA/STY/VPA (70/15/15)	100	210	277
PESSGMA/VPA (70/30)	107	205	327
PESSGMA/VPA (60/40)	64	112	266
PESSGMA/VPA (50/50)	61	81	192

7.4. PROTON CONDUCTIVITY RESULTS

The proton conductivity measurements were conducted in 60°C and 80°C saturated water vapor for 48hrs as explained in the experimental section. Table 7.3 lists the measured proton conductivities of the different polymer membranes at 60°C and 80°C, at the end of approximately 48hrs when the resistance value recorded stabilized. Unfortunately, although the PESSGMA polymer and the PESSGMA/STY copolymer exhibited significantly improved T_g 's, higher thermal stabilities at the higher temperature ranges, and reduced swelling (wt% change) in water, they exhibited significantly reduced proton conductivity values as compared to that of PESS polymer. This may be related to the lower water uptake of the PESSGMA polymers (due to their cross-linked structure) as compared to PESS polymer as the proton transport in membranes requires both well connected ion channels and proper contents of bonded water [66]. Also we suspect that some of the sulfonic acid groups may be lost in a side reaction with glycidyl methacrylate instead of reaction with the aromatic hydroxyls of the PESS prepolymer during the synthesis of PESSGMA. In several other studies, the cross-linking of poly(aryl ether sulfone) type polymers has been reported to reduce the proton conductivity of the resulting membranes [39,66,67,68].

In an example study, Park K.T. *et al.* similarly reported for sulfonated poly(arylether sulfone) copolymers containing carboxyl groups which were cross-linked with hydroquinone in the presence of the catalyst, sodium hypophosphite, that the water uptake and proton conductivity of the membranes were decreased with increasing the degree of cross-linking [39].

In another study [67], Park J.Y prepared a series of sulfonated poly(aryl ether sulfone) with photo cross-linkable moieties and reported that the cross-linked membranes showed less water uptake, a lower level of methanol permeability, and good thermal and mechanical properties compared to non-crosslinked membranes. Although cross-linking decreased the proton conductivity values a reasonable level of proton conductivity was still maintained. Kiran V.*et al.*, in a related study on cross-linked poly(arylether sulfone)s [68], synthesized a sulfonated poly (aryl ether sulfone) copolymer by direct copolymerization of 4,4'-bis(4-hydroxy phenyl) valeric acid, benzene 1,4-diol and synthesized sulfonated 4,4'-difluorodiphenylsulfone. This copolymer (SPAES) was subsequently cross-linked with 4,4'-(hexafluoroisopropylidene) diphenol epoxy resin by thermal curing reaction to synthesize cross-linked membranes. The copolymer (SPAES-H-0) exhibited a proton conductivity of 6.8mScm^{-1} at 30°C which decreased with cross-linking with the EFN resin at 50-70 wt% content. The proton conductivity decreased with increasing crosslink density and was reduced to 3mScm^{-1} at 30°C for the membrane cross-linked with 70wt% EFN resin. In addition reduction in water and methanol uptake, ion exchange capacity, with simultaneous enhancement in oxidative stability was observed for the cross-linked membranes as compared to pristine membrane. In a work by Dongsheng L. *et al.*[66], a series of sulfonated poly(aryl ether sulfone) copolymers (SPSFs) containing phenyl pendant groups with sulfonic acid groups on the backbone was synthesized. The SPSF copolymers were then cross-linked using changing amounts of 4,4'-thiodibenzoic acid (TDA) as a cross-linker. The proton conductivity was again reported to decrease with increasing cross-linking density of the membrane.

On the other hand as can be seen from Table 7.3, introduction of VPA monomer to the PESSGMA matrix improved proton conductivity significantly and the proton conductivities were further increased with increasing VPA content of the matrix from 30wt% to 50wt% due to the introduction of additional phosphonic acid groups to the

system. The use of poly(vinyl phosphonic acid) and its derivatives as polymer electrolyte membranes in fuel cells has been reviewed by Macarie L. *et al.* [69].

The proton transport mechanism in phosphonic acid is different from that in Nafion. In Nafion, a channel-like structured polymer allows the protons to travel through the membrane [70]. The protons are attached to water molecules which are used as vehicles resulting in traveling hydronium ions. This mechanism requires wet state of the membrane and as temperatures above 100°C would cause evaporation of water, these membranes can not be used for high temperature applications. In phosphonic acids a totally different mechanism is involved. Here, the protons travel via the hydrogen bonds of neighbored phosphonic acid groups. Ionic bonds break and form between phosphonic acid groups as the proton is hopping to the next molecule [71]. Thus in some studies the proton conductivities of membranes based on PVPA and its derivatives have been examined at temperatures above 100°C in anhydrous state. In an example study [40], Parvole J. *et al.* prepared membranes by grafting poly(vinylphosphonic acid) side chains onto polysulfones which showed high proton conductivities, e.g., $5 \times 10^{-3} \text{ Scm}^{-1}$ under nominally dry conditions at 120°C and up to $9.3 \times 10^{-2} \text{ Scm}^{-1}$ under 100% relative humidity at the same temperature. In a related study by Sannigrahi A. *et al.* [72], multiblock copolymers were prepared by coupling polyfluoroether (PFE) and polysulfone (PSU) precursor blocks under mild conditions. Lithiation of the PSU block, followed by anionic polymerization of diethyl vinyl phosphonate and hydrolysis led to poly(vinyl phosphonic acid) (PVPA) side chains attached to PSU blocks. Proton conductivities above 80 mScm^{-1} at 120°C were reported for the fully hydrated multiblock copolymer membranes. In another study [43], Göktepe F. *et al.* prepared novel polymer complex electrolytes consisting of chitosan and poly(vinylphosphonic acid), PVPA via in situ polymerization of vinyl phosphonic acid in the presence of chitosan at various monomer feed ratios with respect to D-glucosamine repeat unit. The proton conductivity of CHPVPA₅ polymer electrolyte membrane was reported to be around $3 \times 10^{-5} \text{ S cm}^{-1}$ at 120 °C in the anhydrous state.

Aslan A. *et al.*, in another study [41], prepared graft copolymer electrolytes by grafting of poly(vinyl phosphonic acid), PVPA onto poly(glycidyl methacrylate), PGMA via ring opening of ethylene oxide groups. Several graft copolymers were produced at various stoichiometric ratios with respect to monomer repeat units. The proton conductivity of P(GMA)-graft-P(VPA)₁₀ was reported as $5 \times 10^{-5} \text{ Scm}^{-1}$ at 150 °C in the anhydrous state.

The proton conductivity of the same polymer was measured as 0.03 S cm^{-1} at 80°C under 50% of RH. In a similar study [44], Yazawa T. *et al.* reported a maximum proton conductivity of $3.7 \times 10^{-2} \text{ S cm}^{-1}$ at 80°C under 90% of relative humidity for polyvinyl phosphonic acid, PVPA and 3-glycidoxypropyltrimethoxysilane graft membranes. As can be seen, the proton conductivity values reported for the PVPA copolymers at 80°C under changing relative humidity conditions range from 30 to 37 mS cm^{-1} . The proton conductivities of the PESSGMA /STY/VPA and PESSGMA/VPA (at 30-50wt% VPA content) copolymer membranes at 80°C range from 28 mS cm^{-1} to 42 mS cm^{-1} and therefore are in a comparable range with those reported in literature.

Table 7.3. Proton conductivity data of the different polymer membranes at the end of 48hrs, in saturated water vapor at 60°C and 80°C .

Polymer	Proton Cond. (60°C) (mS cm^{-1})	Proton Cond. (80°C) (mS cm^{-1})
PESS	76.3 ± 3.5	79.40 ± 0.47
PESSGMA	0.87 ± 0.02	2.56 ± 0.24
PESSGMA/STY(70/30)	1.19 ± 0.01	2.45 ± 0.19
PESSGMA/STY/VPA(70/15/15)	16.0 ± 3.1	27.82 ± 1.43
PESSGMA/VPA(70/30)	25.4 ± 2.1	32.21 ± 0.54
PESSGMA/VPA(60/40)	31.52 ± 0.54	35.61 ± 1.06
PESSGMA/VPA(50/50)	28.98 ± 0.96	41.55 ± 2.07

7.4.1. Effect of Temperature

As can be seen from Table 7.3, the proton conductivities of all the PESS and PESSGMA polymer membranes measured at 80°C were significantly higher than those measured at 60°C , and the increase was more pronounced for the PESSGMA and PESSGMA/STY polymers. These results can be attributed to the higher transmission of protons (H^+) through the membranes with increasing temperature since conductivity is directly proportional with temperature. When the temperature increases, the proton conductivity increases as the mobility of proton ions rises at higher temperatures [73].

7.4.2. Effect of Initiator Content

In our previous studies 4wt% initiator (tert-butyl peroxy benzoate, TBPB) content was found to be necessary to prepare fully cross-linked rigid films. Thus all the films were prepared in the presence of 4wt% initiator. In an effort to see, the effect of initiator content on proton conductivity of the PESSGMA polymers, the proton conductivity of the PESSGMA membrane cured with 2wt% initiator was also measured at 80°C and found to be $2.01 \pm 0.03(\text{mS cm}^{-1})$ which was lower than that of the PESSGMA membrane cured with 4wt% initiator ($2.51 \pm 0.06\text{mS cm}^{-1}$ at 80°C). This result indicates that increasing initiator content does not decrease the proton conductivity as the whole initiator content is consumed in the radical polymerization of the PESSGMA system and does not interfere with proton transfer.

7.5. METHANOL PERMEABILITY

For direct methanol fuel cells (DMFCs) a high methanol permeability through the proton exchange membrane leads to a decreased fuel cell performance owing to depolarization of the oxygen reducing cathode. Thus a low methanol permeability is a desirable characteristic of a polymer electrolyte membrane that is designed to be used in DMFC applications. The commercial Nafion membranes suffer from a relatively high methanol permeability in applications for DMFCs. The methanol permeabilities of the polymer membranes prepared in this study were determined as explained in the experimental section using Equation 4.4. Table 7.4 lists the methanol diffusion coefficients of the PESSGMA and PESSGMA copolymer membranes at 60°C. In addition, the methanol diffusion coefficient values of the PESS(60) [38] and the commercial Nafion membrane [74] as reported in literature are also listed. It can be observed that the methanol permeability of the PESSGMA and PESSGMA copolymer membranes were significantly reduced both as compared to the PESS and the Nafion membranes. The methanol diffusion coefficient of the cross-linked PESSGMA polymer membrane which exhibited the lowest methanol permeability decreased about 200 times as compared to that of the PESS polymer membrane and about 2000 as compared to the Nafion membrane. As can be seen from the data in the table, all the PESSGMA crosslinked membranes showed methanol diffusion coefficients below $1.92 \times 10^{-8} \text{ cm}^2 \text{ s}^{-1}$, with the lowest value of $2.37 \times 10^{-9} \text{ cm}^2 \text{ s}^{-1}$,

demonstrating excellent resistance to methanol crossover. On the other hand, the introduction of 30wt% styrene increased the methanol diffusion coefficient slightly as compared to PESSGMA membrane. Also when styrene was replaced with VPA co-monomer at the same content, methanol permeability increased only slightly which can be attributed to the more hydrophilic structure of the VPA co-monomer as compared to styrene as hydrophilic moieties in the polymer structure tend to increase the methanol permeability (methanol cross-over can be reduced with the effect of hydrophobic modification) [75]. In addition the methanol diffusion coefficients of the PESSGMA/VPA copolymers increased again slightly with the increase in VPA content again owing to the increasing hydrophilicity and decreasing cross-link density of the system.

In a study on quinoxaline-based crosslinked sulfonated poly(aryl ether sulfone)s (SPAESs) [76], the cross-linked polymer membranes exhibited lower methanol permeability values than the non-crosslinked membranes. The methanol diffusion coefficients of the cross-linked polymer membranes ranged from 1.9×10^{-7} to $4.9 \times 10^{-7} \text{ cm}^2 \text{ s}^{-1}$ at 25°C changing with the cross-link density of the system. In another study on a series of photo-cross linked sulfonated poly(aryl ether sulfone)s [74], again the crosslinked membranes showed a lower level of methanol permeability compared to pristine (non-crosslinked) membranes while maintaining a reasonable level of proton conductivity. The methanol diffusion coefficients of these membranes decreased with increasing cross-link density and were in the following range : 1.35×10^{-6} - $0.65 \times 10^{-6} \text{ cm}^2 \text{ s}^{-1}$ at 25°C and 3.24×10^{-6} - $2.24 \times 10^{-6} \text{ cm}^2 \text{ s}^{-1}$ at 60°C . For the majority of studies on polymer membranes incorporating VPA or phosphonic acid moieties, proton conductivity data has been reported but methanol permeability data has not been presented. In a related study on phosphonic acid grafted bis(4- γ -aminopropyl-diethoxysilylphenyl) sulfone (APDSPS) poly(vinyl alcohol)(PVA) cross-linked polyelectrolyte membranes [75], the cross-linked PVA-APDSPS membranes exhibited methanol diffusion coefficient values from 2.02×10^{-7} to $1.46 \times 10^{-7} \text{ cm}^2 \text{ s}^{-1}$ at 25°C , decreasing with the increasing hydrophobic APDSPS content of the polymer membranes. In another study on chitosan/poly(vinyl phosphonic acid) complex polymer electrolytes [43], the polymer electrolytes were prepared via in situ polymerization of vinyl phosphonic acid in the presence of chitosan at various monomer feed ratios with respect to D-glucosamine repeat unit. The methanol molar flux of CHPVPA5 complex polymer electrolyte membrane prepared in this work, was reported as $3.39 \times 10^{-9} \text{ mol cm}^{-1} \text{ s}^{-1}$ at 20°C .

°C and $5.42 \times 10^{-9} \text{ mol cm}^{-1} \text{ s}^{-1}$ at 40 °C, which was found to be lower than that of commercial Nafion membrane. As can be seen, the PESSGMA and PESSGMA copolymer membranes prepared in this study exhibited lower methanol permeability data than those reported for polymer membranes based on either cross-linked poly(aryl ether sulfone)s or polymer membranes incorporating phosphonic acid units in their structures.

As described previously in the theory section, a polymer electrolyte membrane suitable to be used in DMFC applications should possess both a high proton conductivity and low methanol permeability. The ratio of proton conductivity to methanol permeability termed as the selectivity parameter (ρ), is an effective parameter to evaluate the performance of membrane in a DMFC system. Thus the selectivity ratios (ρ) of the PESSGMA and PESSGMA copolymer membranes are also listed in Table 7.4 together with the selectivity ratio (ρ) values of the PESS and the commercial Nafion membrane as reported in literature. A quick examination of the selectivity ratios indicates that the PESSGMA/VPA(60/40) polymer exhibits the highest selectivity ratio and is therefore most suitable to be used as a polymer electrolyte membrane in DMFC application if we consider only the proton conductivity and methanol permeability data. One can also suggest that all the PESSGMA copolymers incorporating VPA exhibited comparable ρ values to each other which were also significantly higher than those of the PESS, PESSGMA and PESSGMA/STY membranes and therefore are suitable to be used in DMFCs. However other properties such as modulus, thermal stability and water absorption capacity of the membranes also have to be considered to suggest the formulation with optimum set of properties, which suggest the PESSGMA/STY/VPA membrane as the most suitable candidate. This discussion will be presented in detail in the conclusions section of the thesis.

Table 7.4. Methanol permeability and selectivity ratios of the PESS, PESSGMA and PESSGMA copolymer membranes at 60°C.

Polymer	Methanol Permeability (cm ² s ⁻¹)(60°C)	Selectivity Ratio(ρ) (Ss cm ⁻³)
Nafion	^a 3.20x10 ⁻⁶	5.00x10 ⁴
PESS	^{b*} 5.20x10 ⁻⁷	1.47x10 ⁵
PESSGMA	2.37x10 ⁻⁹	3.67x10 ⁵
PESSGMA/STY(70/30)	5.47x10 ⁻⁹	2.18x10 ⁵
PESSGMA/STY/VPA(70/15/15)	^c 6.52x10 ⁻⁹	2.45x10 ⁶
PESSGMA/VPA(70/30)	7.57x10 ⁻⁹	3.36x10 ⁶
PESSGMA/VPA(60/40)	8.10x10 ⁻⁹	3.89x10 ⁶
PESSGMA/VPA(50/50)	1.92x10 ⁻⁸	1.51x10 ⁶

^aLiterature data (Park J.Y.) [67].

^bLiterature data (Oh Y.S. *et al.*) [38].

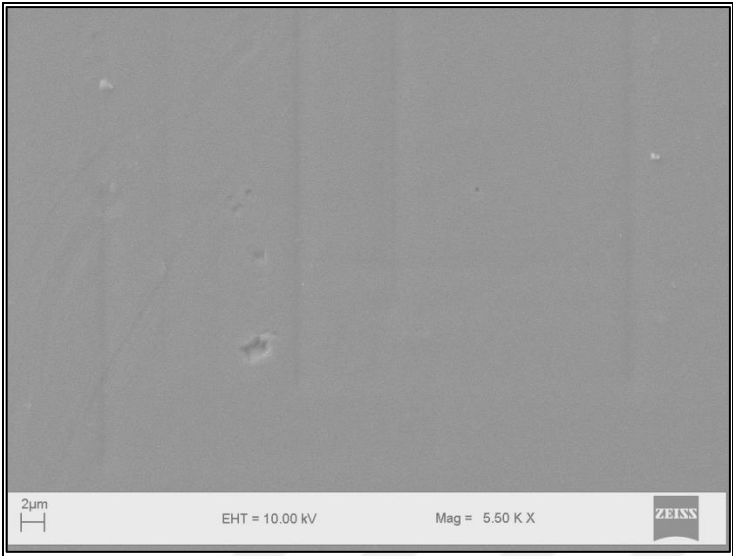
^c Data produced through extrapolation.

* Methanol permeability reported at 25°C.

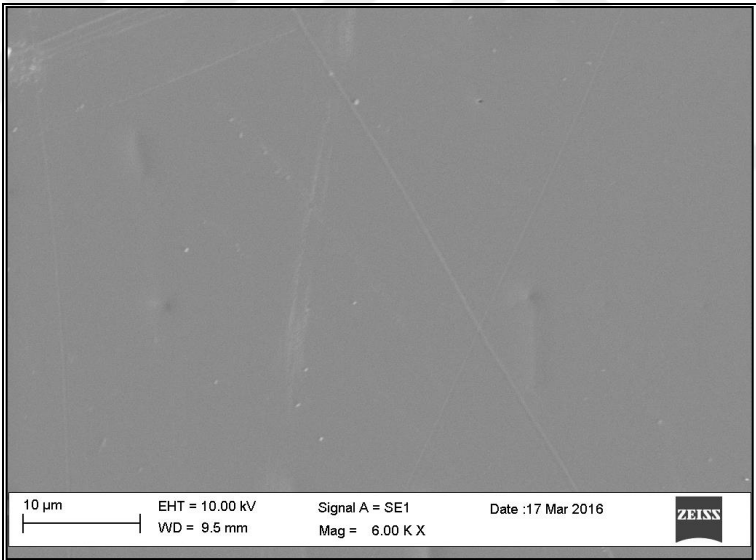
7.6. SCANNING ELECTRON MICROSCOPY (SEM) ANALYSIS

The surface morphology of the different polymer membranes prepared via solution casting method was investigated via scanning electron microscopy as explained in the experimental section. The SEM images of the PESS, PESSGMA, PESSGMA/STY and PESSGMA/VPA polymers are presented in Figure 7.6(a), (b), (c) and (d) respectively. As can be seen from these images at similar magnifications, the PESS, PESSGMA and the PESSGMA/VPA membranes show smooth and flat surfaces whereas the PESSGMA/STY membrane exhibits a porous surface due to solvent or styrene evaporation. As the samples were dried at 100°C for 5 hours and at 110°C for 15 hours under vacuum, there is a

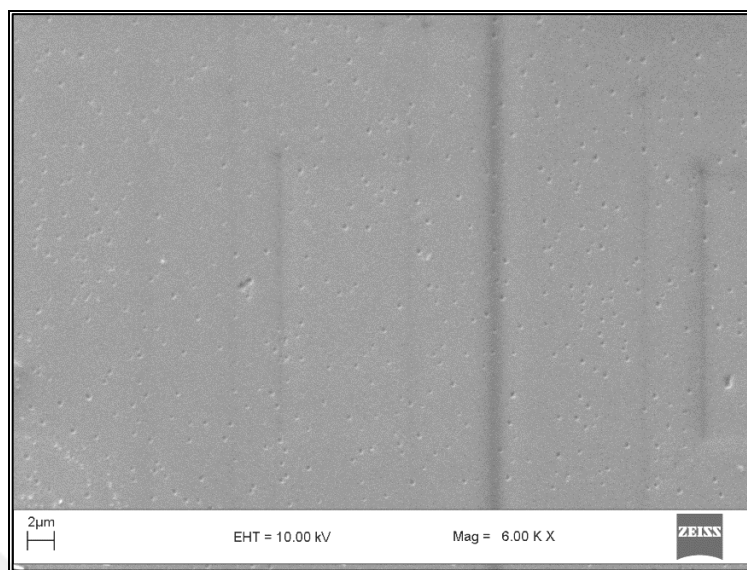
possibility that unreacted styrene trapped in the PESSGMA network can escape and evaporate (boiling point(*styrene*)=145°C) just like the solvent may (boiling point(*dimethyl sulfoxide*)=185°C) during drying of the films, causing the pores on the surface. However we were not able to detect such a porous surface morphology for the PESS, PESSGMA or PESSGMA/VPA membranes even at higher magnifications due to solvent evaporation. The SEM images of the PESSGMA/STY/VPA membrane at different magnifications are presented in Figure 7.7. The images presented in Figure 7.7 clearly indicate that there is phase separation in this system. The SEM images of the PESSGMA/STY/VPA membrane at 4000x and 10000x magnifications presented in Figure 7.7 (b) and (c) respectively, indicate that within the PESSGMA network (matrix), which include styrene and VPA units within its structure, polystyrene, polyvinylphosphonic acid and their copolymers assemble to form spherical domains which are as large as 10 to 30µm and within these domains there are smaller spherical domains whose size can range from 100nm (0.1µm) to around 2 µm. In a study on poly(styrene-*b*-vinylphosphonic acid) diblock copolymers which have been prepared and evaluated as nanostructured polymer electrolytes, analysis of the copolymer membranes by tapping mode atomic force microscopy revealed nanophase-separated morphologies with continuous phosphonated domains [77]. The acidic block copolymers were also found to self-assemble into spherical micellar nanoparticles. As PESSGMA forms the main matrix of the PESSGMA/STY/VPA polymers, and as the polarity of the three components should decrease in the following order VPA> PESSGMA>STY, it is suggested that the larger domains are formed by a polystyrene rich phase within the PESSGMA network and the smaller spherical domains which are distributed both within the polystyrene phase and PESSGMA matrix is formed by the copolymer of poly styrene and vinyl phosphonic acid which must assemble into spherical micellar structures (as observed for poly(styrene-*b*-vinylphosphonic acid) diblock copolymers in the work by Jannasch P. *et.al.*) [78]. However, this phase separation was not detected in the DMA of the PESSGMA/ STY / VPA polymers. Both the E'' and tan delta versus temperature profiles gave single broad bands indicating a heterogenous system, but separate peaks corresponding to the T_g's of the different phases were not present.



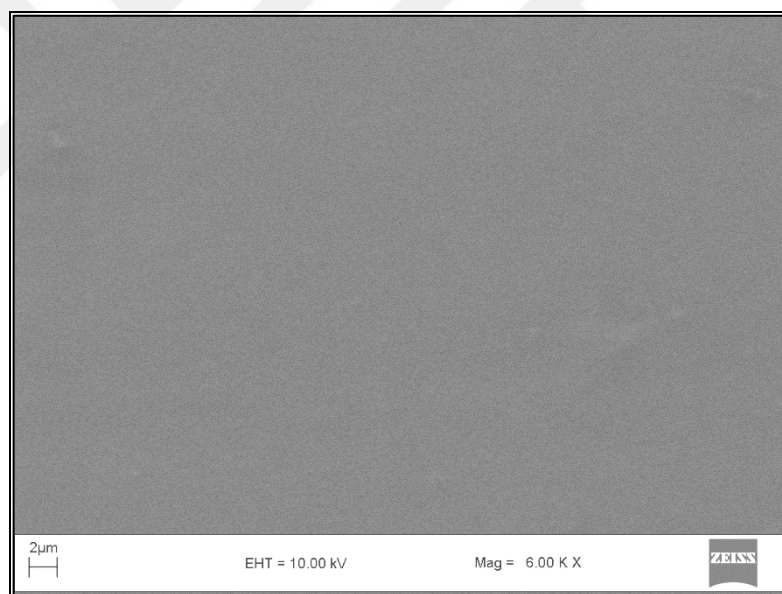
(a)



(b)

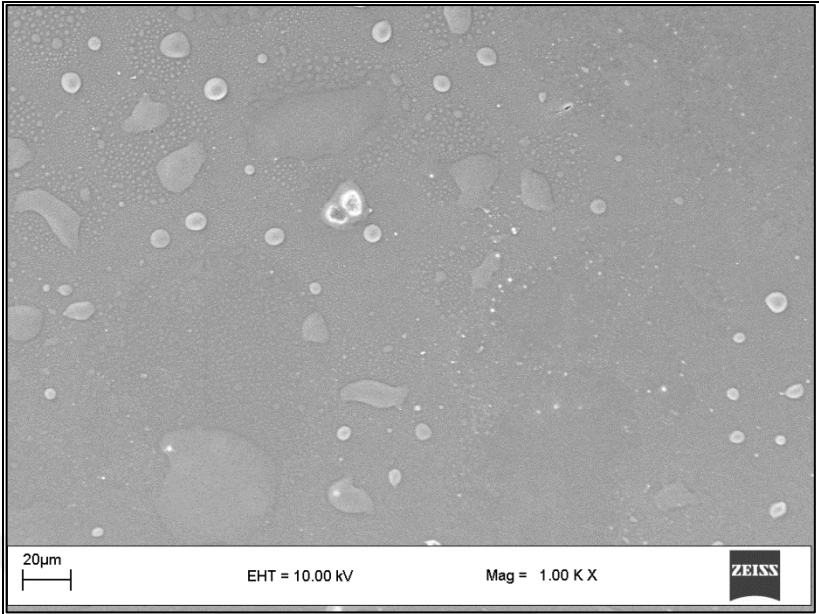


(c)

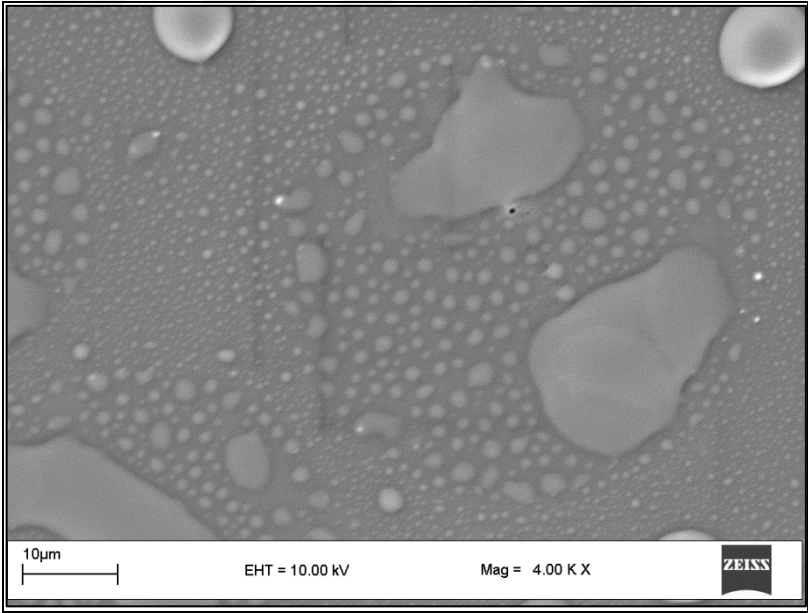


(d)

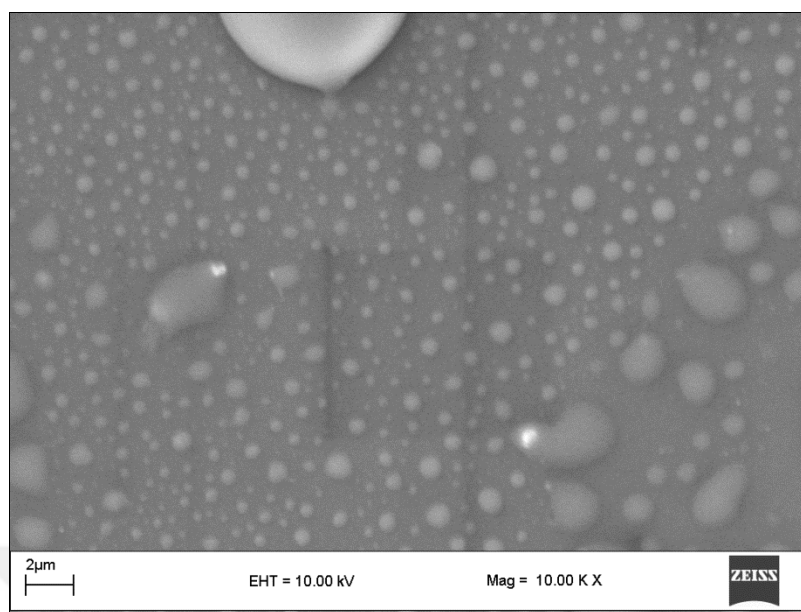
Figure 7.6. SEM images of (a) PESS at 5500x magnification (b)PESSGMA at 6000x magnification, (c)PESSGMA/STY at 6000x magnification, and (d)PESSGMA/VPA at 6000x magnification.



(a)



(b)



(c)

Figure 7.7. SEM images of PESSGMA/STY/VPA at (a) 1000X (b) 4000X (c) 10000X magnifications.

7.7. COST ANALYSIS

Although the performance of a membrane is an important parameter for direct methanol fuel cells, cost also plays a critical role in the commercialization of this type of fuel cells. Currently, the cost of the DMFC systems is thought to be very high, mainly due to the excessive cost created by some key fuel cell components including the polymer electrolyte membranes (PEMs). Several PEMs are commercially available including Nafion (Dupont), Aciplex (Asahi Chemicals Co.), Flemion (Asahi Chemicals Co.) and Dow membranes (Dow Chemical Co.) etc. Of all, Nafion is the most established product that has been widely tested and used in the majority of the available fuel cell systems. The performance of Dow membranes is superior to that of Nafion 117, but they are more expensive than Nafion. These perfluorosulfonic acid membranes are not suitable in large scale commercial applications due to their high price in DMFC applications. In this study PESS and PESSGMA polymer membranes have been developed as alternative PEMs for cost reduction in DMFCs. In order to estimate the cost of the PESS and PESSGMA membranes prepared in this work, the price of each starting chemical was obtained from Sigma-

Aldrich and necessary cost calculations were done by considering all the chemicals used in the synthesis of PESS and PESSGMA polymers and preparation of the membranes. The calculated cost values of all the prepared membranes as well as the commercial Nafion membranes are listed in Table 7.5. The PESS and PESSGMA membranes were prepared with dimensions of 50mm x 50mm x 0.18mm, therefore the price of each membrane with these dimensions were calculated. The cost of commercial Nafion membrane that has sizes 8in x 10in x 0.007in is about 692-1080 €. The price of Nafion® 117 membrane was found as 168.8 € for 50mm x 50mm x 0.18mm dimensions as obtained from Sigma-Aldrich. The lowest price of Nafion®117 membrane from Alfa Aesar was calculated as 54.3€ for the same dimensions. As can be seen from the cost data presented in Table 7.5, the PESS and PESSGMA membranes are much more economic than the commercial Nafion® 117 membranes. Even the price of the most expensive PESSGMA membrane is about the quarter price of the least expensive Nafion membrane.

Table 7.5. Cost values of the PESS, PESSGMA, PESSGMA copolymer membranes and the commercial Nafion® 117 membranes.

Polymer Membrane	Cost(€) for the membrane with (50mm x 50mm x 0.18mm) dimensions
Nafion® 117	¹ 168.8 - ² 54.3
PESS	9.12
PESSGMA	14.34
PESSGMA/STY(70/30)	10.81
PESSGMA/STY/VPA(70/15/15)	12.25
PESSGMA/VPA(70/30)	13.69
PESSGMA/VPA(60/40)	13.48
PESSGMA/VPA(50/50)	13.26

¹Cost obtained from Sigma-Aldrich [79].

²Cost obtained from Alfa Aesar [80].

8. CONCLUSIONS AND FUTURE WORK

8.1. CONCLUSIONS

The main goal of this project was to develop polymer electrolyte membranes based on poly(aryl ether sulfone)s for the direct methanol fuel cells (DMFCs). These membranes should exhibit high proton conductivity, high mechanical and thermal resistance, low methanol permeability and good hydrolytic stability for desired applications. Thus, for this purpose, partially sulfonated poly(aryl ether sulfone) (PESS) was synthesized via polycondensation reaction of sulfonated and non-sulfonated monomers that are 4-florophenyl sulfone (FPS), bisphenol A (BPA) and hydroquinone 2-potassium sulfonate (HPS) using an approximate mole ratio of BPA to HPS of 4:6 and then after acidification, the PESS polymer was functionalized with glycidyl methacrylate (PESSGMA). The PESSGMA pre-polymers were then cross-linked and altered via radical polymerization with co-monomers such as styrene (STY) and vinyl-phosphonic acid (VPA) in an effort to improve the mechanical properties and thermal stability and reduce the swelling in water and the methanol permeability. Five types of polymer membranes were prepared namely the PESS, and its glycidyl methacrylate derivative PESSGMA, and the copolymers of PESSGMA with vinyl phosphonic acid and styrene; PESSGMA/STY, PESSGMA/VPA, PESSGMA/STY/VPA via solution casting method using dimethyl sulfoxide as the solvent, tert-butyl peroxy benzoate or benzoyl peroxide as the radical initiator. The total comonomer content was fixed at 30wt% content for the PESSGMA/STY and PESSGMA/STY/VPA but varied for the PESSGMA/VPA copolymers as 30,40 and 50wt%. Additionally, the potassium salt form of the PESS polymer (PESS(K)) was also synthesized and reacted with glycidyl methacrylate; (PESSGMA(K)), then self-polymerized and copolymerized with styrene and vinyl phosphonic acid in an effort to examine and prevent the possible inhibiting effect of sulfonic acid groups on radical polymerization. However, this synthesis led to the side reaction of sulfonated potassium groups of the PESS(K) polymer with GMA to form undesirable glycidyl methacrylate esters that consumes the sulfonate groups which would be acidified later. Therefore, this synthetic route was found to be inappropriate for the preparation of cross-linked methacrylated derivatives of sulfonated poly(aryl ether sulfone)s. In addition the partially sulfonated poly(aryl ether sulfone) (PESS) was synthesized first by the reaction of 4-

fluorophenyl sulfone (FPS), bisphenol A (BPA) and hydroquinone 2-potassium sulfonate (HPS) using an excess of the diol monomers where the obtained PESS polymer chains terminate with either HPS or BPA monomer as depicted in Figure 4.1. The cross-linking reactions of the glycidyl methacrylated derivatives of this PESS product did not produce network polymers unless post cure cycles at 150 or 180°C were applied. Therefore, a modified procedure for the synthesis stage of PESS polymer was also carried out to ensure that all the PESS polymer chains terminate with BPA monomer that provided to keep the sulfonic acid groups far away from the glycidyl methacrylate functionality. Different temperature cure cycles were applied to the PESSGMA pre-polymers, and the cure cycle was also optimized to obtain membranes with a network structure, which were also processable (eg. not brittle). Thus, the PESSGMA pre-polymer synthesized with the BPA terminated PESS and the optimized cure cycles were used for the preparation of crosslinked PESSGMA polymers and copolymers for further analysis.

The chemical structures of the synthesized PESS and PESSGMA pre-polymers were characterized by FT-IR and ¹H-NMR spectroscopic methods. The ¹H-NMR spectroscopic analysis indicated that the PESS polymers synthesized contained about 60% mol of sulfonated repeating unit. The ¹H-NMR spectroscopic analysis of the product of the reaction of PESS(K) with GMA indicated the addition of GMA to sulfonate groups, which was an undesirable condition as this reaction consumes sulfonate groups which were planned to be acidified after cure reactions to make the membranes proton conductive. Therefore this synthetic route was found to be ineffective in preparation of crosslinked PESSGMA polymers, as discussed above. The number average molecular weight (\bar{M}_n) of the PESS polymer synthesized by the first method (PESS(1)) where an excess of the diol monomers was used, was determined as 50,642(g/mol) and that of BPA terminated PESS polymer synthesized by the second method (PESS(2)) was determined as 35,342(g/mol). The addition of GMA to the PESS polymers synthesized by the two methods both led to a larger molecular weight increase than would be expected for GMA addition to only chain ends (eg +12,518g/mol for PESS(1) and 35,023g/mol for PESS(2)). For the PESS polymer synthesized by the second method, the molecular weight was nearly doubled when reacted with GMA to form the PESSGMA product. Some radical side reactions through methacrylate double bonds, such as di-merization was suggested to be responsible for the increase of molecular weight.

The FT-IR spectroscopic analysis of the PESSGMA/STY, PESSGMA/VPA, PESSGMA/STY/VPA polymers indicated that the PESSGMA pre-polymer was co-polymerized with styrene and vinyl phosphonic acid successfully via radical mechanism moreover, these polymer membranes were found as insoluble in several solvents as expected demonstrating the successful crosslinking of the PESSGMA polymers and network formation when the optimized cure cycle was applied. In addition FT-IR spectroscopic analysis also indicated the condensation of –OH groups of VPA monomer for the PESSGMA/VPA polymers especially for the ones that were post-cured at elevated temperatures (eg.150 or 180°C) which was why post cure at elevated temperatures was avoided.

The PESS polymer (synthesized by the 2nd method) had measured IEC values of 1.88 meq g⁻¹ (powdered polymer) and 2.17 meq g⁻¹(membrane) which were very close to its reported IEC values in the range of 1.8 – 2.2 meq g⁻¹. A decrease of IEC value was observed for the PESSGMA polymer for both un-crosslinked polymer as synthesized and its cross-linked film. This decrease in IEC for the PESSGMA polymer as compared to that of the PESS polymer was attributed to both the increase in molecular weight of the polymer chains as determined from GPC analysis and to loss of the sulfonic acid groups to a certain extent upon possible side reaction with glycidyl methacrylate. The cross-linked PESSGMA and PESSGMA/STY membranes showed decreased IEC values as compared to that of linear PESS polymer membrane which was attributed to the lower swelling of the crosslinked membranes in water which would suppress ion exchange. The IEC values observed for PESSGMA/VPA membranes varied from 4.34 to 7.75 meq./g, which were gradually higher than the corresponding PESS, PESSGMA and PESSGMA/STY membranes which exhibited IEC values between 0.35 - 2.17 meq/g. PESSGMA/VPA membranes exhibited relatively higher ion-exchange capacity since additional acid groups were introduced to the system by the VPA comonomer.

The cross-linking of the PESS polymer led to a considerable decrease in the degree of swelling in water both at room temperature and at 80°C as expected, however the introduction of the VPA co-monomer to the PESSGMA network led to an increase in the extent of swelling in water as compared to PESSGMA and PESSGMA/STY membranes. Swelling in water after 24 hrs at 80°C resulted in 55wt% weight change for the PESS polymer whereas the weight change was less than 10wt% for the PESSGMA and

PESSGMA/STY polymers and approximately 30wt% for the PESSGMA/VPA polymer and nearly 20wt% for the PESSGMA/STY/VPA polymer.

In DSC analysis, a broad endothermic peak at around 105°C for the PESS and at around 115°C for the PESSGMA and PESSGMA/STY polymers was observed which was attributed to the transition of sulfonic acid groups into ionic clusters. These endo peaks shifted to around 125°C and 130°C for the PESSGMA/STY/VPA and PESSGMA/VPA polymers respectively, which was explained by the presence phosphonic acid groups in addition to sulfonic acid groups. Thus, the introduction of a cross-linked structure and phosphonic acid groups to the PESS polymer effected the hydration levels and the transition into ionic clusters as well as the temperature that this transition was observed. The exo peaks observed above 200 °C in the DSC thermograms of all the membranes were attributed to the degradation of the side chain sulfonic acid and/or phosphonic acid groups.

The thermomechanical properties of the PESS and PESSGMA polymer membranes were determined via DMA. The T_g 's of the PESS and PESSGMA polymers as determined from the loss modulus maxima ranged from 94 to 161°C. The glass transition temperatures of all the membranes as determined from the loss moduli maxima were above 90°C indicating that these membranes can be used below their T_g 's at 60-80 °C where they can be used in DMFC applications. The highest T_g was observed at 161°C for the PESSGMA/STY(70/30) polymer, and the lowest T_g was observed at 94 °C for the PESSGMA/VPA(50/50) polymer. The crosslinking of PESS polymer resulted in an increase in T_g for the PESSGMA and PESSGMA/STY polymers whereas the PESSGMA/VPA polymers, although cross-linked exhibited lower T_g 's as compared to that of PESS polymer. This was attributed to the lower T_g of polyvinylphosphonic acid units that may have formed during the crosslinking of PESSGMA with VPA. The T_g 's of the PESSGMA/VPA polymers also decreased with increasing VPA content.

At temperatures below the glass transition temperature (T_g) of PESS and PESSGMA polymers, the storage modulus values decreased in the following order; PESSGMA > PESSGMA/STY(70/30) > PESS > PESSGMA/STY/VPA(70/15/15) > PESSGMA/VPA(70/30) > PESSGMA/VPA(60/40) > PESSGMA/VPA(50/50). Thus the cross-linked nature of PESSGMA and the introduction of the rigid aromatic styrene monomer to the system acted to increase the modulus significantly as compared to the PESS polymer below the T_g of these polymers whereas the introduction of VPA

monomer to the PESSGMA network decreased the storage modulus considerably due to lack of aromaticity in its structure. The storage modulus values of the PESS and PESSGMA polymers at 25°C ranged from 363MPa to 2589 MPa. The storage modulus values of all the PESSGMA copolymers at 30wt% comonomer content ranged from 0.6GPa to 2.1GPa even at 60 °C.

In thermal gravimetric analysis, two major weight loss stages were detected at around 200–360 °C and 400–550 °C which were ascribed to the removal of $-\text{SO}_3\text{H}$ and/or $-\text{PO}_3\text{H}$ groups and the thermal decomposition of the poly(arylether sulfone) polymer main chain respectively. The slight weight loss observed below 200 °C for all the polymer membranes on the other hand were attributed to the removal of water molecules from the polymer matrix or of moisture absorbed from the air. Although the first stage degradation profiles were quite similar, the second stage degradation started at higher temperatures for the PESSGMA and PESSGMA/STY polymers as compared to the PESS polymer and the char residue at 600°C was also higher for the PESSGMA and PESSGMA/STY polymers as compared to that of PESS polymer due to the cross-linked structure. The PESSGMA/VPA polymer exhibited the greatest weight loss for the whole temperature range and the second stage degradation started at the lowest temperature among all the polymers. For the PESSGMA/VPA copolymers the temperatures at which the last stage degradation starts (corresponding to main chain and network degradation) shifted to lower temperatures and the char residue at each temperature decreased as the VPA content increased.

Proton conductivities of the different polymer membranes were measured at 60°C and 80°C in saturated water vapor. In general, higher proton conductivity was significantly based on higher IEC and larger water uptake or vice versa. The PESSGMA polymer and the PESSGMA/STY copolymer exhibited significantly improved T_g 's, higher thermal stabilities at the higher temperature ranges, and reduced swelling in water, however they exhibited significantly reduced proton conductivity values as compared to that of PESS polymer. This result was attributed to the lower water uptake of the cross-linked PESSGMA polymers as compared to PESS polymer since proton transport in membranes requires proper contents of bonded water. In addition, it was suggested that some of the sulfonic acid groups may also be lost in a side reaction with glycidyl methacrylate during the synthesis of PESSGMA. However this handicap was overcome with the introduction of VPA comonomer to the PESSGMA network. The PESSGMA/VPA polymers showed

significantly increased proton conductivities than the PESSGMA polymers, and the proton conductivity increased with increasing VPA content (from 30wt% to 50wt%) due to the introduction of additional phosphonic acid groups to the system. The proton conductivities of all the membranes increased significantly with increasing temperature from 60 °C to 80 °C as the mobility of proton ions rises at higher temperatures. The proton conductivity of the PESSGMA polymer did not increase when the initiator content was decreased from 4wt% to 2wt% initiator content, indicating that all the initiator content was consumed during cure reactions.

The methanol permeabilities of the crosslinked PESSGMA and PESSGMA copolymer membranes were significantly reduced both as compared to the PESS and the Nafion membranes. All the PESSGMA crosslinked membranes exhibited methanol diffusion coefficient values in the range of $2.37 \times 10^{-9} \text{ cm}^2 \text{ s}^{-1}$ – $1.92 \times 10^{-8} \text{ cm}^2 \text{ s}^{-1}$, showing excellent resistance to methanol crossover. When VPA was used as the co-monomer, the methanol permeability increased only slightly as compared to that of PESSGMA and PESSGMA/STY. In addition, the methanol diffusion coefficients of the PESSGMA/VPA membranes increased slightly with the increase in VPA content due to increasing hydrophilicity and decreasing cross-link density of the system.

In SEM analysis of the surface morphologies of the membranes, the PESS, PESSGMA and the PESSGMA/VPA membranes showed smooth and flat surfaces whereas the PESSGMA/STY membrane exhibited a porous surface due to solvent or styrene evaporation. However the PESS, PESSGMA or PESSGMA/VPA membranes did not exhibit such a porous surface morphology even at higher magnifications. The SEM analysis of the PESSGMA/STY/VPA membrane at different magnifications on the other hand showed that there was phase separation in this system. It was postulated that, within the PESSGMA network which involved styrene and vinylphosphonic acid units, polystyrene, polyvinylphosphonic acid and their copolymers assembled to form spherical domains which were as large as 10 to 30 μm and within these domains there were smaller spherical domains whose size ranged from 100nm (0.1 μm) to around 2 μm .

According to cost analysis, application of the PESS, PESSGMA and PESSGMA copolymer membranes have been proved to be an effective approach in reducing their cost in addition to decreasing the methanol permeability significantly as compared to both Nafion membranes and aromatic polymer membranes reported in literature. The cost of all

the PESS, PESSGMA and PESSGMA copolymer membranes with (50mm x 50mm x 0.18mm) dimensions were found to be in the range of 9.12-14.34 € which was significantly lower as compared to the price of the commercial Nafion® 117 membranes with the same dimensions (168.80 - 54.30€).

As a polymer electrolyte membrane suitable to be used in DMFC applications should possess both a high proton conductivity and low methanol permeability, the selectivity parameter (ρ) which is the ratio of proton conductivity to methanol permeability was also determined for the different membranes to evaluate their performance in DMFC applications. All the PESSGMA and PESSGMA copolymer membranes, especially the membranes incorporating VPA exhibited higher selectivity ratios than the PESS and commercial Nafion membrane, indicating considerable improvement. The PESSGMA/VPA(60/40) polymer exhibited the highest selectivity ratio and was therefore most suitable to be used as a polymer electrolyte membrane in DMFC applications if only the proton conductivity and methanol permeability data were considered. However other properties such as the storage modulus, the glass transition temperature (T_g), IEC and water uptake need to be considered to determine the membrane most suitable for DMFC applications. Figure 8.1 shows bar graphs for the T_g 's, and the values of storage modulus, proton conductivity, methanol permeability and selectivity ratio at 60°C as well as the cost for all the PESS, PESSGMA and PESSGMA copolymer membranes. Considering the fact that the PESSGMA/STY/VPA membrane exhibited a relatively high proton conductivity of $(16.0 \pm 3.1) \text{ mS cm}^{-1}$ at 60°C which was increased to $27.82 \pm 1.43 \text{ mS cm}^{-1}$ at 80°C, a very low methanol permeability of $6.52 \times 10^{-9} \text{ cm}^2 \text{ s}^{-1}$ at 60°C, and therefore a high selectivity ratio at the same temperature ($2.45 \times 10^6 \text{ S s cm}^{-3}$) significantly improved as compared to both PESS and Nafion membranes (5.00×10^4 for Nafion), a storage modulus value of $931 \pm 435 \text{ MPa}$ at 60°C ($1066 \pm 374 \text{ MPa}$ at 25°C), a T_g of $(112 \pm 4)^\circ\text{C}$, the highest IEC value among all the membranes ($(7.75 \pm 0.42) \text{ meq./g}$), water absorption of about 22% after 24 hours at 80°C and finally a low cost (12.25€/ (50mm x 50mm x 0.18mm) membrane), it may be proposed to be the membrane with optimum set of properties to be used in DMFC applications.

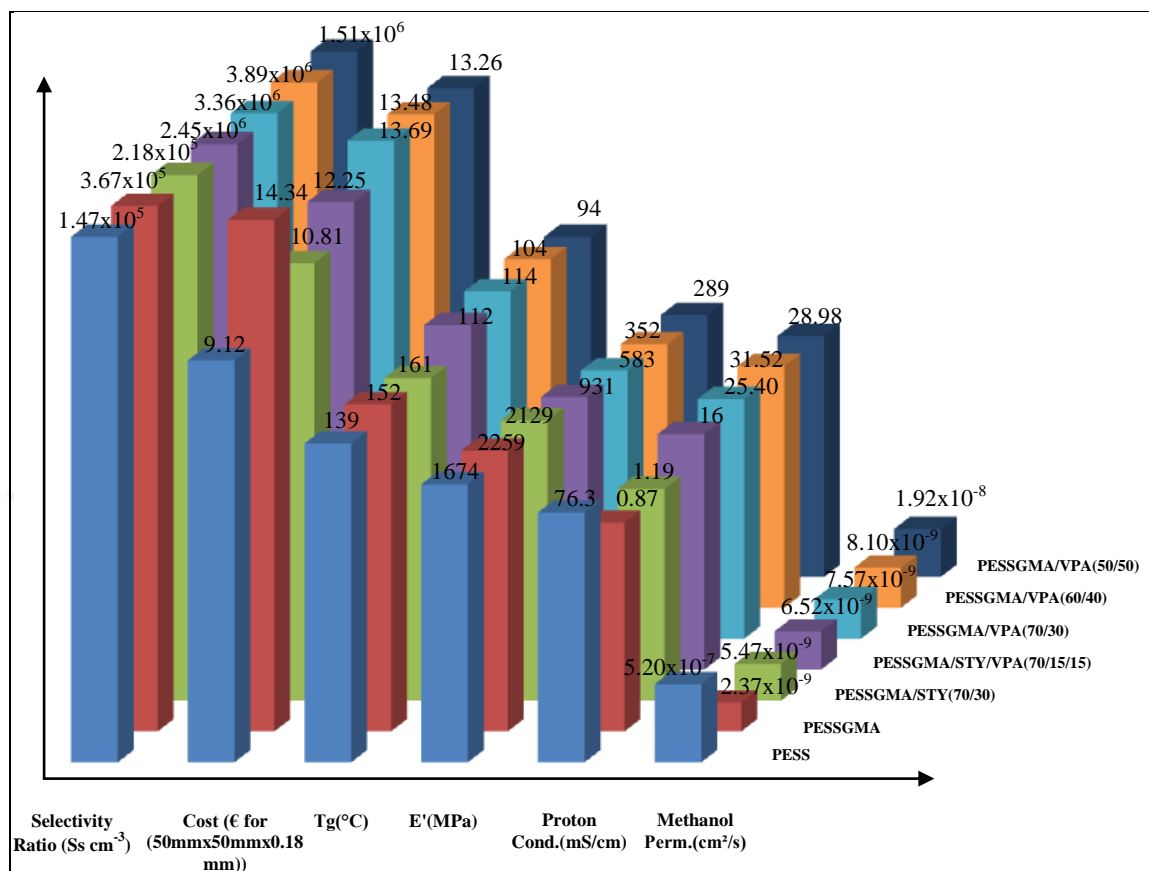


Figure 8.1. Bar graphs for the T_g 's, and the values of storage modulus, proton conductivity, methanol permeability and selectivity ratio at 60°C as well as the cost for all the PESS, PESSGMA and PESSGMA copolymer membranes.

8.2. FUTURE WORK

One necessary future work for this study may be the investigation of the single-cell performance of the PESS and PESSGMA/STY/VPA membranes using a membrane-electrode assembly. In addition, as it is known that the degree of sulfonation of a polymer affects its proton conductivity as well as its swelling in water, PESS polymers with different mol% of sulfonated repeat units groups may be prepared by changing the molar ratio of HPS through the polycondensation reaction in order to improve the proton conductivity of the PESSGMA membranes. In this study the mol% of sulfonated repeat unit groups was kept as 60%, since higher contents of sulfonic acid groups were reported to lead to higher methanol permeability and solubility in water. However sulfonation level

can still be increased since it is now shown that crosslinking of the PESSGMA polymers significantly reduces the methanol cross-over. Finally, in order to avoid the possible consumption of sulfonic acid groups via side reaction with glycidyl methacrylate (GMA), acryloyl chloride or methacryloyl chloride may be used as alternative reagents to modify the PESS pre-polymer and crosslink it via radical polymerization afterwards.



REFERENCES

1. T. Norby, The Promise of Protonics. *Nature*, 410:877, 2001.
2. A. Heinzl, and V. M. Barragan. A Review of the State-of-art of the Methanol Crossover in Direct Methanol Fuel Cell. *Journal of Power Sources*, 84:70, 1999.
3. X. M. Ren, P. Zelenay, S. Thomas, J. Davey and S. Gottesfeld. Recent Advances in Direct Methanol Fuel Cells at Los Alamos National Laboratory. *Journal of Power Sources*, 86:111, 2000.
4. G. Alberti, M. Casciola, L. Massinelli and B. Bauer. Polymeric Proton Conducting Membranes for Medium Temperature Fuel Cells (110–160°C). *Journal of Membrane Science*, 185:73, 2001.
5. K. Miyatake, E. Shouji, K. Yamamoto and E. Tsuchida. Synthesis and Proton Conductivity of Highly Sulfonated Poly(thiophenylene). *Macromolecules*, 30:2941, 1997.
6. Y. S. Kim, F. Wang, M. Hickner, T. A. Zawodzinski and J. E. McGrath. Fabrication and Characterization of Heteropolyacid (H₂PW₁₂O₄₀) Directly Polymerized Sulfonated Poly(aryl ether sulfone) Copolymer Composite Membranes for Higher Temperature Fuel Cell Applications. *Journal of Membrane Science*, 212:263, 2003.
7. D. S. Kim, H. B. Park and Y. M. Lee. Synthesis of Sulfonated Poly(imidoaryl ether sulfone) Membranes for Polymer Electrolyte Membrane Fuel Cell. *Journal of Polymer Science*, 43:5620, 2005.
8. Y. S. Kim, M. A. Hickner, L. Dong, B. S. Pivovar and J.E. McGrath. Sulfonated Poly(aryl ether sulfone) Copolymer Proton Exchange Membranes: Composition and Morphology Effects on the Methanol Permeability. *Journal of Membrane Science*, 243:317, 2004.

9. Smithsonian Institution, "Fuel Cells", <http://americanhistory.si.edu/fuelcells/basics.html>, [retrieved 11 October 2015].
10. Make Your Own Fuel, "Fuel Cell Technology", http://running_on_alcohol.tripod.com/id30.html, [retrieved 25 October 2015].
11. S. B. Reddy, "Proton Exchange Membrane Fuel Cell", <http://www.scribd.com/doc/49628262/Proton-Exchange-Membrane-Fuel-Cell>, [retrieved 2 December 2015].
12. Tech-etch, "Fuel Cells", <http://www.tech-etch.com/photoetch/fuelcell.html>, [retrieved 5 December 2015].
13. A. Hacquard, Improving and Understanding Direct Methanol Fuel Cell (DMFC) Performance. *Worcester Polytechnic Institute, In partial fulfillment of the requirement for the Degree of Master of Science in Chemical Engineering*, May 2005.
14. T. S. Zhao, C. Xu, R. Chen, and W. W. Yang. Mass Transport Phenomena in Direct Methanol Fuel Cells. *Progress in Energy and Combustion Science*, 35:275-292, 2009.
15. P. L. Antonucci, A. S. Arico, P. Crefi, E. Ramunni and V. Antonucci. Investigation of a Direct Methanol Fuel Cell Based on a Composite Nafion-Silica Electrolyte for High Temperature Operation. *Solid State Ionics*, 125:431-437, 1999.
16. A. S. Arico, S. Srinivasan and V. Antonucci. *Fuel Cells*, 1:133-161, 2001.
17. F. R. Kalhammer, P. R. Prokopius, V. P. Roan and G. E. Voecks. Status and Prospects of Fuel Cells as Automobile Engines. *A Report of the Fuel Cell Technical Advisory Panel*, July 1998.
18. J. R. Jurado and M. T. Colomer. Protonic Conductors for Proton Exchange Membrane Fuel Cells. *Chemistry and Industry*, 56:264-272, 2002.

19. V. R. Gowariker, N. V. Viswanathan, and J. Shreedhar, *Polymer Science*, New Age International, New Delhi, 2005.
20. M. A. Clinton, Polymer Cross-linking Information. <http://www.r-scc.com/pdf/tech-electronics.pdf>, [retrieved 5 December 2015].
21. F. W. Billmeyer, *Textbook of Polymer Science*, 3rd Edition, John Wiley and Sons, Inc., USA, 1984.
22. Polymer Journal, "Free-radical Chain Polymerization", <http://www.nature.com/pj/journal/v42/n9/full/pj201066a.html>, [retrieved 8 December 2015].
23. R. J. Young and P. A. Lovell, *Introduction to Polymers*, 3rd Edition, CRC Press Taylor and Francis Group, NW, USA.
24. R. O. Ebevele, *Polymer Science And Technology*, CRC Press, Department of Chemical Engineering University of Benin, Benin City, Nigeria, 2000.
25. W. D. Callister and D. G. Rethwisch, Linear Polymers, *Materials Science and Engineering*, 8th Edition SI Version, 2014.
26. Dr. Breinan, Branched Polymers, *Polymers Expectations, Introduction and Structures*, Breinan Chemistry , 2005.
27. C. A. Harper, Polymer Structure and Synthesis, *Handbook of Plastics, Elastomers, and Composites*, 4th Edition, The McGraw-Hill Companies, 2002.
28. National Programme on Technology Enhanced Learning, "Thermoplastics and Thermosets, <http://nptel.ac.in/courses/112107085/module4/lecture1/lecture1.pdf>, [retrieved 25 December 2015].
29. T. Osswald, Thermal Transitions. *Polymer processing: modeling and simulation*, Hanser Verlag, 2006.

30. W. D. Callister, Crystallization. *Materials Science and Engineering an Introduction*, Wiley, 2003.
31. W. D. Callister, Melting. *Materials Science and Engineering an Introduction*, Wiley, 2003.
32. W. D. Callister, Glass Transition Temperature. *Materials Science and Engineering an Introduction*, Wiley, 2003.
33. Advanced Lab, "Polymer Science", http://polymerscience.physik.huberlin.de/anleitg/dsc12_hu.pdf, [retrieved 03 January 2016].
34. Shodhganga, a Reservoir of Indian Thesis, " Polymers", http://shodhganga.inflibnet.ac.in/bitstream/10603/10198/2/a_patel_chapter-1.pdf, [retrieved 05 January 2016].
35. M. Y. Kariduraganavar, R. K. Nagarale, A. A. Kittur and S .S. Kulkarni. Ion-exchange Membranes: Preparative Methods for Electrodialysis and Fuel Cell Applications. *Desalination*, 197:225-246, 2006.
36. L. M. Sánchez, Literature Review on the Properties of Proton Exchange Membranes. *Phd Thesis*, The Lorraine University, France, November 2012.
37. S. J. Peighambardoust, S. Rowshanzamir, and M. Amjadi. Review of the Proton Exchange Membranes for Fuel Cell Applications. *International Journal of Hydrogen Energy*, 35:9349-9384, 2010.
38. Y. S. Oh, H. J. Lee, M. Yoo, H. J. Kim, J. Han and T. H. Kim. Synthesis of Novel Crosslinked Sulfonated Poly(ether sulfone)s Using Bisazide and Their Properties for Fuel Cell Application. *Journal of Membrane Science*, 323:209-315, 2008.
39. K. T. Park, J. H. Chun, S. G. Kim, B. H. Chun, and S. H. Kim. Synthesis and Characterization of Crosslinked Sulfonated Poly(aryl ether sulfone) Membranes for High

Temperature PEMFC Applications. *International Journal of Hydrogen Energy*, 36:1813-1819, 2011.

40. J. Parvole and P. Jannasch. Polysulfones Grafted with Poly(vinylphosphonic acid) for Highly Proton Conducting Fuel Cell Membranes in the Hydrated and Nominally Dry State. *Macromolecules*, 41:3893–903, 2008.

41. A. Aslan, S. Ü. Çelik and A. Bozkurt. Proton-conducting Properties of the Membranes Based on Poly(vinyl phosphonic acid) Grafted Poly(glycidyl methacrylate). *Solid State Ionics*, 180:1240–1245, 2009.

42. A. Aslan, and A. Bozkurt. An Investigation of Proton Conductivity of Nanocomposite Membranes Based on Sulfated Nano-titania and Polymer. *Solid State Ionics*, 239:21–27, 2013.

43. F. Göktepe, S. Ü. Çelik and A. Bozkurt. Preparation and The Proton Conductivity of Chitosan/poly(vinylphosphonic acid) Complex Polymer Electrolytes. *Journal of Non-Crystalline Solids*, 354:3637–42, 2008.

44. T. Yazawa, T. Shojo, A. Mineshige, S. Yusa, M. Kobune and K. Kuraoka. Solid Electrolyte Membranes Based on Polyvinyl Phosphonic Acid and Alkoxysilane for Intermediate-temperature Fuel Cells. *Solid State Ionics*, 178:1958-1962, 2008.

45. EG&G Services, Fuel Cell Handbook, Fifth Edition, <http://www.fuelcells.org/info/library/fchandbook.pdf>, [retrieved 10 January 2016].

46. J. W. Robinson, *Undergraduate Instrumental Analysis*, 5th edition, Marcel Dekker, pages 93; 114;121-122, 1994.

47. T. Williams, Gel Permeation Chromatography. A Review Journal of Materials Science. *Journal of Membrane Science*, 5:811-820,1970.

48. Waters, "GPC - Gel Permeation Chromatography" http://www.waters.com/waters/en_T

R/GPCGelPermeationChromatographyBeginner%27s- Guide/nav. htm?cid=10167568&locale=en_TR, [retrieved 12 January 2016].

49. Olin College of Engineering, "TA Instruments Differential Scanning Calorimeter (DSC) Operating Instructions" , <http://faculty.olin.edu/~jstolk/matsci/Operating%20Instructions/DSC%20Operating%20Instructions.pdf>, [retrieved 12 January 2016].

50. J. Schawe, R. Riesen, J. Widmann and M. Schubnell, *Interpreting DSC curves Part 1: Dynamic Measurements*, UserCom, Sweden, 2000.

51. Perkin Elmer, "Thermogravimetric Analysis (TGA), A Beginners Guide", <http://www.perkinelmer.com/cmsresources/images/4474556gdetgabeginnersguide.pdf>, [retrieved 15 January 2016].

52. The Science Education Resource Center at Carleton College, "Scanning Electron Microscopy(SEM)", http://serc.carleton.edu/research_education/geochemsheets/techniques/SEM.html, [retrieved 17 January 2016].

53. J. Zhang, J. Wu, H. Zhang, and J. Zhang. Proton Conductivity Measurements. *PEM Fuel Cell Testing and Diagnosis*, pages 143-159, Newnens, 2013.

54. M. Bello, Assessment of Electrochemical Methods for Methanol Crossover Measurement through PEM of Direct Methanol Fuel Cell. *International Journal of Engineering and Technology*, 11:92, 2011.

55. E. E. Ünveren, T. Y. İnan and S. S. Çelebi. Partially Sulfonated Poly(1,4-phenylene ether-ether-sulfone) and Poly(vinylidene fluoride) Blend Membranes for Fuel Cells. *Fuel Cells*, 13:862–872, 2013.

56. Antech, "Gas Chromatography", <http://www.antech.ie/hintstips.html>, [retrieved 18 January 2016].

57. C. A. Dai, C. P. Liu, Y. H. Lee, C. J. Chang, C. Y. Chao and Y. Y. Cheng. Fabrication of Novel Proton Exchange Membranes for DMFC via UV Curing. *Journal of Power Sources*, 117:262-272, 2008.
58. H. Bi, J. Wang, S. Chen, Z. Gao, L. Wang and K. Okamoto. Preparation and Properties of Cross-linked Sulfonated Poly(aryl ether sulfone)/sulfonated Polyimide Blend Membranes for Fuel Cell Application. *Journal of Membrane Science*, 350: 109-116, 2010.
59. S. H. Almeida and Y. Kawano. Thermal Behaviour of Nafion Membrane. *Journal of Thermal Analysis and Calorimetry*, 58:569-577, 1999.
60. E. Can, E. Kınacı and G. R. Palmese. Preparation and Characterization of Novel Vinyl Ester Formulations Derived from Cardanol. *European Polymer Journal*, 72:129–147, 2015.
61. W. F. Su, Chemical and Physical Properties of Polymers. *Principles of Polymer Design and Synthesis*, Chapter 4, pages 68, Springer Science and Business Media, 2013.
62. K. Matyjaszewski, B. S. Sumerlin, N. V. Tsarevsky and J. Chiefar. Controlled Radical Polymerization: Mechanisms. I. B. Coutelier, S. Reynaud, B. Grassl, M. Destarac, editors, *Aqueous RAFT/MADIX Polymerization of Vinylphosphonic Acid under Microwave Irradiation*, pages 283-294, American Chemical Society, 2015.
63. Dynamic Mechanical Analysis, "Principles of DMA", http://files.hanser.de/hanser/docs/20041012_2411215439-82_3-446-22673-7.pdf, [retrieved 18 January 2016].
64. L. J. Broadbelt, M. T. Klein, B. D. Dean and S. M. Andrews. Thermal Stability High Performance Polyarylether Sulfones. *Industrial and Engineering Chemistry Research*, 33:2265–2271, 1994.
65. C. L. Beyler and M. M. Hirschler. Thermal Decomposition of Polymers. *Handbook of Fire Protection Engineering*, 2nd Edition, pages 111-131, National Fire Protection Association, 1995.

66. L. Dongsheng, L. Zhimin, H. Fei, L. Shengru, Z. Gang and Y. Jie. Pendant Crosslinked Poly(aryl ether sulfone) Copolymers Sulfonated on Backbone for Proton Exchange Membranes. *Polymer Engineering and Science*, 54:9, 2014.
67. J. Y. Park, Crosslinked Sulfonated Poly(aryl ether sulfone) Membranes for Fuel Cell Application. *International Journal of Hydrogen Energy*, 37:2603-2613, 2012.
68. V. Kiran, S. Awashi, B. Gaur. Hydroquinone Based Sulfonated Poly (aryl ether sulfone) Copolymer as Proton Exchange Membrane for Fuel Cell Applications. *Express Polymer Letters*, 9:1053–1067, 2015.
69. L. Macarie and G. Iliu. Poly(vinylphosphonic acid) and Its Derivatives. *Progress in Polymer Science*, 35:1078-1092, 2010.
70. K. D. Kreuer, S. J. Paddison, E. Spohr and M. Schuster. Transport in Proton Conductors for Fuel-cell Applications: Simulations, Elementary Reactions and Phenomenology. *Chemical Reviews*, 104:4637–768, 2004.
71. K. D. Kreuer, Proton conductivity: Materials and Applications. *Chemistry of Materials*, 8:610–41, 1996.
72. A. Sannigrahi, S. Takamuku and P. Jannasch. Block Selective Grafting of Poly(vinyl phosphonic acid) From Aromatic Multiblock Copolymers for Nano-structured Electrolyte Membranes. *Polymer Chemistry*, 4:4207-4218, 2013.
73. J. Y. Park, T. H. Kim, H. J. Kim, J. H. Choi and Y. T. Hong. Crosslinked Sulfonated Poly(aryl ether sulfone) Membranes for Fuel Cell Application. *International Journal Energy*, 37:2603-2613, 2012.
74. J. Y. Park, Crosslinked Sulfonated Poly(aryl ether sulfone) Membranes for Fuel Cell Application. *International Journal of Hydrogen Energy*, 37:2603-2613, 2012.

75. B. P. Tripathi, A. Saxena and V. K. Shahi. Phosphonic Acid Grafted Bis(4- γ -aminopropyl diethoxysilylphenyl) Sulfone (APDSPS)-poly(vinyl alcohol) Cross-linked Polyelectrolyte Membrane Impervious to Methanol. *Journal of Membrane Science*, 318:288–297, 2008.
76. P. Chen, X. Chen, Z. Ana, K. Chen and K. Okamoto. Quinoxaline-based Crosslinked Membranes of Sulfonated poly(aryl ether sulfone)s for Fuel Cell Applications. *International Journal of Hydrogen Energy*, 36:12406-12416, 2011.
77. R. Perrin, M. Elomaa and P. Jannasch. Nanostructured Proton Conducting Polystyrene–Poly(vinylphosphonic acid) Block Copolymers Prepared via Sequential Anionic Polymerizations. *Macromolecules*, 42:5146–5154, 2009.
78. E. L. Lutz, W. H. Heath, R. R. Odle, T. L. Guggenheim, J. J. R. Ordenez and J. R. G. Pena. Poly(aryl ether sulfone) Composition and Method of Making. Patent WO2013066784A1, May 2013, <http://www.google.com/patents/WO2013066784A1?hl=tr&cl=en>, [retrieved 12 March 2016].
79. Sigma Aldrich, "Nafion Perfluorinated Membrane", <http://www.sigmaaldrich.com/catalog/product/aldrich/274674?lang=en®ion=TR&gclid=CLjT2ZqLgNICFQ4R0wodBWoGsg>, [retrieved 31 January 2017].
80. Alfa Aesar, "Nafion 117 Membrane", <https://www.alfa.com/en/catalog/042180/>, [retrieved 31 January 2017].